INVESTIGATION OF BUCKLING MODES AND CRITICAL BUCKLING PRESSURES FOR CLAMPED SPHERICAL CAPS

by

Donald Earle Milks

A Thesis Submitted to the Faculty of the

DEPARTMENT OF CIVIL ENGINEERING

In Partial Fulfillment of the Requirements
For the Degree of

MASTER OF SCIENCE

In the Graduate College

THE UNIVERSITY OF ARIZONA

1 9 6 4

STATEMENT BY AUTHOR

This thesis has been submitted in partial fulfillment of requirements for an advanced degree at The University of Arizona and is deposited in the University Library to be made available to borrowers under rules of the Library.

Brief quotations from this thesis are allowable without special permission, provided that accurate acknowledgement of source is made. Requests for permission for extended quotation from or reproduction of this manuscript in whole or in part may be granted by the head of the major department or the Dean of the Graduate College when in his judgment the proposed use of the material is in the interests of scholarship. In all other instances, however, permission must be obtained from the author.

SIGNED: Donald E. Milks

APPROVAL BY THESIS DIRECTOR

This thesis has been approved on the date shown below:

H. P. Harrenstien

H. P. Harrenstien
Professor of Civil Engineering

6 May 64
Date

ACKNOWLEDGEMENTS

The author acknowledges and appreciates the suggestions made by Dr. Howard P. Harrenstien, Dr. Richmond C. Neff, Dr. Ralph M. Richard and Dr. Morris W. Self in reviewing the manuscript, the advice of Dr. Don A. Linger on the experimental phase, the assistance of Brooks L. Muterspaugh in the machining of the shell molds and in the building of the forming and testing apparatus, and the encouragement of his wife Alyce.

TABLE OF CONTENTS

LIST OF TABLES

LIST OF ILLUSTRATIONS

LIST OF ILLUSTRATIONS--Continued

ABSTRACT

The buckling pressure of uniformly loaded clamped spherical caps is determined experimentally by testing a statistically sufficient number of shells for each of five different values of a ratio representing the rise of the shell divided by the thickness. A technique leading to the forming of the plastic shells using a vacuum former is presented and discussed. The variation of the measured quantities of buckling pressure, radius of curvature and thickness at the point of buckling for each sheet of material and for each shape of spherical cap is noted. The experimentally determined buckling pressure is compared to other experimental results and theoretical investigations. This comparison indicates reasonably good agreement. The von Karman-Tsien theory shows the best agreement throughout the range of testing. Results of the tests indicates that the ratio of radius of curvature divided by thickness has a more significant effect on the buckling pressure than does the degree of shallowness of the spherical caps. This investigation shows that spherical shells formed by a vacuum former technique can give reliable results for the buckling pressure when tested. It is also demonstrated that the experimental determination of buckling pressures of spherical caps is feasible

and it is thus expected that this procedure can be extended to more complicated situations.

CHAPTER ONE

INTRODUCTION

A shell structure results when a material is formed into a curved surface which is required to transmit loads and respective displacements. The middle surface of the shell is that surface which bisects the thickness. If the form of this middle surface is known, as well as the normal thickness, the geometry of the shell is completely defined. When the thickness is small as compared to the other dimensions, the principle action of the forces in the shell is that of a membrane, that is, a state of direct forces which may be a combination of tension, compression, and shear, the directions of which lie parallel to the plane of the middle surface. In certain cases, however, the situation is complicated by the boundary disturbances which may lead to the condition where bending and normal shearing forces become dominant rather than neglible.

The history of the use of these structures in building construction is a relatively long one. However, in the past few decades engineers have been able to place greater emphasis on the application of shell structures, not only in the building

construction field, but in other areas as well. One reason for the increased use of shell structures has been caused by a better understanding of the theoretical shell action. This has been brought about by mathematical analyses which are based on idealized conditions.

Many mathematical models of each of the different shell types have been developed by engineers or mathematicians, and the results of these analyses are readily available. It is noted that these analyses usually contain approximations or assumptions which are made in order to formulate the mathematical model in a way which admits a solution. When one takes into account these limitations and present construction practices, it is not unreasonable to expect a lack of agreement between the theoretical and the true behavior of shell structures.

The phenomenon of the buckling of a shell is a particularly difficult situation to formulate mathematically. To develop workable equations, a symmetrical type of deflection is usually assumed along with the assumption that the shell is shallow. Even with these simplifications, the solutions of the nonlinear differential equations which result are generally difficult and lengthy, if at all possible. Moreover, the simplifications often made in order to obtain a solution may or may not be acceptable in the light of the actual physical behavior of the shell.

As a possible alternate approach, it is suggested that the buckling problem be formulated experimentally rather than mathematically. If it proves feasible to obtain buckling pressures through this experimental approach for a simple case, the procedure might be extended to more difficult situations.

The particular problem to be discussed here is that of the buckling of clamped spherical caps subjected to uniform pressure. The spherical cap is a segment of a sphere. If one had a complete sphere and removed a segment by passing any plane through the sphere, and then hollowed out the inside portion, a spherical cap would result. The term thin, in thin spherical caps, refers to the thickness of the material. For the majority of applications, this thickness is small compared to the radius of curvature of the shell, and the general assumptions of thin shell theory are applicable. It is also observed that this thickness is usually uniform. The term shallow refers to the rise of the peak of the shell from the base plane. A shallow shell would have a small rise as compared to the radius of the base plane. The parts of the spherical cap, as well as some of the notation to be used, are indicated in Figure 1.

The classical theory of the buckling of spherical shells assumes that a complete, initially perfect spherical shell which is subjected to external pressure contracts in size with little bending

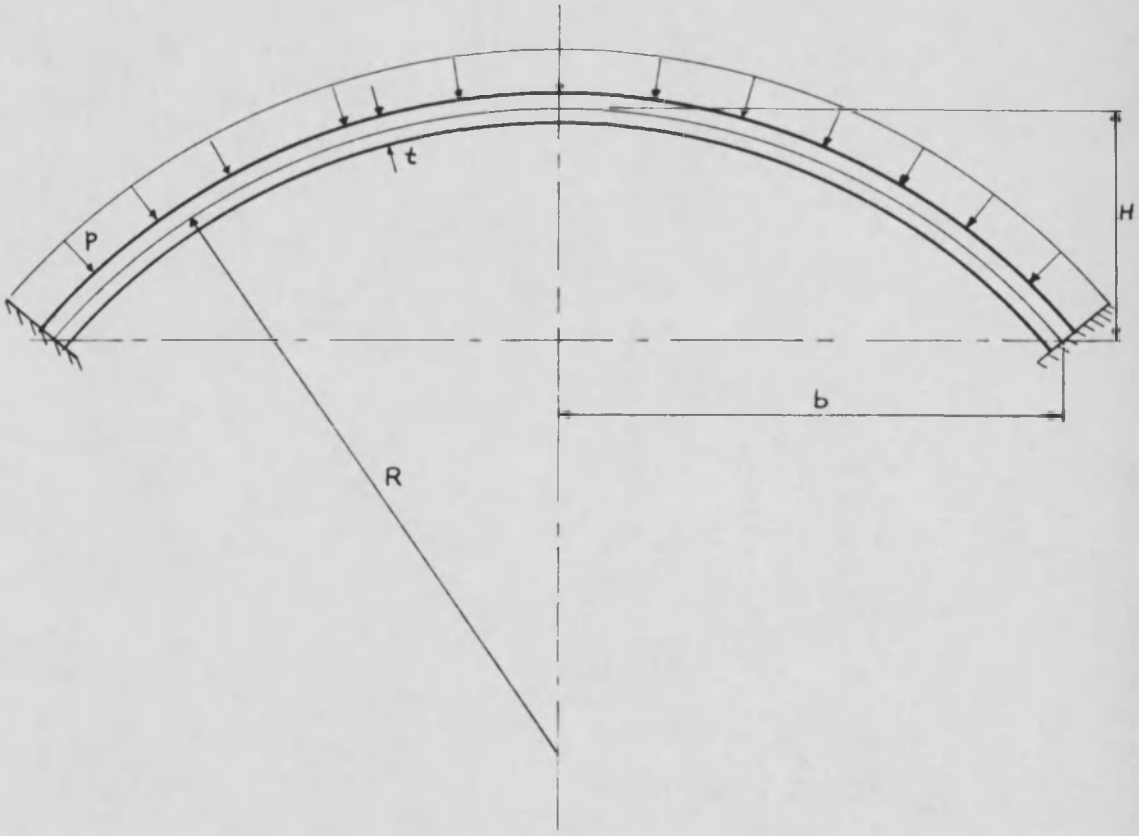

FIGURE 1

Shell Cross Section Showing Notation

t - shell thickness in inches
R- radius of curvature of the middle surface in inches
H- rise of the shell from the base plane to the apex in inches
b - radius of the base plane in inches
p - pressure in pounds per square inch

until the critical buckling pressure is reached. Practically speaking, initial geometrical imperfections in the complete shell and changes in the radius due to membrane strains permit bending to start immediately upon the application of pressure. As a consequence, experimentation shows that buckling pressures of complete shells are generally lower than the theoretical buckling pressures for ideally perfect shapes under the usual assumptions.

Spherical caps may distort axisymmetrically out of shape at the beginning due to the application of pressure. In this manner the pressure may make its own "initial" imperfections in addition to the geometrical ones which may already be present. However, it does not necessarily follow that the lowest buckling pressure is related to an axisymmetrical buckling situation. There exists the possibility of an instability associated with unsymmetrical distortions which may occur prior to the reaching of the axisymmetrical buckling. It is also possible that the unsymmetrical initial imperfections might have a more significant effect than the axisymmetrical ones.

As Archer[1] explains the buckling criterion, it is assumed that a given state of equilibrium becomes unstable when there are equilibrium positions infinitesimally near to that state of equilibrium for the same external load. To obtain a solution, it is necessary

to obtain the pressure-deflection relationships for a given problem and to interpret properly the buckling pressure according to the above criterion. In the work of Simons,[2] the center deflection to pressure relationship is generalized by interpreting buckling from a maximum deflection to pressure relationship in order to reveal the buckling in cases where the deflection modes become more involved.

Another explanation of the buckling of spherical caps is that of von Karman, Dunn, and Tsien.[3] They consider the case of a curved bar under the action of a single concentrated load P at the center with the ends laterally restrained as shown in Figure 2. Starting from the undeformed position, P is gradually increased, and a symmetrical type of deflection is assumed. During this initial stage the bar behaves in a manner similar to that of a straight beam under the action of a concentrated load. That is, the load increases with the center deflection. However, large deflections in a curved bar with fixed ends produces a shortening of the centroidal axis and consequently an increase in compression. This is contrary to the case of a straight beam with fixed ends where large deflections produce tension. A beam under end compression is much weaker in sustaining a lateral load than one without end compression. In fact, when the end compression in a straight beam reaches the Euler load,

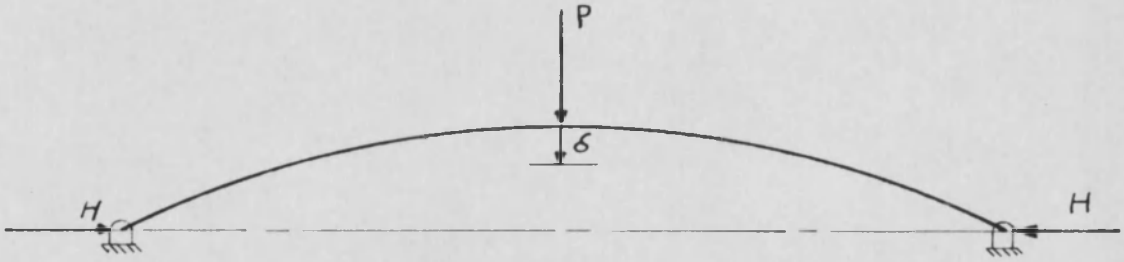

FIGURE 2

Curved Bar

the beam loses all its ability to sustain a lateral load. This general property applies also to curved bars. Thus, with increasing compression in the bar due to an increasing deflection at the center, the effective rigidity of the bar to sustain the lateral load P is gradually reduced. In other words, the slope of the load versus deflection curve decreases with increasing deflection. Thus, as the load P is increased, a point will be reached where the slope is zero. Therefore a maximum load P is obtained.

Beyond this point the load P will decrease with increasing deflection. That is, this part of the load versus deflection curve indicates that the structure is unstable. If the material is elastic, this instability will continue until the actual shape of the bar has a curvature opposite to that of the undeformed bar. In other words, if the undeformed bar is curved downward, the bar has to be deformed so far as to curve upward before the decreasing process of the load stops. The reason for this phenomenon can be explained by the change in the end compression in the bar. Once the curvature of the bar is reversed, then the increase of the deflection will decrease the compression in the bar. This decrease in the end compression will increase its ability to carry lateral loads.

For slender bars the situation is further complicated by the appearance of an anti-symmetrical type of deflection. Marguerre,

as reported by von Karman, Dunn and Tsien,[3] found that when the end compression in the curved bar reaches a value which is four times the Euler load for a straight bar, an anti-symmetrical deflection appears together with the symmetrical one. In the load-deflection curve, Figure 3, the loading will start from the origin and follow the curve corresponding to a symmetrical deflection up to point A_o. Then the anti-symmetrical component sets in, and the bar follows the straight line to point B'. From then on, the deflection of the bar is symmetrical. In a testing machine, the bar will actually "jump" from point A_o to some point C, depending upon the rigidity of the machine, with violent vibration due to a sudden release of energy.

It is evident the load-deflection relationship is highly complicated and not linear. The buckling phenomenon may occur completely within the elastic range. The load-deflection relationship for the structure is nonlinear even though the stress-strain relationship for the material is linear.

Consider now a spherical shell under external pressure with clamped edges as shown in Figure 4. The action is similar to the curved bar. Assuming that the bending stiffness, which is proportional to the cube of the thickness, can be neglected, the strain energy consists only of the energy due to extension or

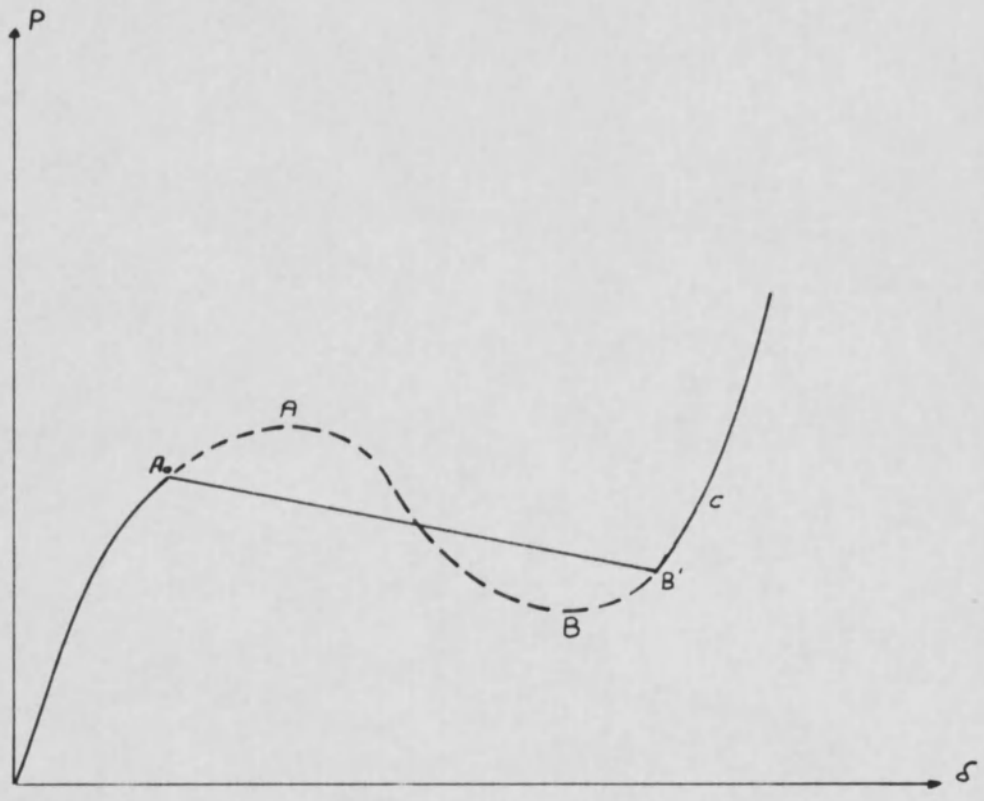

FIGURE 3

Load-Deflection Curve

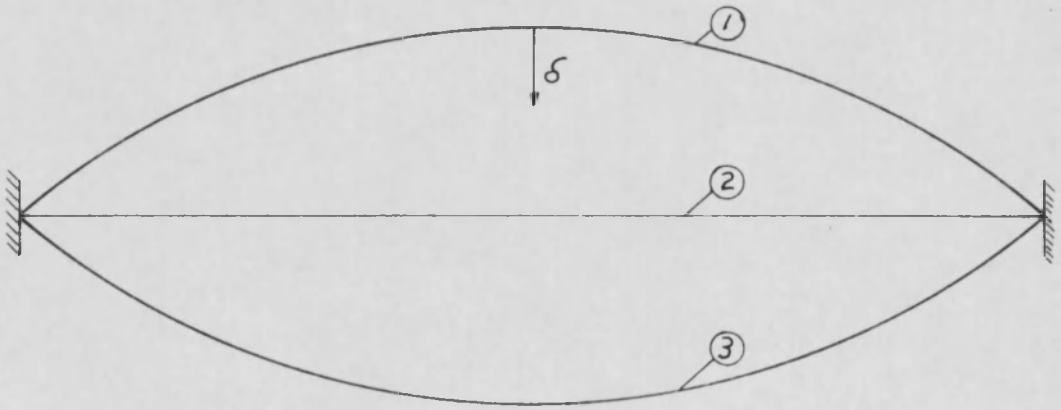

FIGURE 4

Spherical Shell Cross Section

compression of the shell. The strain energy is zero in the deflection position 3, if it is zero in the undeflected position 1. It is in equilibrium in position 3 without the aid of external pressure.

Above position 2, the intermediate positions involve compression of the shell. The shell can be held in equilibrium in these positions only by an external pressure. However, as with the curved bar, the compression in the shell elements tends to reduce its pressure-carrying ability. Thus, if only a rotationally symmetrical type of deflection is considered, the initial part of the pressure versus maximum deflection curve again has a decreasing slope with increasing deflection. When the deflection goes beyond position 2 and above position 3, a negative external pressure is necessary to maintain equilibrium as the compressed elements tend to force the shell to take the equilibrium position 3. The pressure-deflection curve under the assumption of negligible bending stiffness and symmetrical deflection is of the form of curve A_1, of Figure 5. The effect of the bending stiffness is to increase the positive external pressure necessary to hold the shell in equilibrium. In other words, the pressure-deflection curves with increasing bending stiffness are of the form of curves A_2, A_3, etc.

With an anti-symmetrical type of deflection in a spherical cap, the instability might occur before the peak is reached, as in the

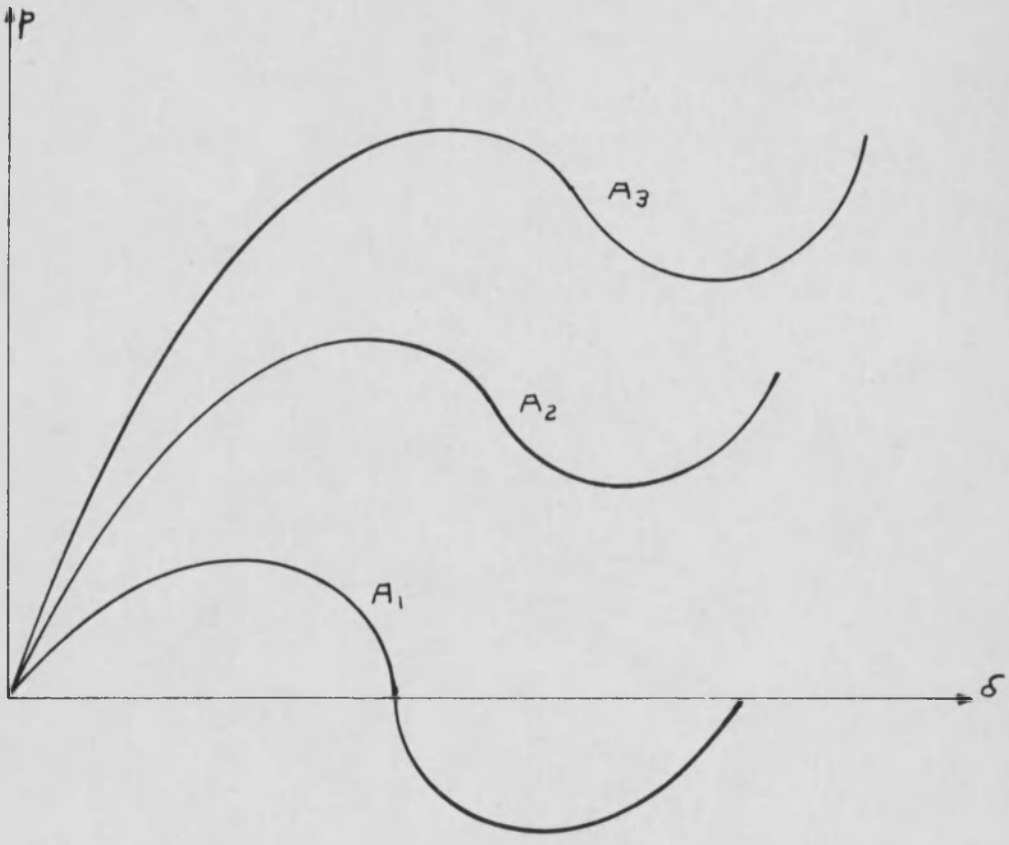

FIGURE 5

Pressure-Deflection Curves

curved bar. Furthermore, without care in the laboratory, the "jump" might occur as with the curved bar. In any event, the load-deflection curve is not a straight line and has an unstable portion within the elastic range.

The investigation of nonlinear buckling of thin spherical caps under uniform pressure had its beginnings immediately prior to World War II through the investigation of von Karman and Tsien.[4] This theory was based upon energy criteria for determining buckling loads. Archer[1] used a similar set of equations that were solved by means of a perturbation technique. Simons[2] solved the nonlinear equations by means of a power series. A numerical procedure employing finite differences was formulated by Keller and Reiss.[7] Solutions by power series were made by Reiss, Greenberg and Keller[8] as well as by Weinitschke.[9,10] Murray and Wright[11] proposed a theory based on power series expansion to circumvent the singularity at the initial boundary and then a step-by-step integration procedure. Other theories have been developed, but these generally follow one of the above mentioned approaches.

Many investigators make note of discrepancies between various theories. Since there is more than one way to develop a theory, either through energy minimization, power series, perturbations, wave action, linearization, to name a few, it is not

particularly surprising that the results are in some disagreement. It is noted that each of these procedures, of necessity, contains some simplification so that the problem can be solved.

What also seems significant is the lack of agreement between experimental results and developed theories. This is of great concern since any actual shell construction or fabrication might be expected to conform more closely to well conducted experimental results rather than certain theoretical ones. Those who have developed the various theories have noted these discrepancies and have suggested plausible causes for the lack of agreement. Some of these reasons include initial imperfections, such as thickness or curvature variations, a failure to achieve full fixity around the edge, or a failure to meet some other initial assumption of idealized behavior. This then raises the question as to whether an ideal shell can actually be achieved. If it cannot, then the theories are at best a guide and, depending upon the simplifications, few can be expected to yield accurate results.

The purpose of this paper is to approach the problem through the experimental route. A statistically sufficient number of models was constructed and tested. Shells with different radii of curvature were included to determine the effect of the assumption of shallowness, which most of the theories demand. There are no

assumptions of ideal conditions; thus the results should indicate realistic behaviors rather than idealized ones.

It is hoped that the techniques developed may be applied to more complex situations with confidence as a result of the success of this investigation.

CHAPTER TWO

REVIEW OF LITERATURE

The purpose of this chapter is to summarize a few of the significant publications on the buckling of clamped spherical caps. Appendix A discusses the theories in somewhat greater depth.

Apparently, the first theoretical publication on the buckling of clamped spherical caps under a uniform load was that of von Karman and Tsien.[4] An expression for the total energy was developed, with certain assumptions, and this expression was minimized. This yielded the minimum buckling load which is that load required to keep the shell in a deflected shape. By modifying the strain energy expression to include the effects of uniform compression prior to buckling, the authors again obtained the lower buckling load. In addition they discussed an upper buckling load which is the highest value on the load-deflection curve. The necessity of extreme care in the experimental determination of the upper value was pointed out.

A subsequent publication by Friedrichs[5] discussed the vertical deflection assumption made by von Karman and Tsien.

Friedrichs found that the influence of this assumption was to double the buckling load.

Tsien[6] later modified the original theory to account for the findings of Friedrichs. He obtained a somewhat different value for the minimum value of the buckling stress. A later publication by Tsien[12] discussed the lower buckling load and how it may differ from what has previously been observed.

Chien[13] developed a theory which did not require all of the assumptions of the von Karman-Tsien theory. This led to fundamental equations for the determination of the buckling pressure of a small segment of a spherical shell. The neglecting of two terms in the equation yielded the same equation as that of von Karman and Tsien.

Reissner's[14-17] major contribution to this subject involved the development of general equations. Starting with the Marguerre equilibrium equations, he obtained equations for stresses and displacements as well as strain quantities. Reissner also developed equations for the symmetrical bending of thin elastic shallow shells.

The experimental work of von Kloppel and Jungbluth, on non-shallow shells, as reported by Reiss,[18] indicated the buckle formed near the boundary rather than the symmetrical case which

is generally assumed. Initial stresses and thickness variations were felt to be the cause of the unsymmetrical situation.

Simons[2] used the equations developed by Reissner[14] and a series solution to obtain a buckling criterion. His conditions indicated that instability cannot occur for a flat plate nor for a shell which is very shallow. He determined a critical load parameter in terms of Poisson's ratio. This load parameter is a function of the uniform pressure. There was a lack of agreement between the theory of Simons and the results of Kaplan and Fung.[19]

Reiss has contributed several publications to the field, both as a sole author,[18,20] and in conjunction with Greenberg and Keller.[7,8] Using different loading and geometric parameters, he uncovered modes of buckling in the theory of Kaplan and Fung.[19] This led to a better correlation between the theoretical and experimental results of Kaplan and Fung. Using the equations developed by Chien,[13] a theory was developed which yielded critical buckling pressures which verified the previously mentioned buckling modes. A linearized theory was reported in a different publication,[18] which indicated similar buckling modes. In comparing his theories to experimental results of others, Reiss noted fair agreement and attributed the discrepancies to initial imperfections, difficulties in measuring the radius of curvature in shallow shells, a small

experimental error in determination of the geometric parameter leading to a large error in the buckling pressure, the shallow shell assumption and the failure to achieve a completely clamped edge condition. Reiss indicated the need for additional experimentation.

Klein[21,22] attempted to reduce the scatter between experimental and theoretical results through the use of an eccentricity parameter. This parameter was a function of both initial thickness and curvature variations.

Archer[1] worked with the equilibrium equations developed by Reissner[14] and a power series solution to determine a buckling criterion and a critical buckling pressure. Comparison with the works of Kaplan-Fung[19] and Tsien[6] was satisfactory at particular points, but not throughout the range of the geometric parameter. Archer attributed the discrepancy to the "jumping" of the shell during testing.

The approach of Weinitschke[9,10] was through the equations developed by Reissner,[14] power series, and an iterative technique on a digital computer. He indicated agreement between his work and previous theoretical results for low values of the geometric parameter, that is, for very shallow shells. The lack of agreement with previous experimental results was attributed to initial discrepancies. In a different publication,[23] Weinitschke supports

Klein[22] in his claim that initial irregularities are responsible for the scatter between theory and experiment.

Von Willich[24] derived energy equations and then used an application of the principle of minimum potential energy to obtain the critical buckling pressures. He solved the problem only for small values of the geometric parameter.

Budiansky[25] began with the equilibrium equations of Reissner.[14] Simplifications were made, and the use of operators and transformations yielded two integral equations. These equations were solved numerically by an iterative technique which yielded values of critical buckling pressure in terms of the geometric parameter. Budiansky also developed a theory based on initial imperfections. The procedure was the same as previously mentioned for the shell with no initial imperfections. This again yielded values of critical buckling pressure in terms of the geometric parameter.

A publication coauthored by Budiansky and Weinitschke[26] indicated their stability curves were in agreement despite the differences in the two independent theories. A lack of agreement with the Kaplan-Fung[19] results was noted.

Experimental work by the Avco Corporation, carried out by Homewood, Brine and Johnson,[27] resulted in buckling pressures for caps of various radius-thickness ratios. They found no important

differences in buckling characteristics between shallow and non-shallow caps. The buckling occurred abruptly and the majority of the buckles remained when the pressure was released. The shells were hot rolled steel which were formed by spinning. A later publication by Johnson and Homewood[28] indicated work on forming plastic shells by a vacuum snapback technique.

Grigolyuk[29] worked with the Marguerre equilibrium equations, a power series expansion, and Bubnov's method to obtain two nonlinear equations. Solution of these equations yielded the expression for the critical buckling pressure.

Nash and Modeer[30] developed a theory for the buckling of clamped, uniformly loaded spherical caps by two different approximations. The first neglected the second invariant of the middle surface strains, while the other retained only the linear terms in the second invariant. The approach was based on minimizing the total energy expression. The advantage of either of these assumptions was that the governing nonlinear equations were uncoupled.

Murray and Wright[11] developed a theory by a step-by-step integration of the differential equilibrium equations. They eliminated many of the usual assumptions and claimed a higher accuracy. For a specific radius of curvature and thickness, the upper buckling load as well as the minimum one was obtained. Comparison with the

von Karman-Tsien[4] results indicated a difference by a factor of two. It was concluded that the results of the Rayleigh-Ritz solution by von Karman and Tsien did not satisfy equilibrium. Good agreement was obtained in comparing their results with those of Keller and Reiss.[7] However, these results did not agree with the Kaplan-Fung results.[19]

Thurston[31] began with the Reissner[14] equilibrium equations and obtained a final solution by assuming an approximate solution and then solving for a correction, thereby obtaining upper and lower buckling curves. The upper curve agreed with Weintschke[9] and Budiansky[25] while the lower curve agreed with the Keller-Reiss[7] results. The Kaplan-Fung[19] experimental results were between the two curves.

Gjelsvik and Bodner[34] developed a theory for the nonsymmetrical snap buckling of uniformly loaded clamped spherical caps. They used an energy minimization procedure to determine an upper buckling load and an energy load for both the symmetrical and nonsymmetrical cases, that is, with or without consideration of the effects of the boundary layer. The energy load corresponds to a minimum or lower buckling load. They also developed an expression for the minimum value of the geometric parameter at which snap

buckling can occur. Their work is limited to shallow caps where the ratio of the rise of the shell to the radius of curvature is 1/8 or less.

CHAPTER THREE

EXPERIMENTAL INVESTIGATION

This chapter contains the description of the author's experimental investigation. The first part is concerned with the determination of the best technique for forming spherical caps with a vacuum former. The second part consists of the results obtained from the buckling test of each shell as well as a description of these tests.

Forming Technique

In an investigation of this type, it is necessary to fabricate many nearly identical shells. A vacuum former is ideally suited since many shells can be formed rapidly at a minimum expense. Of even greater importance is the knowledge that each shell formed will be similar to its predecessor, assuming there has been no change in the machine settings.

The operation of the vacuum former is to heat the material and then to form the plastic to the desired shape by means of the vacuum. There are many variations which enter into the forming technique such as the decision of whether to use a concave or convex

mold, the mold material, the shell material, the amount of heat, whether to allow the material to partially form to the shape of the mold before the application of the vacuum, as well as others. For this investigation, it was decided to use an aluminum mold, in part because of the ease of machining in forming the other mold shapes. The shell material, chosen because of its reported good thickness tolerances and properties, was a polyvinyl chloride, Boltron 6200 Normal Impact Type 1, obtained in sheets from the General Tire and Rubber Company. Each sheet was approximately 30 by 60 inches.

Five different shapes were considered in this investigation. The radius of the base plane of the mold was kept constant and the radius of curvature varied by decreasing the rise of the shell above the base plane. Figure 6 is a sketch showing the five formed shapes with the corresponding values of radius of curvature and rise.

The forming technique was determined by working with the shell with the greatest curvature, that is, the hemisphere. When the best technique was developed, all subsequent shells were formed with a similar procedure, not only for the hemisphere, but for all shells formed.

The shell forming operation is illustrated by Figures 7, 8, and 9. In Figure 7, the mold with the collar attached is shown

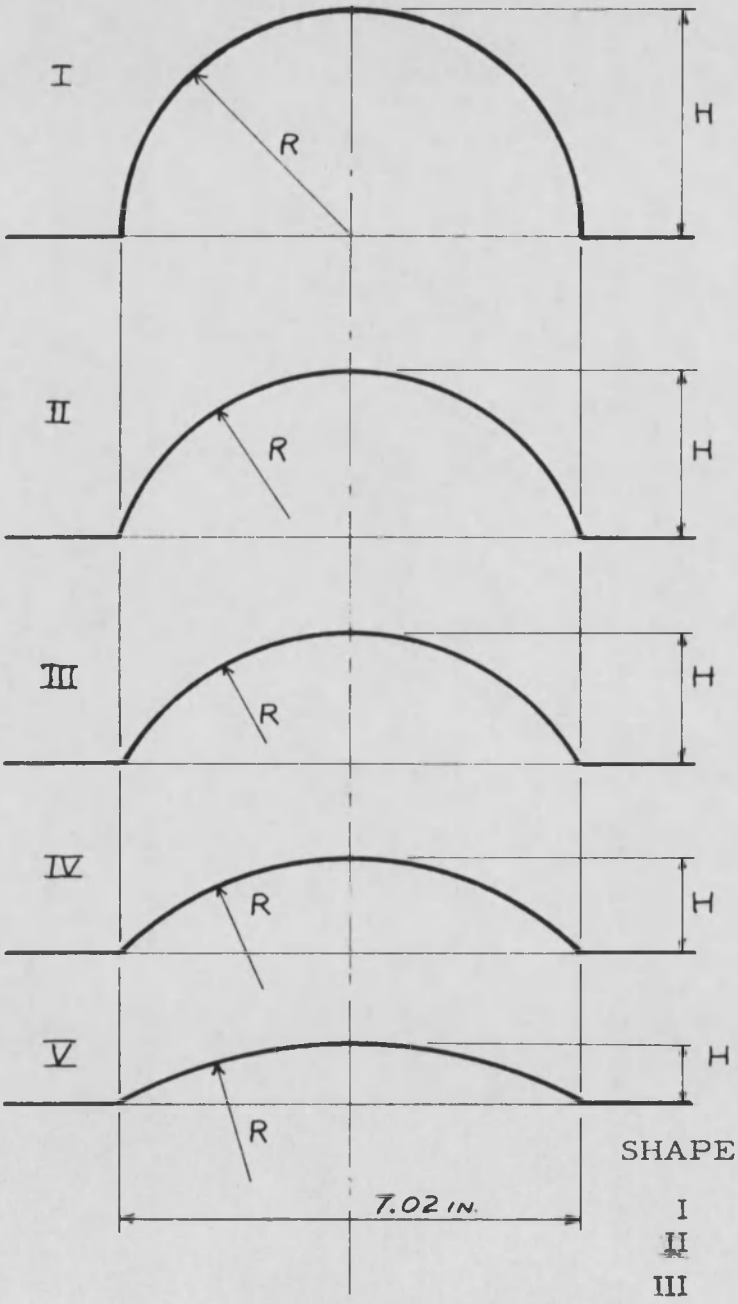

SHAPE	R in in.	H in in.
I	3.51	3.51
II	3.78	2.65
III	4.21	2.12
IV	5.33	1.53
V	9.64	0.96

FIGURE 6

Geometry of Formed Shapes

FIGURE 7

Forming Mold in Vacuum Chamber

FIGURE 8

Vacuum Former with Heating Element Forward

FIGURE 9

Formed Shell in Frame of Vacuum Former

sitting on top of the platform in the vacuum chamber. Figure 8 shows the former with the heating element forward heating the plastic prior to the actual forming. When the heating cycle is completed the heating element returns to the rear position and the frame holding the heated plastic moves down over the mold. The final forming is accomplished by applying the vacuum. Figure 9 shows the formed shell in the frame of the vacuum former. Figure 10 shows the five different shapes which were formed and Figure 11 shows the array of shells which were formed for the buckling tests.

The variables of the vacuum former which can be varied during the forming operation are:

1. percentage of time the heating element is on
2. length of time the heating element is over the plastic
3. height of the stops which control the distance the frame comes down
4. distance of the mold platform from the machine base
5. amount of vacuum

Several tests were run to determine the combinations which yielded the best shells. To compare forming techniques, the radius of curvature and thickness were measured at twenty-five grid points on the shell as shown in Figure 12.

FIGURE 10

The Five Different Formed Shapes

FIGURE 11

Formed Shells for Test Program

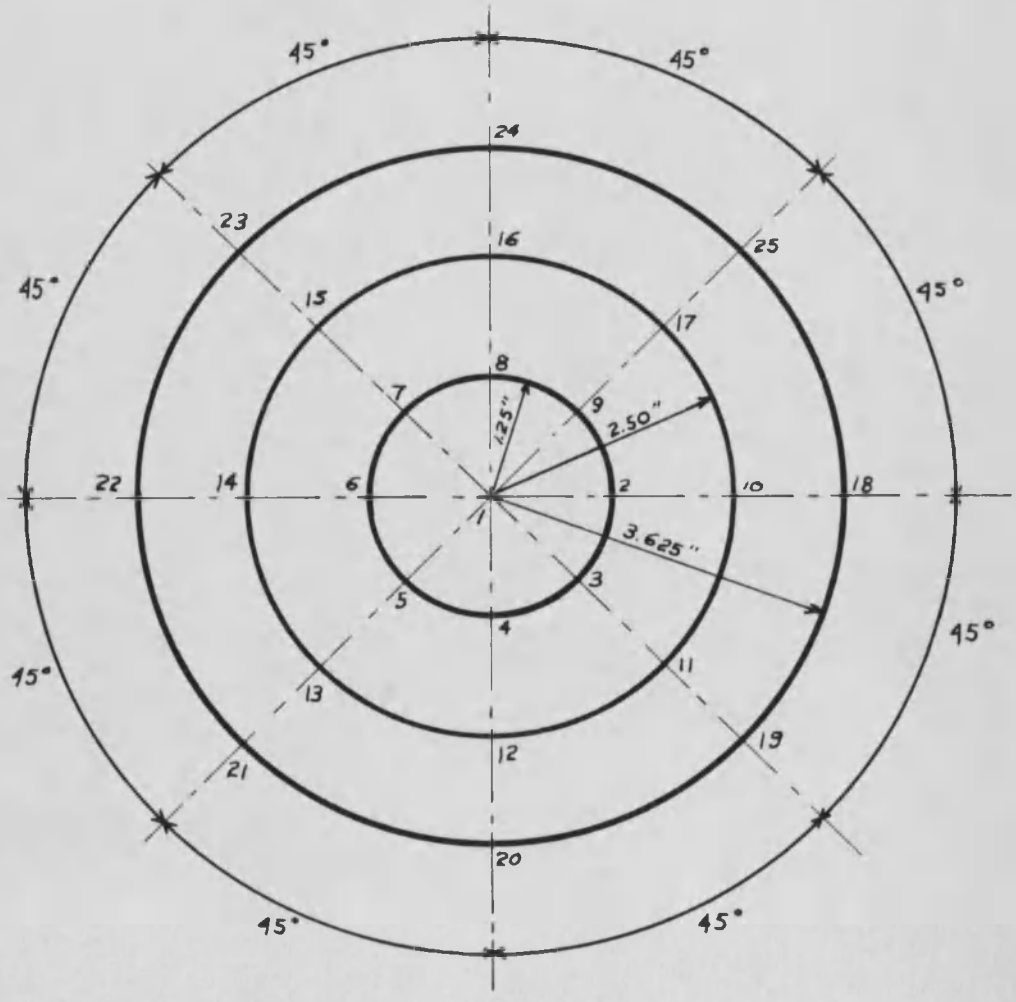

FIGURE 12

Grid Points on Shell

The radius of curvature was measured by the device shown on the left in Figure 13. The three points, two fixed and the third attached to the dial gage, were placed on the shell surface and the minimum gage reading recorded. The radius of curvature of the middle surface of the shell was then $R = \frac{g}{2} + \frac{1}{8g} - \frac{t}{2}$, where R is the radius of curvature, g is the gage reading and t is the thickness of the shell at that point.

The thickness was measured by the device shown on the right in Figure 13. The apparatus was held in a vise and the shell placed between the point on the frame and the pointer attached to the dial gage at the position where the thickness was desired. For each point, the shell was rotated until a minimum dial reading was obtained. This reading was the normal thickness at the point in question.

Average values and standard deviations of thickness and radius of curvature were computed for each forming technique and are included in Appendix C.

Because it is desirable to have the models of uniform thickness and curvature, various techniques of forming were investigated. It was not difficult to obtain consistent curvatures because the formed plastic adhered very closely to the mold which had been machined to a hemispherical shape. However, keeping the

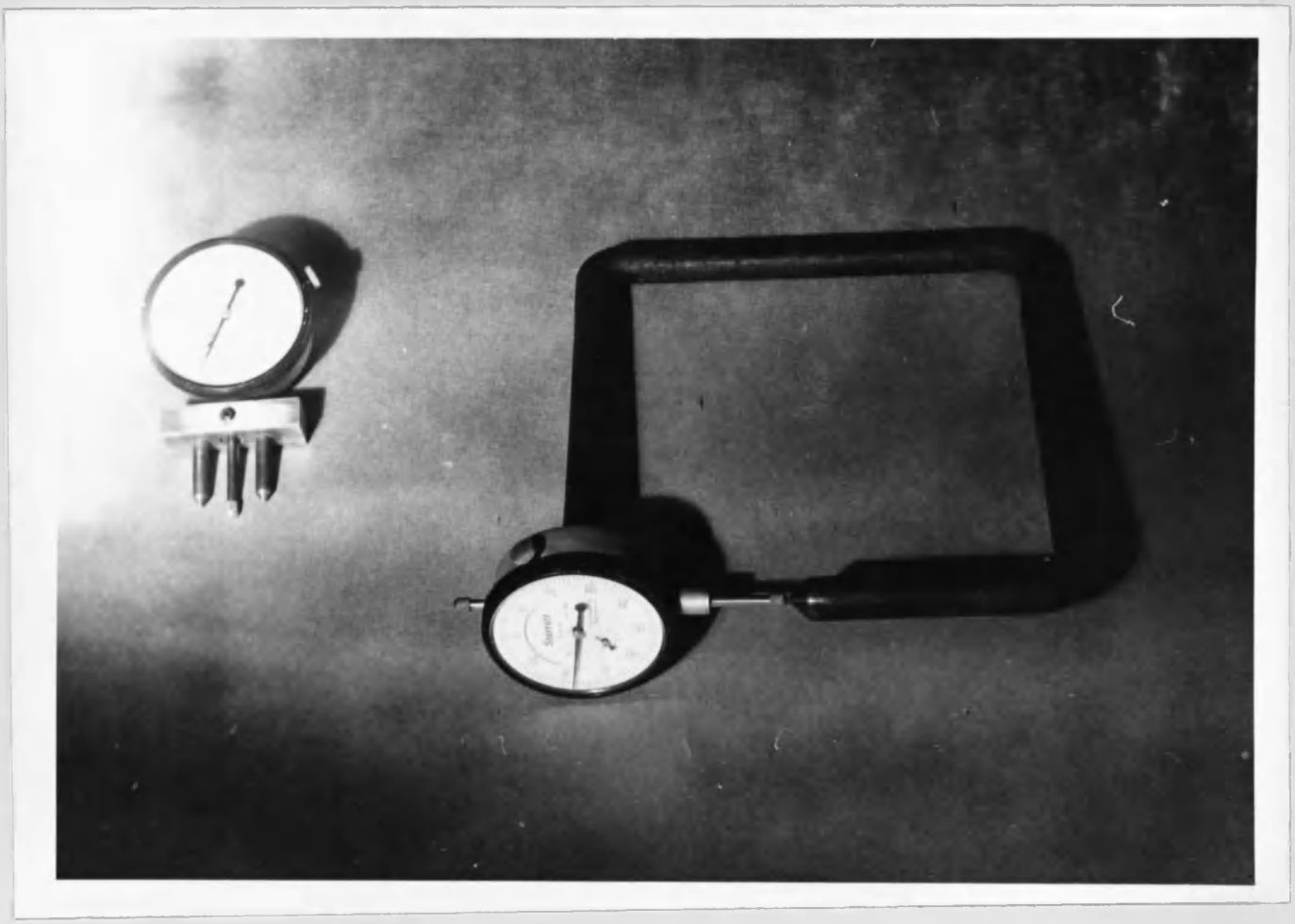

FIGURE 13

Measuring Devices

thickness constant represented a more difficult problem. In each of the formings, the shell was thickest at the peak and thinnest at the base of the mold. Several combinations of the variable settings were attempted to obtain a minimum thickness variation.

It became apparent that a short heating cycle and a low "percent on" of the heating element resulted in less flowing of the plastic during the draping of the plastic over the mold. Using the heat on 35% of the time with a heating cycle of 50 seconds resulted in the least amount of thickness variation.

The elevation of the platform holding the mold above the machine base had an effect upon the thickness variation. The higher the mold the more the drape, and this larger drape caused a thinning out of the plastic near the base of the mold thus resulting in larger thickness variations. Hence, a lower platform elevation was decided to be advantageous. There was a minimum value for this elevation, because too low a setting required more draw for a sharp edge at the shell boundary than could be accomplished during the vacuum operation. An elevation of 5.33 inches above the base of the machine was an acceptable compromise.

The collar between the platform and the mold had two purposes. It provided an edge for the clamping of the shells during the buckling tests, and it allowed for a lower setting of the

mold platform. Without the collar, it was necessary to use a higher platform setting to obtain a sharp draw between the shell and the mold platform.

The height of the stops, which controlled the amount that the frame holding the plastic moved down, was important since a good air seal was necessary between the plastic and the top of the vacuum chamber. This was determined by a trial and adjustment procedure.

Application of the vacuum was another important operation. Of the several variations in the vacuum technique attempted, it appeared the thickness variation was a minimum when the vacuum was applied as the plastic moved down toward the mold after the heating cycle. The vacuum was left on until the plastic had drawn as much as possible. The plastic was then allowed to cool before it was removed from the mold and the frame.

In summary then, the best forming technique had these settings:

1. heat on - 35% of the time
2. heating cycle - 50 seconds
3. vacuum time - a burst of about 10 seconds beginning as the plastic moved down toward the mold
4. platform elevation above the machine base - 5.33 inches

5. mold - sitting on top of a collar on the platform

Testing of Shells

The buckling of each shell was accomplished by placing it in a test chamber and applying air pressure to a water chamber. It was the water in the test chamber under pressure which buckled the shell. Figure 14 is a photograph showing the buckling test apparatus before the shell is positioned. Figure 15 shows the shell in position with the tapered collar and brackets in place. The tapered collar is the same collar that was used in the forming technique. The plate on top of the test chamber had a similar taper; thus with the shell in position and the collar attached, a clamped edge condition was achieved.

Two quantities were determined directly from the test on each shell. One was the mercury level in the manometer, and the other was the volume change in the water chamber. The first can be related to pressure and is therefore the critical buckling pressure. The second gives an insight into the buckling action. In addition to these observations, the point on the shell at which buckling occurs was recorded. This allowed for the measurement of the thickness and radius of curvature at the point of buckling using the devices shown in Figure 13.

FIGURE 14

Buckling Test Apparatus

FIGURE 15

Test Chamber with Shell in Test Position

Each shell was tested, and the results of these tests are shown in Appendix D. Table 1 is a summary of these results. Measured quantities such as p the buckling pressure in pounds per square inch, R the radius of curvature of the middle surface of the shell at the point of buckling in inches, and t the thickness of the shell at the point of buckling in inches are listed for each sheet. Table 2 is a summary of the results for each shape.

For each of the shapes formed after the hemisphere, three sheets of the plastic were used. This resulted in the formation of approximately thirty-three shells of each shape. This number of shells and subsequent tests was the result of an examination of the variation of the quantity $p\,(R/t)^2$ for the hemispherical shape. Table 3 shows the average value and standard deviation of this quantity, and Table 4 indicates the value of t_1 which was determined after each sheet of shells was tested. The t_1 is Student's t which is used to compare sample mean values. Values of t_1 are tabulated in most books on statistics in terms of the confidence level and the number of degrees of freedom. t_1 is calculated by the relationship,[32] $t_1^2 = kd^2/S^2$, where k is the sample size, S^2 is the variance and d is the magnitude of the desired bound. A total of fifty-one shells were buckled, but it was seen that t_1 decreased after the third sheet of

TABLE 1

Test Results for Each Sheet

SHEET	NUMBER OF SHELLS	AVERAGE VALUES p in	R in	t in	R/t	STANDARD DEVIATIONS p in	R/t
5	9	4.4	3.57	.023	159	.57	11.0
6	10	5.0	3.53	.025	143	.34	5.6
7	11	5.5	3.48	.025	140	.91	4.5
8	11	5.9	3.47	.025	140	.57	5.4
9	10	3.7	3.53	.021	167	.54	5.4
10	10	4.0	3.78	.024	160	.37	9.5
11	11	5.0	3.77	.025	149	.34	6.7
12	10	4.9	3.78	.026	148	.39	6.8
13	11	4.6	4.30	.028	156	.30	3.9
14	11	4.8	4.19	.028	148	.35	6.7
15	11	4.6	4.13	.028	150	.26	5.8
16	8	3.4	5.41	.032	172	.15	6.4
17	10	3.2	5.28	.031	173	.09	4.7
18	11	3.3	5.32	.031	172	.24	4.5
19	11	1.0	9.64	.031	312	.07	8.8
20	11	1.1	9.64	.031	307	.04	8.7
21	10	1.1	9.64	.032	297	.04	4.4

TABLE 2

Test Results for Each Shape

SHAPE	NUMBER OF SHELLS	AVERAGE VALUES				STANDARD DEVIATION	
		p_{in}	R_{in}	t_{in}	R/t	p_{in}	R/t
I	51	4.9	3.51	.024	149	1.01	12.9
II	31	4.7	3.78	.025	152	.57	9.6
III	33	4.7	4.21	.028	151	.33	6.4
IV	29	3.3	5.33	.031	172	.18	5.2
V	32	1.1	9.64	.032	306	.06	9.7

TABLE 3

Values of $p(R/t)^2$ After Each Sheet Tested of Shape I

SHEET	NUMBER OF SHELLS	AVERAGE psi	STANDARD DEVIATION psi
5	9	11.0×10^4	1.15×10^4
5-6	19	10.6×10^4	1.29×10^4
5-7	30	10.7×10^4	1.57×10^4
5-8	41	10.9×10^4	1.51×10^4
5-9	51	10.8×10^4	1.53×10^4

TABLE 4

Values of t_1 After Each Sheet Tested of Shape I

SHEETS TESTED	NUMBER TESTED	t_1
5	9	.96
5-6	19	1.01
5-7	30	1.02
5-8	41	.99
5-9	51	.98

shells tested. Therefore, about thirty shells of the other shapes were expected to give reliable results.

To determine the relationship between pressure and volume change, intermediate readings were made on some of the shells during the loading. The reading of water level in the water chamber and mercury level in the manometer, which are directly related to volume change and pressure, are in Appendix E. Figure 16 is a typical plot of water level versus mercury level for the shells where these quantities were measured. The curves for the other shells tested are in Appendix E. The point whose coordinates represent the maximum water drop and highest mercury level, that is the total volume change and buckling pressure, was plotted but was not connected to the rest of the points because there was a slight volume change after the buckling pressure had been reached. This was apparently the volume of water that occupied the buckle itself. Due to the nature of the test operation, it was not practical to stop the flow of water from the water chamber to the test chamber at the instant that buckling occurred. Pressure-volume readings were not obtained on Shape V because the total volume change was much smaller than the other shapes.

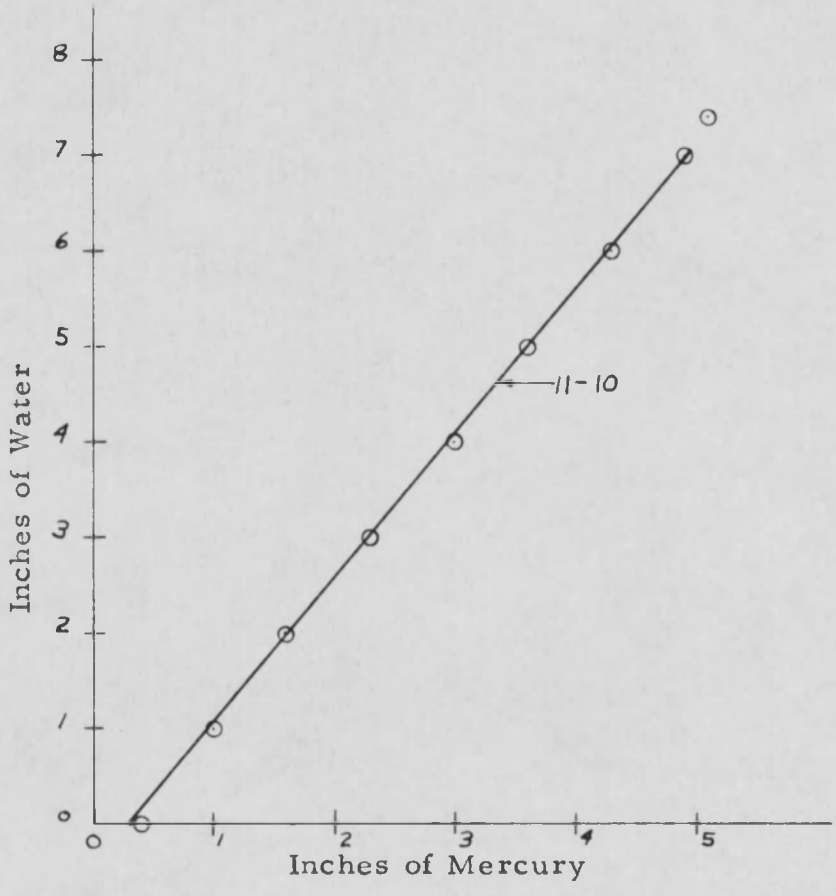

FIGURE 16

Typical Pressure-Volume Curve

The total volume change was measured on all shells. Table 5 is the average volume change in cubic inches of water and the standard deviation for each shape.

Figure 17 is a plot of log p versus log R/t using the experimental results of each sheet tested. Many publications indicate a general relationship of the form $p = A (R/t)^b$ where p is the buckling pressure, R is the radius of curvature, t the thickness and A and b are constants. The curve indicates a linear relationship, within experimental accuracy, between the quantities.

The variation of experimental results within each shape was determined by an examination of the quantity $p(R/t)^2$. Table 6 shows the average value and standard deviation for all shapes. Figures 18 through 22 indicate the frequency and Figures 23 through 27 show the distribution on a probability plot, for each shape, of $p(R/t)^2$.

TABLE 5

Volume Change for Each Shape

SHAPE	AVERAGE VOLUME CHANGE in^3	STANDARD DEVIATION in^3
I	2.6	.90
II	4.3	.95
III	4.1	.52
IV	3.0	.77
V	1.1	.24

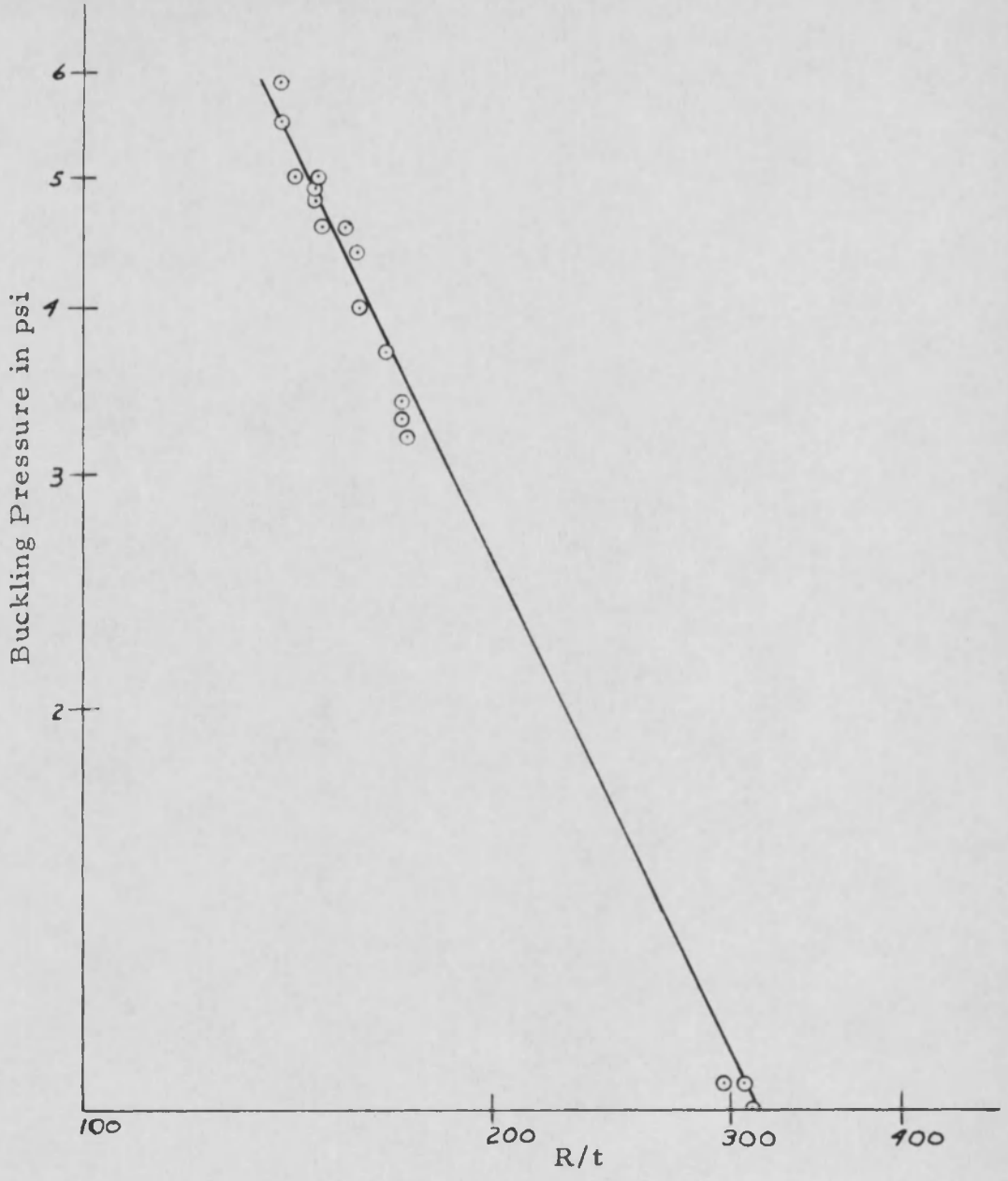

FIGURE 17

Log p versus Log R/t

TABLE 6

Values of $p(R/t)^2$ for Each Shape

SHAPE	AVERAGE VALUE OF $p(R/t)^2$ psi	STANDARD DEVIATION psi
I	10.8×10^4	1.53×10^4
II	10.7×10^4	1.14×10^4
III	10.7×10^4	$.97 \times 10^4$
IV	9.8×10^4	$.62 \times 10^4$
V	10.2×10^4	$.72 \times 10^4$

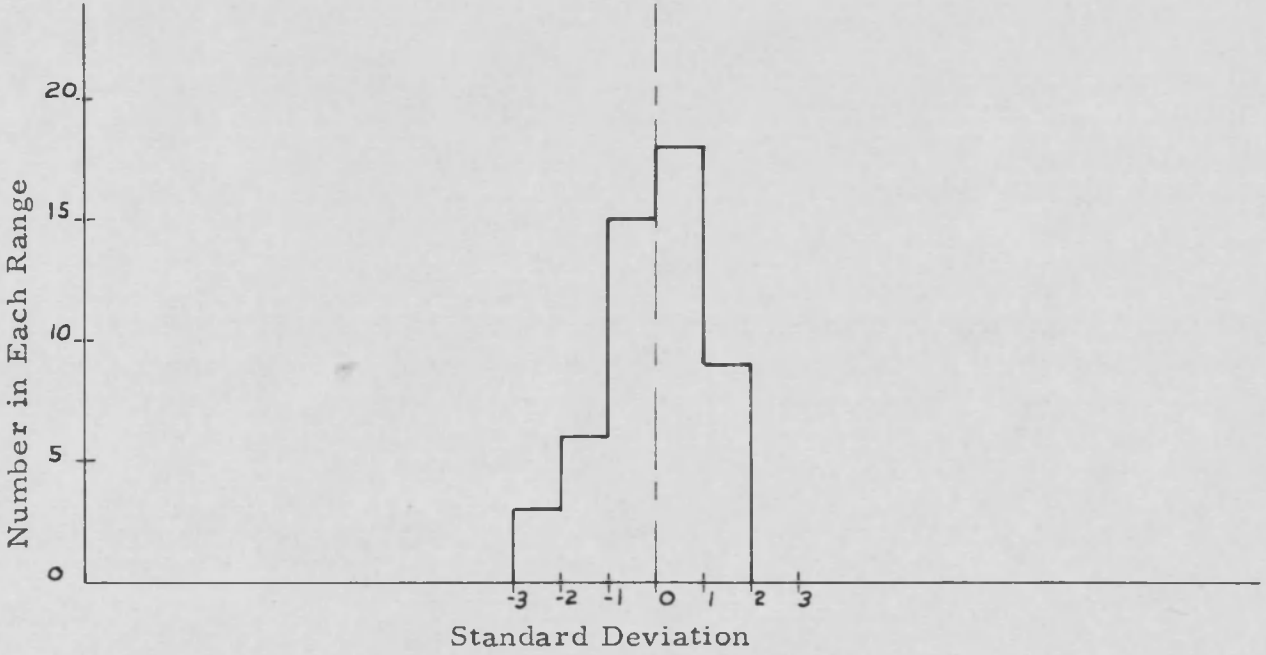

FIGURE 18

Frequency Histogram of $p(R/t)^2$ for Shape I

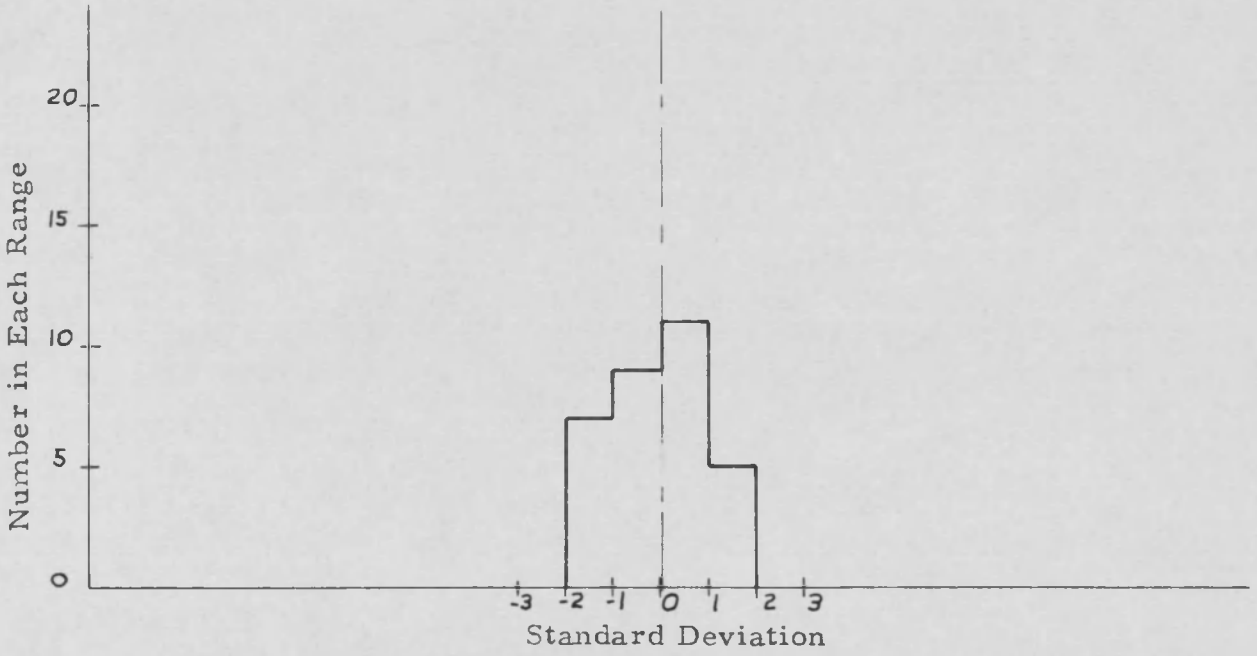

FIGURE 19

Frequency Histogram of $p(R/t)^2$ for Shape II

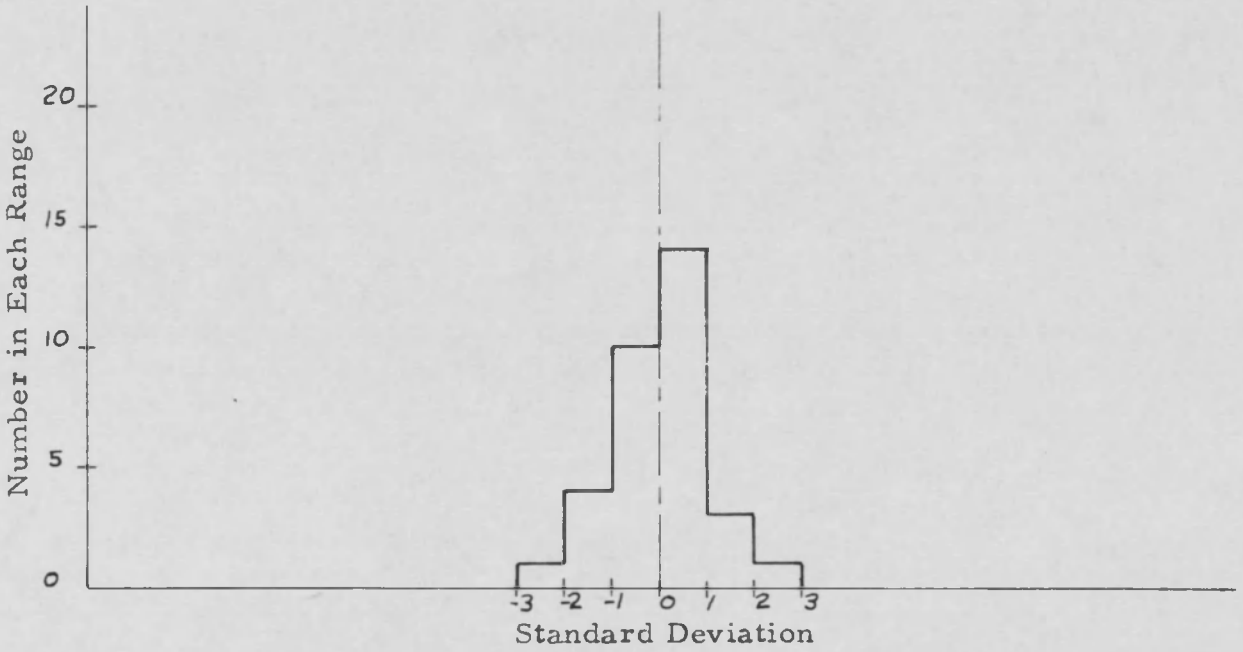

FIGURE 20

Frequency Histogram of $p(R/t)^2$ for Shape III

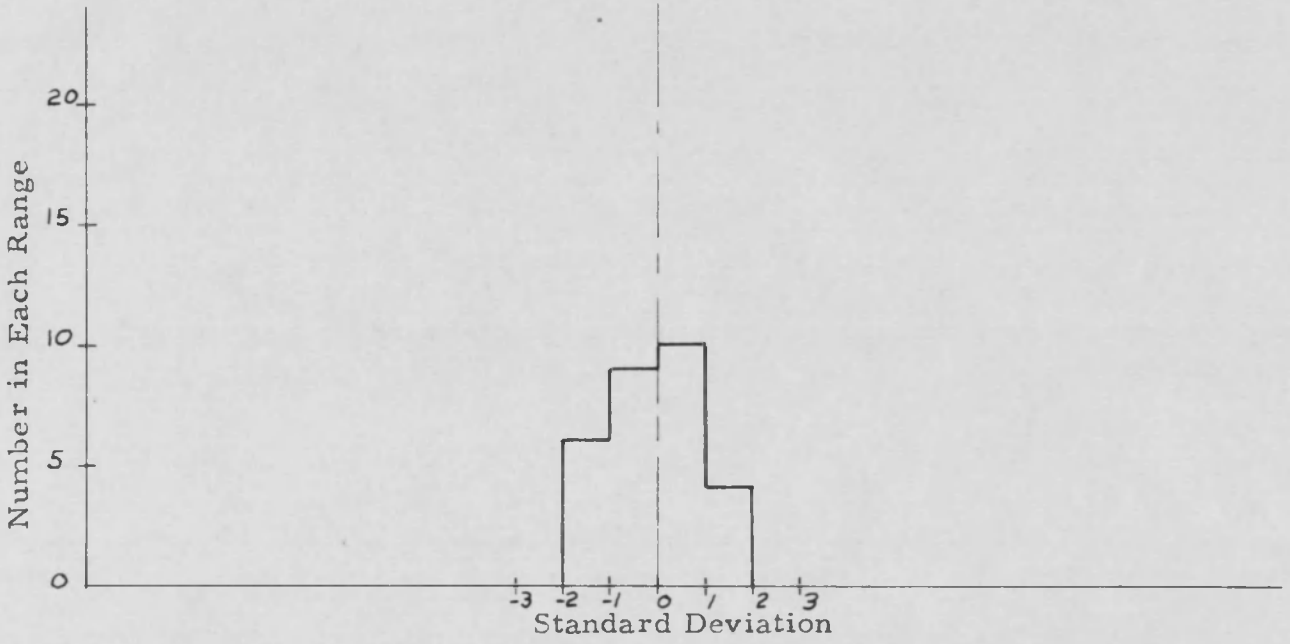

FIGURE 21

Frequency Histogram of $p(R/t)^2$ for Shape IV

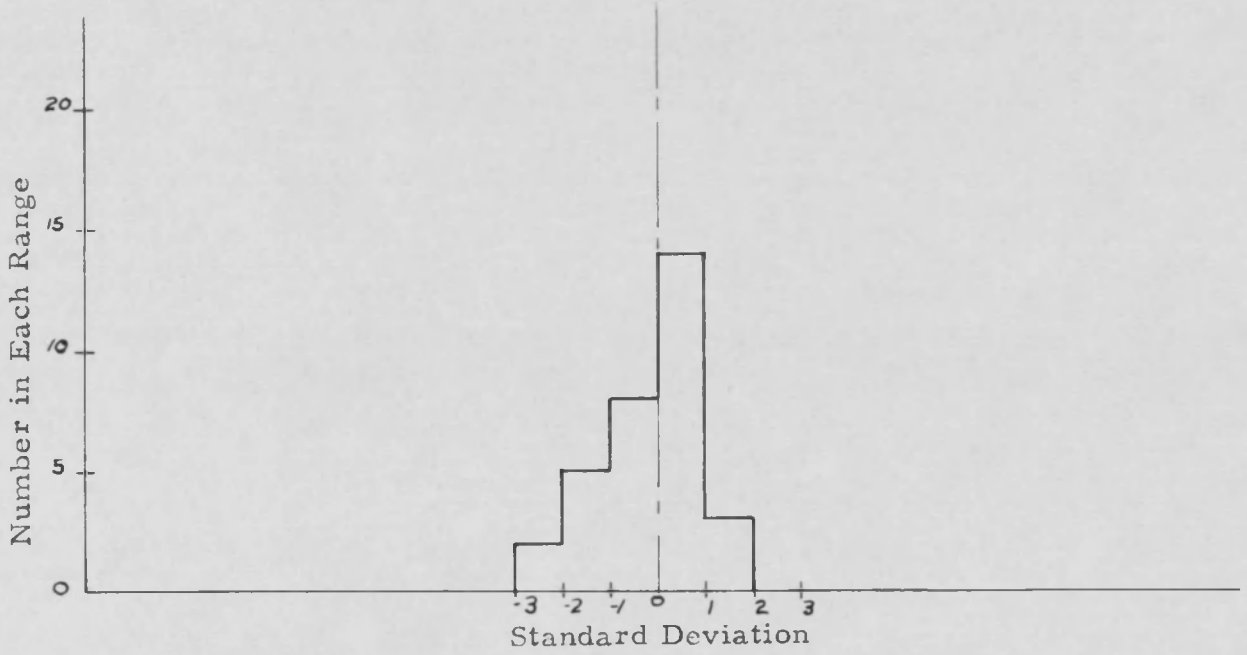

FIGURE 22

Frequency Histogram of $p(R/t)^2$ for Shape V

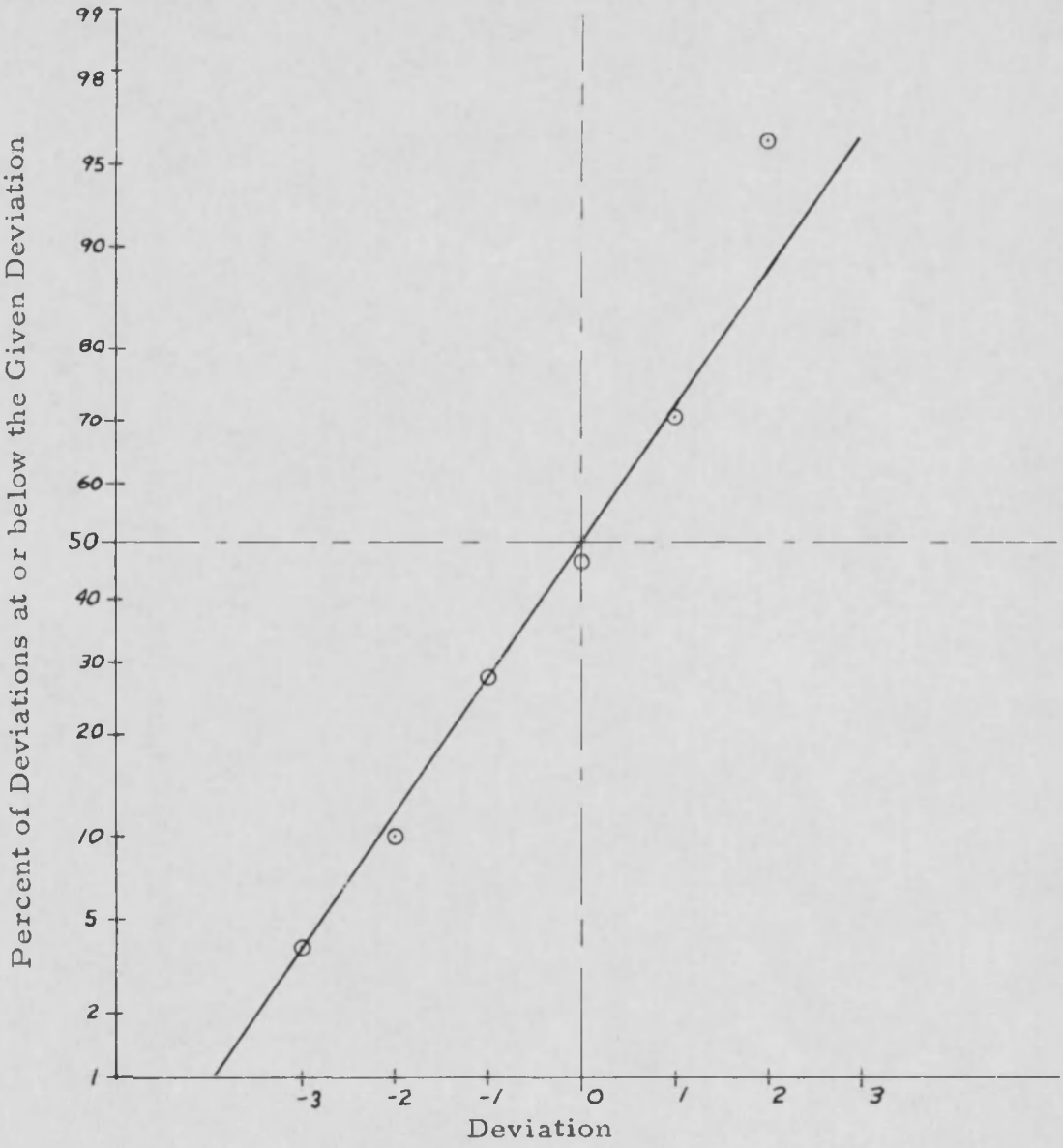

FIGURE 23

Distribution Diagram of $p(R/t)^2$ for Shape I

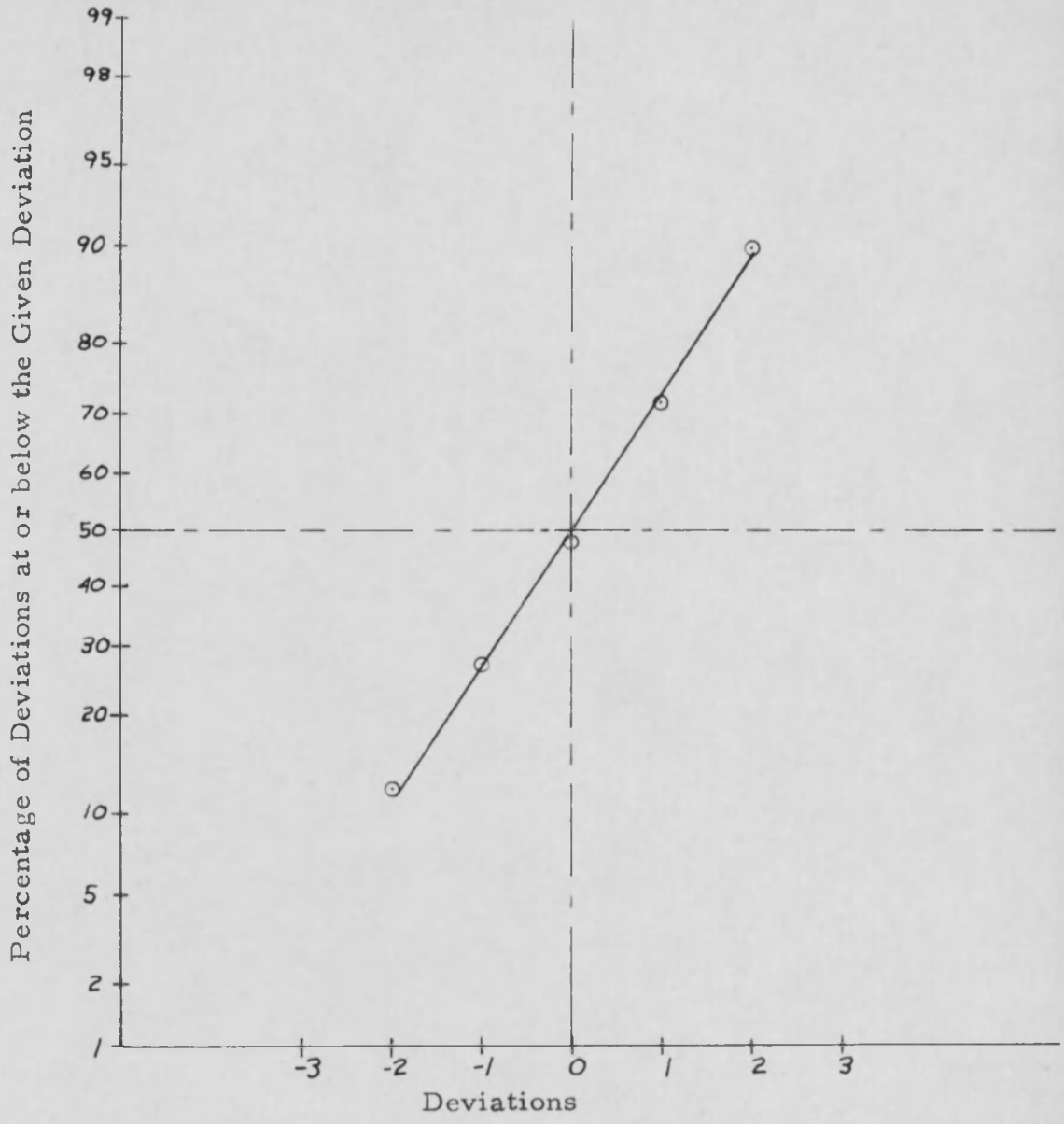

FIGURE 24

Distribution Diagram of $p(R/t)^2$ for Shape II

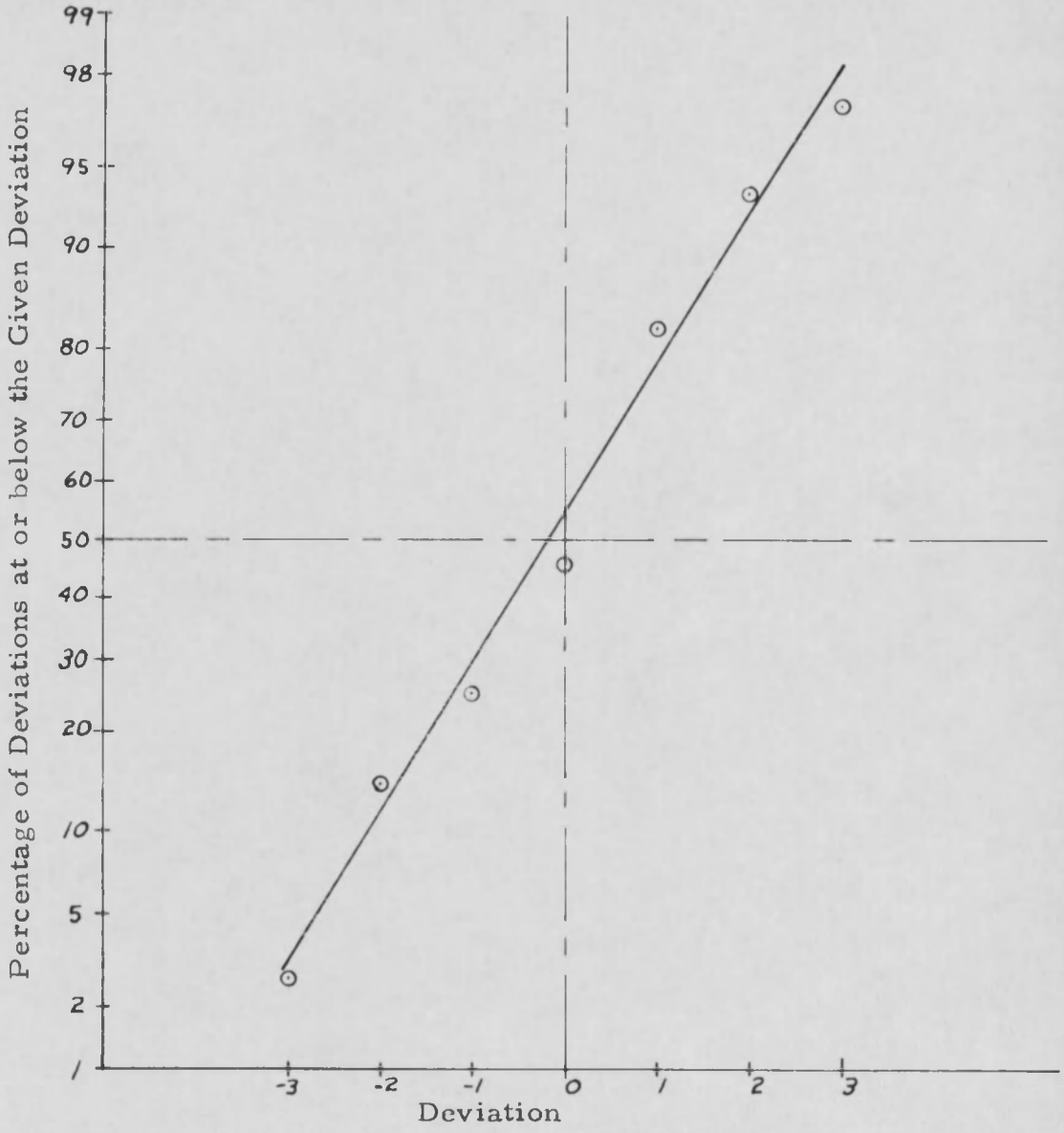

FIGURE 25

Distribution Diagram of $p(R/t)^2$ for Shape III

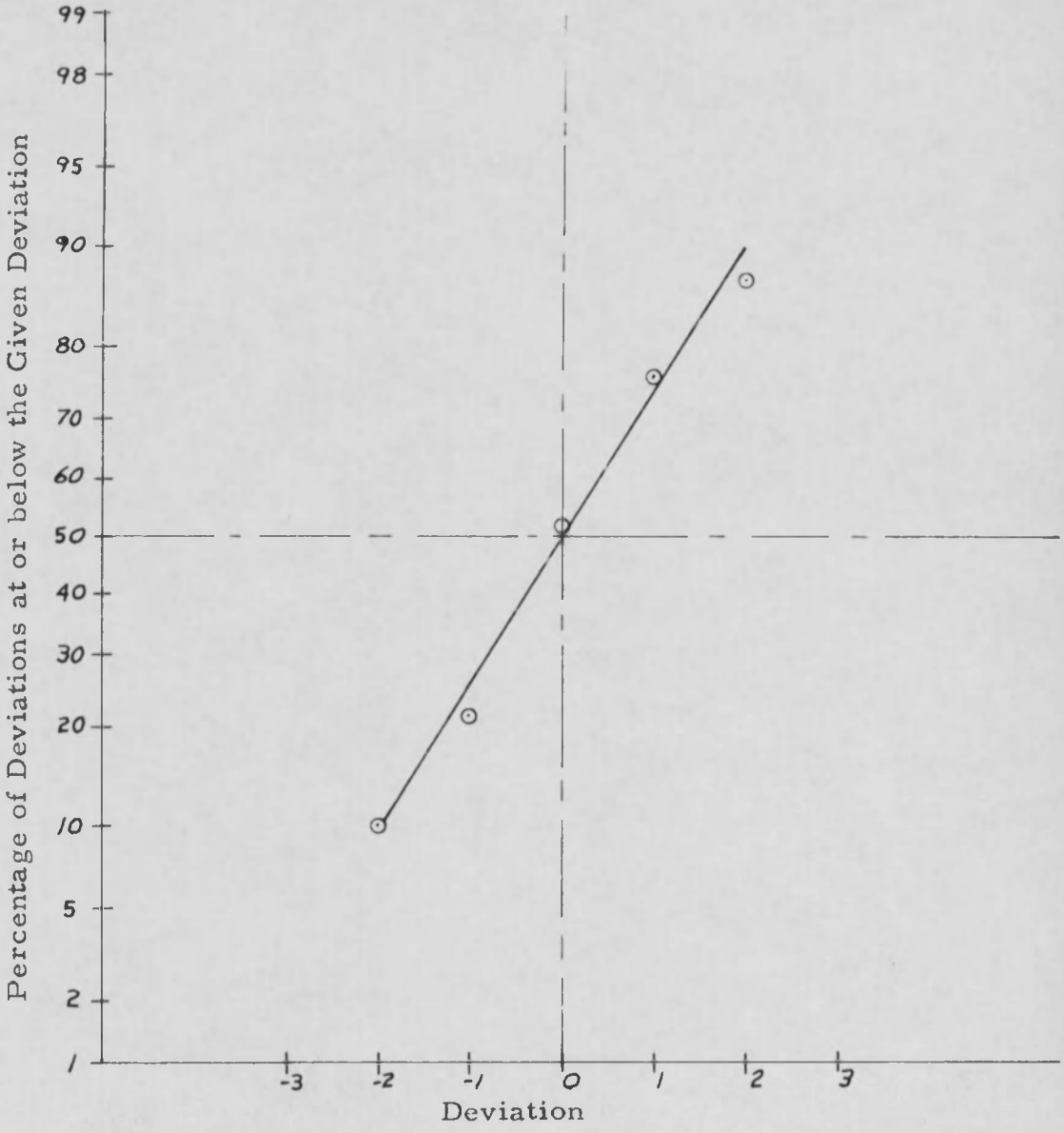

FIGURE 26

Distribution Diagram of $p(R/t)^2$ for Shape IV

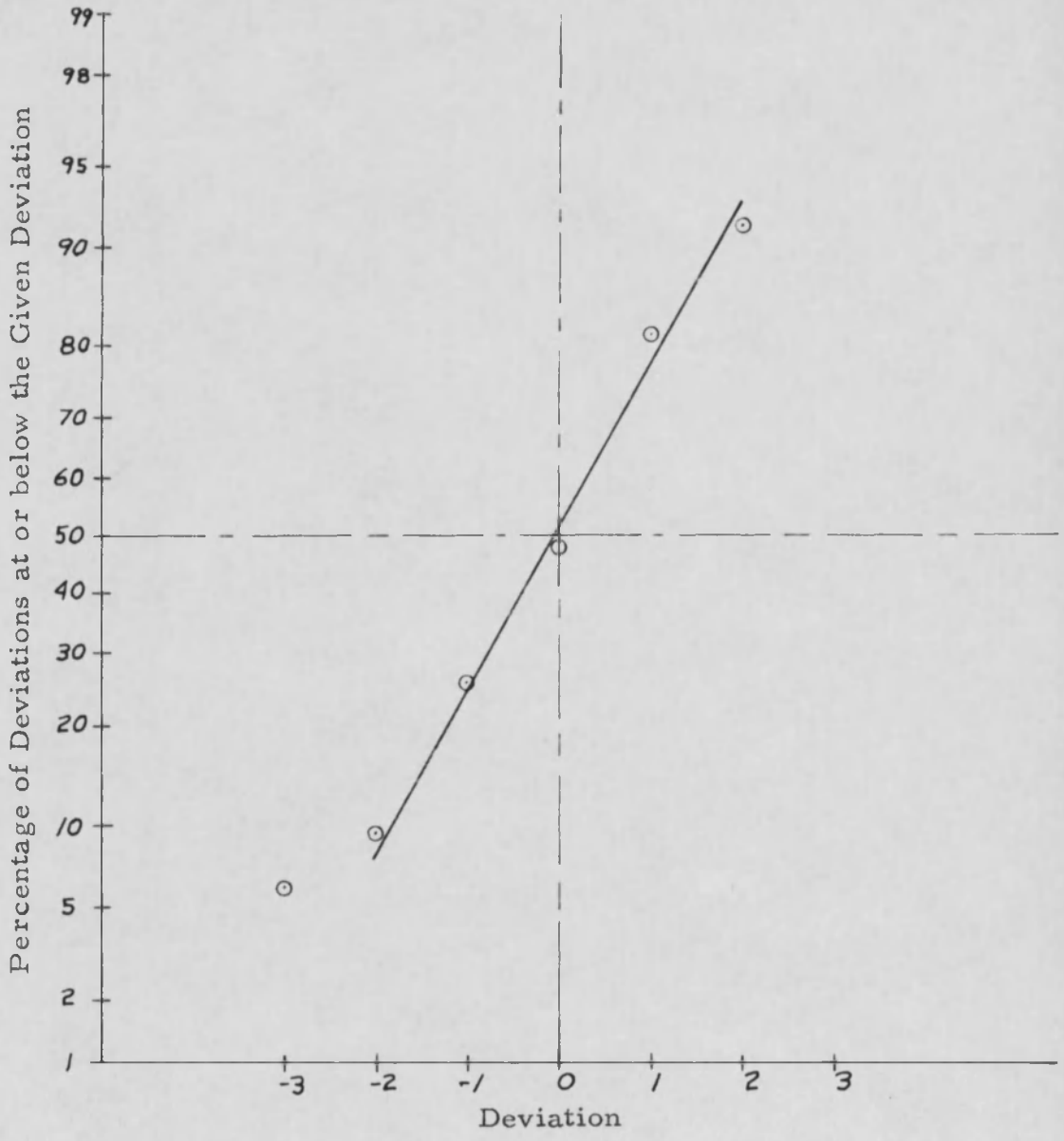

FIGURE 27

Distribution Diagram of $p(R/t)^2$ for Shape V

CHAPTER FOUR

COMPARISON OF RESULTS

It is the purpose of this chapter to compare the experimental results of this investigation with other experimentation as well as with the results of theoretical investigations. The chapter is divided into two parts; the first is concerned with the comparison of results between this investigation and previous publications, and the second part consists of the development, with modifications, of the theory or theories showing the best agreement with this experimental investigation throughout the range of testing.

Comparison

For purposes of comparison, the material properties of the formed shells must be determined. Testing revealed the modulus of elasticity to be 2.79×10^5 pounds per square inch and Poisson's ratio to be 0.47. The results of this test are in Appendix B. It is assumed that, within the accuracy of the determination of the buckling pressures, the variation of the material property values from sheet to sheet is insignificant.

The material properties of polyvinyl chloride have been determined in another investigation[32] and indicate some disagreement. The modulus of elasticity was found to be in the range 430,000 to 500,000 psi and Poisson's ratio to be about 0.4. It is also noted that the observed modulus was very strongly dependent on the length of the sample, long specimens having twice the modulus of short specimens. In the same publication it is shown that 4/9 of the variance in the buckling pressure of spherical shells is due to errors in measuring the thickness, 4/9 due to errors in measuring the radius of curvature and only 1/9 is due to errors in measuring the modulus of elasticity.

There is a problem in the consistency of notation when comparing to results of other publications. Most authors refer to a geometric parameter and a loading parameter. However, these are defined differently in the different investigations. Not only does one encounter the parameters defined differently, it is not uncommon to find the same symbol used for a parameter by two different authors but the parameter itself defined differently in each development. Furthermore, the use of symbols for radius of curvature, thickness, etc., has not been standardized. When referring to a publication, the notation and parameters referred to will be those originally adopted by the author.

Not all of the references mentioned in the Introduction or in Appendix A contain independent theories or experimental results. There are several publications which contain background material or material of general interest on the problem of the buckling of the clamped spherical cap.

In the development of some of the theories, the authors limit their investigation to a shallow spherical cap. Therefore, there is a maximum value of their geometric parameter for which their theory is applicable. If the shallowest shell tested in this investigation has a geometric parameter value exceeding these maximum values, it is not possible to make any comparison. In the theories of Budiansky,[25] Keller and Reiss,[7] Murray and Wright,[11] Reiss,[18] Reiss, Greenberg and Keller,[8] Simons,[2] Thurston,[31] Weinitschke[9,10] and von Willich[24] the largest permissible value of their geometric parameter is smaller than the smallest one of this present study. Therefore, no real agreement is possible with these publications, although reasonableness of results can be compared if the values of the geometric parameter are relatively close.

There are at least two theories which suggest a possible modification to meet the experimental conditions of this paper.

Those of Budiansky[25] and Klein[21] suggest a function relating the departure of thickness and curvature of the actual shell from a true shell.

Budiansky[25] uses a geometric parameter of $\lambda = 2\left[3(1-\nu^2)\right]^{\frac{1}{4}}\left(\frac{H}{t}\right)^{\frac{1}{2}}$ and a load parameter of q_{cr}/q_o, where q_{cr} is the buckling pressure, $q_o = \frac{2E}{\left[3(1-\nu^2)\right]^{\frac{1}{2}}}\left(\frac{t}{R}\right)^2$, H is the rise above the base plane, t is the thickness, ν is Poisson's ratio and R is the radius of curvature of the middle surface of the shell. The value of this parameter for the shallowest shell tested is $\lambda = 13$. For this value $q_{cr}/q_o = 0.30$. For $\lambda = 12$, Budiansky obtains $q_{cr}/q_o = 0.96$, which exceeds the value found experimentally. However, the Budiansky value is based on a true shell. Introducing the surface equation as $Z_o = H\left\{1-\left(\frac{r}{a}\right)^2 - \epsilon\left[1-\left(\frac{r}{a}\right)^2\right]^2\right\}$, where H is the rise of the shell above the base plane whose radius is a, he obtains $q_{cr}/q_o = 0.83$ and 0.75 for values of ϵ equal to 0.025 and 0.050 respectively. Therefore, it might be possible to extend Budiansky's theory for the slightly imperfect shell by using a larger value of ϵ.

Klein[21] does not develop a theory for the problem, but he does propose plotting $\frac{p_{cr}R \times 10^3}{2tE}$ versus R/t to reduce the scatter. The range of R/t considered is from 175 to 800 which includes the shallowest shell of this paper where R/t = 306. At this value of

R/t, Klein obtains $\frac{\sigma_{cr} \times 10^3}{E} = 0.8$ for $\frac{e}{\sqrt{Rt}} = 0.025$ where R is the radius of curvature of the middle surface, t is the thickness, p_{cr} is the critical buckling pressure and e is the average maximum initial departure from the mean shell radius. This yields $p_{cr} = 1.5$ psi and the experimental value is $p_{cr} = 1.1$ for this R/t ratio. So again the possibility exists of using a larger value of the error function to obtain predicted results comparable with the observed results through the plot proposed by Klein.

Simons[2] does not indicate the range of the geometric parameter for which his theory is valid. He does make the assumption of a shallow shell, however. When comparing the results of critical buckling pressure with his theory, one finds the observed value to be about 1/4000 of the theoretical value for the hemisphere. The discrepancy decreases with the shallower shells. For the shallowest one tested in this investigation, the observed value is about 1/5 of the theoretical value. Thus it appears the Simon's theory is for shallow shells only, even shallower than the shallowest one tested. Simons does obtain a minimum value of the geometric parameter for which buckling can occur. In the experimental investigation, the shallowest shell buckled at a value larger than the minimum. Thus there is agreement with this portion of the theory of Simons.

Because of the shallowness assumption of Gjelsvik and Bodner,[33] the only shape for which comparison is possible is the shallowest one of this investigation where the geometric parameter is $\lambda = 13$. At this point they determine the loading parameter to be 0.41 for the energy load without the boundary layer and 0.14 when including the effect of the boundary layer. The appropriate value of 0.30 of this investigation is between the two values of Gjelsvik and Bodner.

There are two known theories, the results of which, when evaluated at comparable points in this investigation, indicate a discrepancy. Archer[1] uses an H/h ratio of from 1 to 35, where H is the rise above the base plane and h is the thickness. The shallowest shell tested had an H/h of 30 which is within this range. For this value Archer obtains $p = e/e_{cr} = 0.95$, where $e_{cr} = \frac{4E}{[12(1-\nu^2)]^{1/2}} \left(\frac{h}{a}\right)^2$, e is the buckling pressure, ν is Poisson's ratio and a is the radius of curvature. For the shallowest shell tested, p = 0.30. Reiss[18] uses a geometric parameter of $\rho = \kappa^{-1/2} \Lambda^2 \frac{R}{h}$ where $k = \frac{2}{3(1-\nu^2)}$, Λ is the semi-angle opening, h is half the thickness and R is the radius of curvature. His linear theory predicts $P_{cr} = \frac{\omega_3^2}{\rho}$; $78.2 < \rho < 158.5$, where $\omega_3 = 10.174$ and $P_{cr} = \frac{p_{cr}}{2EK^{1/2}} \left(\frac{R}{h}\right)^2$. The only shell

of this investigation falling within the range of the geometric parameter is the shallowest one where $\rho = 92$. Reiss predicts $P_{cr} = 1.15$ for this shape whereas the experimental value is $P_{cr} = 0.78$.

A search of the literature discloses three previous experimental investigations on the buckling of clamped spherical caps. It is fortunate that the same geometric and loading parameters are used in each. The geometric parameter is $\lambda = 2\left[3(1-\mu^2)\right]^{1/4}\left(\frac{H}{t}\right)^{1/2}$ and the loading parameter is $p/q_{cr} = \frac{p}{2E}\left[3(1-\mu^2)\right]^{1/2}\left(\frac{R}{t}\right)^2$ where h is the rise above the base plane, t is the thickness, R is the radius of curvature, μ is Poisson's ratio and p is the buckling pressure. Table 7 shows the value of the geometric and loading parameter for the five shapes tested in this study.

Homewood, Brine and Johnson[27] tested shells for which the geometric parameter was as high as 20.5. This range includes the two shallowest ones of this investigation and is close to the third shape. The values of the loading parameter which are applicable are listed in Table 8. There is a discrepancy indicated for the fourth shape, but the third and fifth shapes are in good agreement.

Kaplan and Fung[19] obtain values of the loading parameter for a geometric parameter only as high as $\lambda = 10$. At this point, they find $p/q_{cr} = 0.33$. This is in general agreement with the shallowest shell of this study where $\lambda = 13$ and $p/q_{cr} = 0.30$.

TABLE 7

Values of Geometric Parameter and Loading Parameter for Each Shape

SHAPE	λ	p/q_{cr}
I	28	.30
II	25	.30
III	20	.29
IV	16	.27
V	13	.28

TABLE 8

Geometric and Loading Parameter Results
of Homewood, Brine and Johnson[27]

λ	p/q_{cr}
13.1	.32
14.0	.18
14.0	.29
14.3	.22
16.0	.43
20.5	.29

Homewood, Brine and Johnson[27] report that von Kloppel and Jungbluth obtained values of γ in the higher ranges of the geometric parameter. Their values of the loading parameter for corresponding values of the geometric parameter which are applicable are indicated in Table 9. The largest four values of the geometric parameter of this investigation lie in the range of the study of von Kloppel and Jungbluth. There is general agreement although the results of this investigation slightly exceed those of von Kloppel and Jungbluth at each corresponding point.

The two theories showing the best agreement with the experimental results of this study are the publications by von Karman and Tsien[4] and the later modification by Tsien.[6] In the first paper, the authors obtain an expression for the lower buckling stress of $\sigma = 0.18258\ Et/R$ where $\sigma = pR/2t$, p is the buckling pressure, R is the radius of curvature and t is the thickness. Table 10 shows the observed and predicted values of the buckling pressure for the values of the geometric parameter of the five shapes tested in this investigation. In the revision of the theory by Tsien,[6] expressions for both the upper and lower buckling stresses are given. The same notation is used as in the original publication. The values of the lower buckling pressure as predicted by Tsien for the five shapes are shown in Table 11. The agreement with the

TABLE 9

Geometric and Loading Parameter Results of von Kloppel and Jungbluth[27]

γ	p/q_{cr}
29	.19
29	.14
28	.16
27	.18
24	.22
22	.22
22	.25
21	.19
21	.26
20	.23
20	.19
18	.20

TABLE 10

Comparison with von Karman and Tsien[4] Results

SHAPE	R/t	p (observed) psi	p (predicted) psi
I	149	4.9	4.6
II	152	4.7	4.4
III	151	4.7	4.5
IV	172	3.3	3.4
V	306	1.1	1.1

TABLE 11

Geometric and Loading Parameter Results of Tsien[6]

SHAPE	R/t	BUCKLING PRESSURE psi
I	149	Not Applicable
II	152	2.9
III	151	2.9
IV	172	2.5
V	306	1.1

larger values of the geometric parameter in this investigation is not as good as with the original von Karman-Tsien theory; however, the agreement in the lower range of the parameter is reasonably good.

To indicate the disagreements in other publications, Table 12 shows the predicted and observed buckling pressures for one particular shape, for theories which are applicable or nearly applicable. The shape chosen is shape V in this study, where the geometric parameter is $\lambda = 13$, because more theories are found to be near this value of the geometric parameter than any other. For purposes of analysis, results of theories when λ is close to 13 are included and the nearest value of the geometric parameter is noted. It is seen that there is disagreement of a significant nature. Not only is there a lack of agreement with the results of this investigation where the buckling pressure was 1.1 psi, but the several theories and experimental results are not in agreement.

In comparing the results of this investigation to other publications, the following conclusions can be reached:

1. Some of the theories are not comparable to even the shallowest shell tested because of the shallowness assumption.

TABLE 12

Buckling Pressure for γ = 13 and R/t = 306

BUCKLING PRESSURE psi	SOURCE
3.7	Archer[1]
2.9	Budiansky[25] (γ = 12)
1.2	Homewood, Brine and Johnson[27]
0.6	Gjelsvik and Bodner[33] (γ = 11.4)
1.3	Kaplan and Fung[19] (γ = 10)
1.1	von Karman and Tsien[4]
1.5	Klein[21]
0.8	von Kloppel and Jungbluth[27] (γ = 18)
1.7	Murray and Wright[11] (R/t = 362.5)
1.6	Reiss[18]
5.1	Simons[2]
1.1	Tsien[6]
2.6	Weinitschke[10] (γ = 12)
2.8	von Willich[24] (γ = 9.5)
1.1	This experimental investigation

2. The theories of Archer[1] and of Reiss[18] are in disagreement. At applicable values of the geometric parameter, Archer predicts a buckling pressure of about three times the observed pressure, while Reiss predicts a pressure about one and one-half times the observed pressure.
3. The "error functions" of Budiansky[25] and Klein[21] could allow for agreement with a particular value for the departure from an "exact" condition.
4. Published experimental results, that of Homewood, Brine and Johnson,[27] Kaplan and Fung,[19] and von Kloppel and Jungbluth,[27] are in substantial agreement.
5. The original von Karman-Tsien theory[4] and the Tsien[6] modification are in satisfactory agreement.

Figure 28 shows the results of this investigation for the loading parameter versus the geometric parameter compared to the experimental results of Kaplan and Fung, von Kloppel and Jungbluth, and Homewood, Brine and Johnson. The parameters have been previously defined. It should be pointed out that the five plots of this investigation represent averages for each shape while the other points represent the results of a single test.

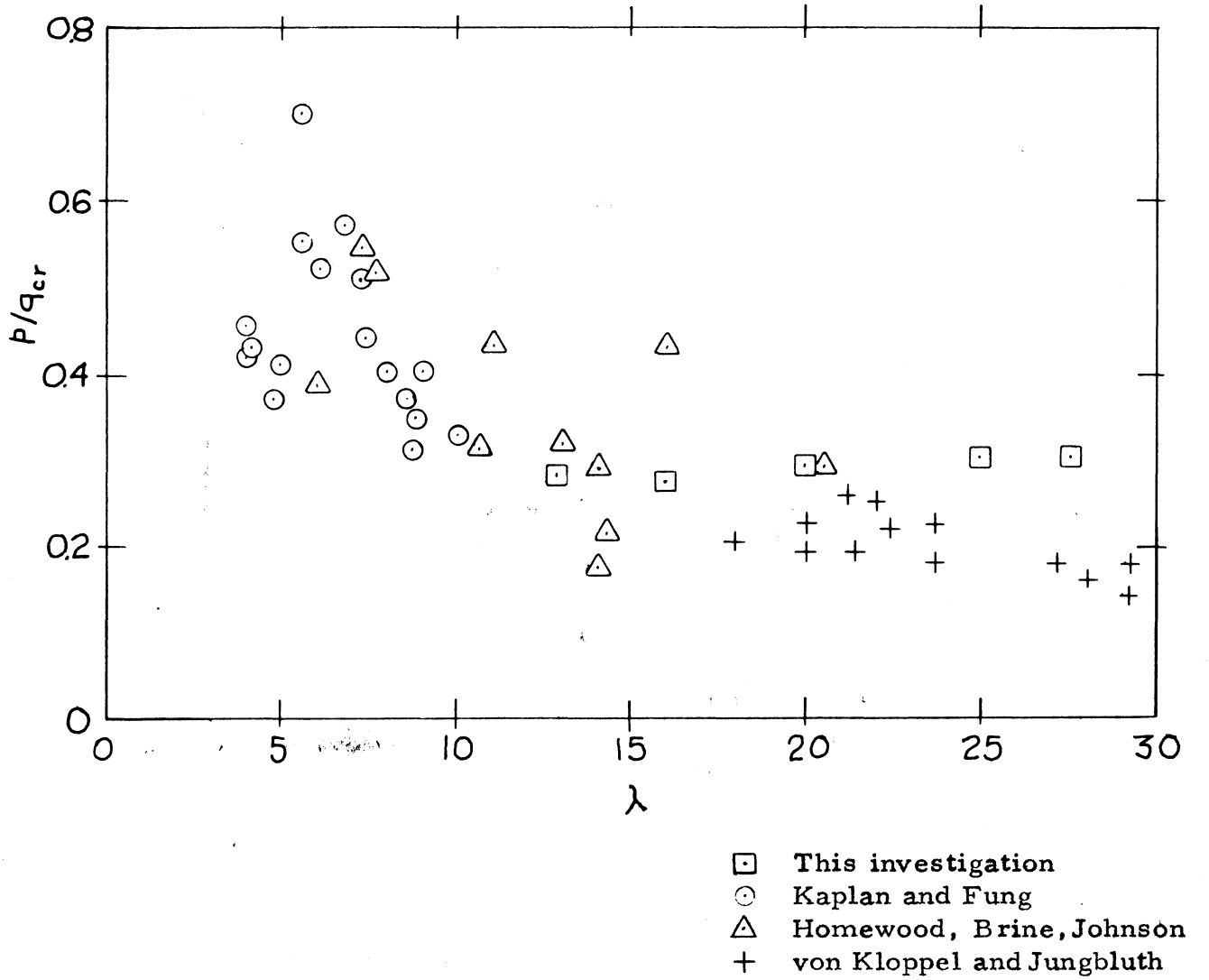

FIGURE 28

Comparison of Experimental Results

Theoretical Development

On the basis of a comparison of the results of this investigation with other publications, it is now considered possible to support an existing theory with experimental verification. The von Karman-Tsien[4] theory was found to be in the best agreement throughout the range of the geometric parameter in this study. This theory is based on developing an expression for the minimum buckling pressure through the Rayleigh-Ritz method with an assumed deflection form. The simplifications involve the assumption of axially symmetrical deflections with the deflections being parallel to the axis of rotational symmetry, and small angle approximations.

The total energy W is equal to W_1, the strain energy due to axial forces, W_2 the strain energy due to bending, and W_3 the potential energy corresponding to the work done by the external pressure. The strain energy due to the axial forces is of the general form, $W_1 = \int \frac{\sigma\epsilon}{2} dV$ or $\frac{E}{2}\int \epsilon^2 dV$. Consider the element from Figure 29a. Sketches b and c show that the length before deformation is $\frac{dr}{\cos\alpha}$ and after deformation is $\frac{dr}{\cos\theta}$. Assuming the deflection is rotationally symmetrical and the deflection of any element is parallel to the axis of symmetry, the

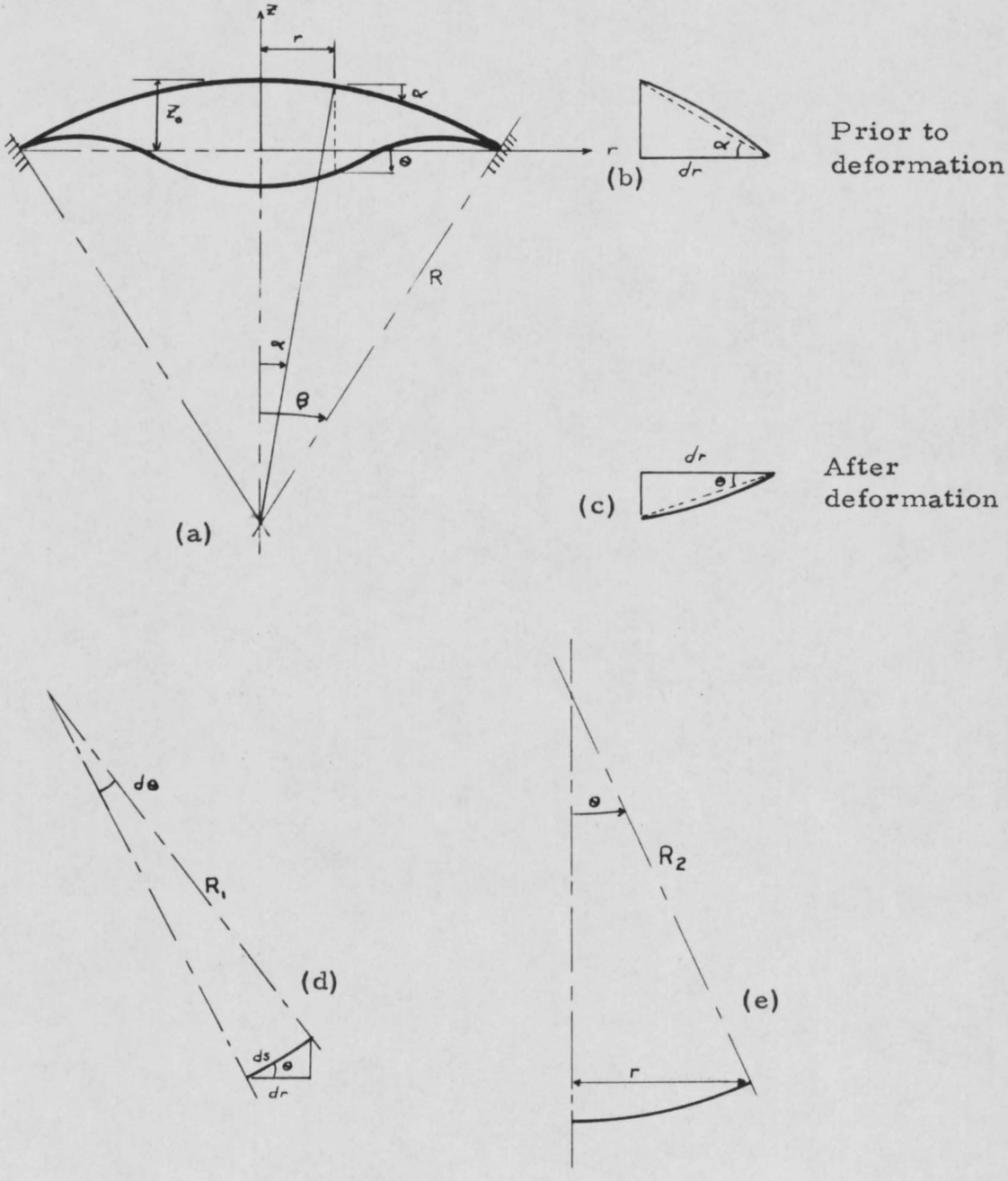

FIGURE 29

Shell Cross Section

strain in the meridian direction is $\epsilon_1 = \dfrac{\frac{dr}{\cos\theta} - \frac{dr}{\cos\alpha}}{\frac{dr}{\cos\alpha}} = \dfrac{\cos\alpha}{\cos\theta} - 1$.

There is also an additional strain due to that produced by the uniform compression prior to buckling; $\sigma_2 = \frac{pR}{2t}$ or $\epsilon_2 = \frac{pR}{2Et}$.

The two strains are of opposite sign, hence the total strain is

$$\epsilon = \epsilon_1 - \epsilon_2 = \frac{\cos\alpha}{\cos\theta} - 1 - \frac{pR}{2Et} = \frac{\cos\alpha - \cos\theta}{\cos\theta} - \frac{pR}{2Et} .$$

Using the Taylor series for the cosine expressions and dropping terms higher than the third power yields,

$$\epsilon = \frac{\left(1 - \frac{\alpha^2}{2}\right) - \left(1 - \frac{\theta^2}{2}\right)}{1 - \frac{\theta^2}{2}} - \frac{pR}{2Et} = \frac{-\alpha^2 + \theta^2}{2\left(1 - \frac{\theta^2}{2}\right)} - \frac{pR}{2Et} ,$$

and assuming θ to be small, $\epsilon = \frac{\theta^2 - \alpha^2}{2} - \frac{pR}{2Et}$.

The element of volume is $dV = 2\pi r t \frac{dr}{\cos\alpha}$, or since

$r = R\sin\alpha$; $dr = R\cos\alpha\, d\alpha$

$$dV = 2\pi R \sin\alpha\, t R \frac{\cos\alpha}{\cos\alpha} d\alpha = 2\pi R^2 t \sin\alpha\, d\alpha$$

or again using the small angle approximation, $dV = 2\pi R^2 t \alpha\, d\alpha$.

Now $W_1 = \frac{E}{2}\int \epsilon^2 dV = \frac{E}{2}\int_0^\beta \left(\frac{\theta^2 - \alpha^2}{2} - \frac{pR}{2Et}\right)^2 2\pi R^2 t \alpha\, d\alpha$

or $$\frac{W_1}{\pi R^3} = \frac{Et}{R}\int_0^\beta \left(\frac{\theta^2 - \alpha^2}{2} - \frac{pR}{2Et}\right)^2 \alpha\, d\alpha$$

The strain energy due to bending is of the general form

$W_2 = \int \frac{1}{2} M \Delta\phi\, ds$; where $\Delta\phi$ is the change of curvature

and the moment $M = EI\Delta\phi = \frac{Et^3}{12}\Delta\phi\, b$. The element of volume is again $2\pi R^2 t \sin\alpha\, d\alpha$. The change in curvature consists of the change in the meridian section $\Delta\phi_1$, plus the change in the section orthogonal to the meridian section $\Delta\phi_2$. For each section the original curvature is 1/R.

In Figure 29d,

$$\frac{1}{R_1} = \frac{d\theta}{ds} = \frac{\frac{d\theta}{d\alpha}}{\frac{ds}{d\alpha}}$$

$$ds = \frac{dr}{\cos\theta} \quad \text{AND} \quad dr = R\cos\alpha\, d\alpha$$

$$\text{SO } \frac{1}{R_1} = \frac{1}{R}\,\frac{d\theta/d\alpha}{\frac{\cos\alpha}{\cos\theta}\,\frac{d\alpha}{d\alpha}} = \frac{1}{R}\,\frac{\cos\theta}{\cos\alpha}\,\frac{d\theta}{d\alpha}$$

$$\text{AND } \Delta\phi_1 = \frac{1}{R_1} - \frac{1}{R} = \frac{1}{R}\left(\frac{\cos\theta}{\cos\alpha}\,\frac{d\theta}{d\alpha} - 1\right).$$

In Figure 29c,

$$R_2 = \frac{r}{\sin\theta} = R\,\frac{\sin\alpha}{\sin\theta}$$

$$\text{so } \Delta\phi_2 = \frac{1}{R_2} - \frac{1}{R} = \frac{1}{R}\left(\frac{\sin\theta}{\sin\alpha} - 1\right).$$

$$\text{Now } W_2 = \int \frac{M}{2t}(\Delta\phi_1 + \Delta\phi_2)\, dV = \int_0^{\beta} E\left[\frac{(\Delta\phi_1)^2 + (\Delta\phi_2)^2}{24}\right] 2\pi R^2 t^3 \sin\alpha\, d\alpha$$

$$= \frac{Et^3\pi}{12}\int_0^{\beta}\left[\left(\frac{\cos\theta}{\cos\alpha}\,\frac{d\theta}{d\alpha} - 1\right)^2 + \left(\frac{\sin\theta}{\sin\alpha} - 1\right)^2\right] \sin\alpha\, d\alpha$$

$$\text{or } \frac{W_2}{\pi R^3} = \frac{E}{12}\left(\frac{t}{R}\right)^3 \int_0^{\beta}\left[\left(\frac{d\theta}{d\alpha} - 1\right)^2 + \left(\frac{\theta}{\alpha} - 1\right)^2\right] \alpha\, d\alpha$$

where the small angle approximations have again been used.

The potential energy corresponding to the work done by the external pressure is equal to the pressure p times the volume enclosed between the initial and deflected surface of the shell. This volume is composed of two parts: V_1, the volume between the initial surface and the plane of the circular edge, and V_2, the volume between the deflected surface and the plane.

$$V_1 = \int \pi r^2 d\rho = \int \pi R^2 \sin^2\alpha (-R \sin\alpha \, d\alpha)$$

$$= -\pi R^3 \int_0^\beta \sin^3\alpha \, d\alpha$$

$$= -\pi R^3 \int_0^\beta \sin^2\alpha \tan\alpha \cos\alpha \, d\alpha.$$

$$V_2 = \int_0^\beta 2\pi r z \, dr = \pi r^2 z \Big|_0^\beta - \int_0^\beta \pi r^2 \frac{dz}{dr} \, dr$$

$$= 0 - \int_0^\beta \pi R^2 \sin^2\alpha \tan\theta \, R \cos\alpha \, d\alpha$$

$$= -\pi R^3 \int_0^\beta \sin^2\alpha \cos\alpha \tan\theta \, d\alpha.$$

Now $V = V_1 - V_2 = \pi R^3 \int_0^\beta \sin^2\alpha \cos\alpha (\tan\theta - \tan\alpha) \, d\alpha$

and $W_3 = \pi R^3 p \int_0^\beta \sin^2\alpha \cos\alpha (\tan\theta - \tan\alpha) \, d\alpha$

or $\frac{W_3}{\pi R^3} = p \int_0^\beta \alpha^2 (\theta - \alpha) \, d\alpha$

using the small angle approximations.

Now the total energy is the sum of W_1, W_2 and W_3;

$$\frac{W}{\pi R^3} = \frac{Et}{R}\int_0^\beta \left(\frac{\theta^2-\alpha^2}{2} - \frac{pR}{2Et}\right)^2 \alpha\, d\alpha + \frac{E}{12}\left(\frac{t}{R}\right)^3 \int_0^\beta \left[\left(\frac{d\theta}{d\alpha}-1\right)^2 + \left(\frac{\theta}{\alpha}-1\right)^2\right] \alpha\, d\alpha$$
$$+ p\int_0^\beta \alpha^2(\theta-\alpha)\, d\alpha$$

which can be written as; $\frac{W}{\pi R^3} = \frac{Et}{R} I_1 + \frac{E}{12}\left(\frac{t}{R}\right)^3 I_2 + p I_3$.

The assumed deflection form for the Rayleigh-Ritz method is

$\theta = \alpha\left[1 - K\left(1 - \frac{\alpha^2}{\beta^2}\right)\right]$ which satisfies the boundary conditions of $\theta = 0$ AT $\alpha = 0$; $\theta = \beta$ AT $\alpha = \beta$.

$$I_1 = \int_0^\beta \left(\frac{\theta^2-\alpha^2}{2} - \frac{\sigma}{E}\right)^2 \alpha\, d\alpha \quad \text{WHERE} \quad \sigma = \frac{pR}{2t}$$

AND $$\frac{\theta^2-\alpha^2}{2} - \frac{\sigma}{E} = -K\alpha^2\left(1-\frac{\alpha^2}{\beta^2}\right) + \frac{K^2\alpha^2}{2}\left(1-\frac{\alpha^2}{\beta^2}\right)^2 - \frac{\sigma}{E}$$

or $$I_1 = \int_0^\beta \left\{\frac{K^4}{4}\left(\alpha^5 - 4\frac{\alpha^7}{\beta^2} + 6\frac{\alpha^9}{\beta^4} - 4\frac{\alpha^{11}}{\beta^6} + \frac{\alpha^{13}}{\beta^8}\right) - K^3\left(\alpha^5 - \frac{3\alpha^7}{\beta^2} + \frac{3\alpha^9}{\beta^4} - \frac{\alpha^{11}}{\beta^6}\right)\right.$$
$$+ K^2\left(\alpha^5 - \frac{2\alpha^7}{\beta^2} + \frac{\alpha^9}{\beta^4}\right) - \frac{\sigma K^2}{E}\left(\alpha^3 - \frac{2\alpha^5}{\beta^2} + \frac{\alpha^7}{\beta^4}\right) + \frac{2\sigma K}{E}\left(\alpha^3 - \frac{\alpha^5}{\beta^2}\right)$$
$$\left. + \frac{\sigma^2\alpha}{E^2}\right\} d\alpha$$

so $$I_1 = \frac{K^4\beta^6}{840} - \frac{K^3\beta^6}{120} + \frac{K^2\beta^6}{60} - \frac{\sigma K^2\beta^4}{24E} + \frac{\sigma K\beta^4}{6E} + \frac{\sigma^2\beta^2}{E^2}.$$

Now $$I_2 = \int_0^\beta \left[\left(\frac{d\theta}{d\alpha}-1\right)^2 + \left(\frac{\theta}{\alpha}-1\right)^2\right] \alpha\, d\alpha$$

$$\left(\frac{d\theta}{d\alpha}-1\right)^2 + \left(\frac{\theta}{\alpha}-1\right)^2 = K^2\left(2 - 8\frac{\alpha^2}{\beta^2} + 10\frac{\alpha^4}{\beta^4}\right)$$

$$\text{so } I_2 = \int_0^{\beta} K^2 \left(2\alpha - 8\frac{\alpha^3}{\beta^2} + 10\frac{\alpha^5}{\beta^4}\right) d\alpha$$

$$\text{or } I_2 = \frac{2K^2}{3}\beta^2.$$

$$\text{Now } I_3 = \int_0^{\beta} \alpha^2(\theta - \alpha)\, d\alpha$$

$$\theta - \alpha = K\left(-\alpha + \frac{\alpha^3}{\beta^2}\right)$$

$$\text{so } I_3 = \int_0^{\beta} K\left(-\alpha^3 + \frac{\alpha^5}{\beta^2}\right) d\alpha$$

$$\text{or } I_3 = -\frac{K\beta^4}{12}.$$

THE EQUILIBRIUM POSITION IS $\frac{\partial W}{\partial K} = 0 = \frac{Et}{R}\frac{\partial I_1}{\partial K} + \frac{Et^3}{12R^3}\frac{\partial I_2}{\partial K} + p\frac{\partial I_3}{\partial K}$;

$$\frac{\partial I_1}{\partial K} = \frac{K^3\beta^6}{210} - \frac{K^2\beta^6}{40} + \frac{K\beta^6}{30} - \frac{\sigma K\beta^4}{12E} + \frac{\sigma\beta^4}{6E},$$

$$\frac{\partial I_2}{\partial K} = \frac{4K}{3}\beta^2,$$

$$\frac{\partial I_3}{\partial K} = -\frac{\beta^4}{12},$$

$$\text{so } 0 = \frac{Et}{R}\beta^4\left(\frac{K^3}{210} - \frac{K^2}{40} + \frac{K}{30}\right) + \frac{\sigma t\beta^2}{12R}(2-K) + \frac{Et^3}{9R^3}K - \frac{\sigma t\beta^2}{6R}$$

$$\text{or } \frac{\sigma}{E} = \frac{\beta^2}{70}(4K^2 - 21K + 28) + \frac{4t^2}{3R^2\beta^2}.$$

To simplify this expression, K is expressed in terms of β and the maximum center deflection δ ;

$$Z_o = \int_o^\beta dr \, \text{TAN}\,\alpha = \int_o^\beta \text{TAN}\,\alpha \; R \cos\alpha \, d\alpha$$

AFTER DEFORMATION THE CENTER DEFLECTION IS,

$$\delta_1 = \int_o^\beta dr \, \text{TAN}\,\theta = \int_o^\beta R \cos\alpha \; \text{TAN}\,\theta \, d\alpha$$

$$\text{or } \delta = Z_o - \delta_1 = R \int_o^\beta \cos\alpha \, (\text{TAN}\,\alpha - \text{TAN}\,\theta) \, d\alpha$$

$$\text{so } \delta = R \int_o^\beta (\alpha - \theta) \, d\alpha \quad \text{USING A SMALL ANGLE APPROXIMATION.}$$

$$\text{Now } \alpha - \theta = K\alpha \left(1 - \frac{\alpha^2}{\beta^2}\right)$$

$$\text{so } \delta = RK \int_o^\beta \left(\alpha - \frac{\alpha^3}{\beta^2}\right) d\alpha = \frac{RK\beta^2}{4} \qquad \text{or } K = \frac{4\delta}{R\beta^2} .$$

$$\text{Now } \frac{\sigma}{E} = \frac{\beta^2}{70}\left[4\left(\frac{16\delta^2}{R^2\beta^4}\right) - 21\left(\frac{4\delta}{R\beta^2}\right) + 28\right] + \frac{4t^2}{3R^2\beta^2}$$

$$\text{or } \frac{\sigma}{E} = \frac{2}{5}\beta^2 - \frac{6\delta}{5R} + \frac{1}{\beta^2}\left(\frac{4t^2}{3R^2} + \frac{32\delta^2}{35R^2}\right) .$$

The minimum value of $\frac{\sigma}{E}$ for a given value of $\frac{\delta}{R}$ is determined by varying β^2 ;

$$\frac{\partial}{\partial\beta^2}\left(\frac{\sigma}{E}\right) = 0 = \frac{2}{5} - \frac{1}{\beta^2}\left(\frac{4t^2}{3R^2} + \frac{32\delta}{35R^2}\right)$$

$$\text{or } \beta^2 = \sqrt{\frac{10}{3}\left(\frac{t}{R}\right)^2 + \frac{16}{7}\left(\frac{\delta}{R}\right)^2} .$$

Now $\left(\frac{\sigma}{E}\right)_{MIN}$ FOR A GIVEN $\frac{\delta}{R} = \frac{2}{5}\sqrt{\frac{10}{3}\left(\frac{t}{R}\right)^2 + \frac{16}{7}\left(\frac{\delta}{R}\right)^2} - \frac{6\delta}{5R}$

$$+ \frac{\frac{4}{3}\left(\frac{t}{R}\right)^2 + \frac{32}{35}\left(\frac{\delta}{R}\right)^2}{\sqrt{\frac{10}{3}\left(\frac{t}{R}\right)^2 + \frac{16}{7}\left(\frac{\delta}{R}\right)^2}}$$

OR $\frac{\sigma R}{Et} = \frac{2}{5}\sqrt{\frac{16}{7}\left(\frac{\delta}{t}\right)^2 + \frac{10}{3}} - \frac{3\delta}{2t} + \frac{\frac{8}{7}\left(\frac{\delta}{t}\right)^2 + \frac{5}{3}}{\sqrt{\frac{16}{7}\left(\frac{\delta}{t}\right)^2 + \frac{10}{3}}}$

SO $\frac{\sigma R}{Et} = \frac{4}{5}\left[\sqrt{\frac{16}{7}\left(\frac{\delta}{t}\right)^2 + \frac{10}{3}} - \frac{3\delta}{5t}\right]$

The minimum value of $\frac{\sigma R}{Et}$ is now determined by varying $\frac{\delta}{t}$

$$\frac{\partial\left(\frac{\sigma R}{Et}\right)}{\partial\frac{\delta}{t}} = 0 = \frac{4}{5}\left\{\frac{1}{2}\left[\frac{16}{7}\left(\frac{\delta}{t}\right)^2 + \frac{10}{3}\right]^{-\frac{1}{2}} 2\left(\frac{16}{7}\right)\left(\frac{\delta}{t}\right) - \frac{3}{2}\right\}$$

or $\frac{\delta}{t} = \sqrt{\frac{735}{8}}$ is the value for minimum $\frac{\sigma R}{Et}$

AND $\left(\frac{\sigma R}{Et}\right)_{MIN} = \frac{4}{5}\left[\sqrt{\frac{16}{7}\left(\frac{735}{8}\right) + \frac{10}{3}} - \frac{3}{5}\sqrt{\frac{735}{8}}\right]$

OR $\frac{\sigma R}{Et} = 0.1825742$, USING $\frac{\sigma R}{Et} = 0.1826$

THEN $\sigma = \frac{pR}{2t} = 0.1826\frac{Et}{R}$,

OR $p = \frac{.3652E}{(R/t)^2}$ is the minimum buckling pressure.

CHAPTER FIVE

SUMMARY AND CONCLUSIONS

This investigation has been concerned with the development and evaluation of a new technique for the reliable experimental determination of critical buckling pressures for shell structures. The specific types of shell structure on which this technique was performed were uniformly loaded clamped spherical caps. In addition, this investigation has attempted to contribute knowledge to a topic on which the previous works have not been in complete agreement. The reasons for the discrepancies, noted in Table 12, have not been the purpose of this presentation. It is sufficient to mention the existence of these discrepancies, however, in order to indicate that some of the theories are not applicable in certain ranges.

From a statistical viewpoint, because of the large number of shells of each shape tested in this study, it is felt that more reliance can be placed on these results than on those obtained from an experimental program where only one shell of each shape is tested. The experimental results of this investigation indicate a

reasonably good agreement with previous experimentation on shells having the same loading and boundary conditions. The theoretical development showing the best agreement with this investigation is the von Karman-Tsien theory[4] which, because of this, has been analyzed in detail.

The buckling action for each of the shells was similar in all cases. The buckle dimple occurred suddenly at a point about one-third of the distance from the edge to the center. When the pressure was released, this buckle disappeared. When the pressure was reapplied to the shell, a slightly lower critical pressure resulted although the buckle occurred at the same point. When this pressure was increased past the critical value, the buckle increased in size until a "crinkling" resulted. The occurrence of the buckle was more abrupt for shells with a higher rise above the base plane as compared to the shallower shells. The pressure-volume data indicates a relationship which is approximately linear, up to the point of buckling. This was true for all shapes tested.

For the shapes tested, there was no evidence of any shallowness effect, a condition which is often assumed. This observation confirms those of Homewood, Brine and Johnson.[27] It is noted that all shells of each shape behaved in a similar manner in

this regard. It is possible, however, that the effect of shallowness would be noticed in the region where the geometric parameter $\lambda = 2\left[3(1-\mu^2)\right]^{1/4}\left(\frac{H}{t}\right)^{1/2}$ is smaller than that of the shallowest shell tested in this investigation.

Shapes II and III resulted in approximately the same value of the ratio of radius of curvature to thickness. This unplanned situation occurred because shape II had a smaller radius of curvature but a larger rise above the base plane than the corresponding values for shape III. Since shape III was shallower, there was less thinning out of the material during the forming process. The result was that the buckling pressure, and hence the loading parameter $p/q_{cr} = \lambda^2\left(\frac{R}{t}\right)^2\left[\frac{3(1-\mu^2)}{2E}\right]^{1/2}$ was approximately the same despite the fact that the geometric parameter λ was different for the two shapes of spherical caps.

Based on this investigation of uniformly loaded clamped spherical shells, the following conclusions may be made:

1. A reasonable value for the critical buckling pressure of a shell can be determined experimentally with confidence for a simple case by testing a sufficient number of models.
2. An adequate technique for forming many nearly identical shells can be developed by use of a vacuum former.

3. The relationship between pressure and volume change is approximately linear up to the point of buckling.
4. The effect of the shallowness of the shell on the buckling pressure is insignificant as compared to the effect of the ratio of radius of curvature divided by thickness.
5. The von Karman-Tsien theory appears to give results which are most consistent with reliable experimental observations.

APPENDIX A

This section is an alphabetic list of recent publications which are pertinent to the problem of the buckling of uniformly loaded clamped spherical caps. None of the theories are developed in detail, but rather the general approach, limitations, assumptions and solution are discussed. The theory which agrees best with the experimental results of this paper is thoroughly analyzed in Chapter Four.

Archer, Robert R.[1]

Archer notes that the previous work on buckling of spherical shells falls into two parts. One part represents the work of von Karman-Tsien,[4] Friedrichs[5] and others and involves the buckling pressure determination by minimizing a potential energy expression with respect to a deflection function. The other part represents the work of Kaplan-Fung,[19] Simons,[2] and others and is based on integration of the nonlinear differential equations.

Archer uses the "classical criterion," as opposed to the "energy criterion," whereby a given state of equilibrium becomes unstable when there are equilibrium positions infinitesimally near to that state of equilibrium for the same external load.

Beginning with the equations for finite deflections of shallow spherical shells under uniform radial pressure as derived by Reissner,[14] he puts the equations into a non-dimension form with new variables; $p = -p/p_{cr}$ where p_{cr} is the minimum buckling pressure for the corresponding complete sphere from the linear theory, $p_{cr} = \frac{4E}{[12(1-\nu^2)]^{1/2}}\left(\frac{h}{a}\right)^2$ and $\lambda^2 = \xi_e^2 m^2 \frac{a}{h}$. In these expressions a is the radius of curvature, h is the thickness, $m^4 = 12(1-\nu^2)$ and ξ_e is one half of the opening angle of the shell.

The problem then is to obtain the solution of the two differential equations in β^* and ψ^* with appropriate boundary conditions. Archer expands the variables and the pressure into a power series in terms of W, a perturbation parameter. This leads to a system of linear differential equations. Use of Bessel functions and boundary conditions yields the coefficients. The buckling pressure is determined from $2p = \sum_{\ell=1}^{\infty} p_\ell W^\ell$ by the condition $dp/dW = 0$.

Archer numerically determines the value of p by computing the expansion coefficients through use of a digital computer. He then compares his results based on two terms in the perturbation series with:

a. the theoretical results of Kaplan and Fung[19]

b. the experiments of Kaplan and Fung[19]

c. the theoretical results of Tsien[6]

and d. the experiments of Tsien.[6]

He found no real agreement throughout the range of λ although certain values of p versus λ agree with previous work.

Archer accounts for the increased deviation between his results and previous experimentation as λ increases, by the shell jumping to a nearby buckled state before reaching the buckling pressure predictated theoretically. The cause of the jumping is attributed to outside disturbances during testing. The theory allows for only a continuous load-deflection relation.

Budiansky, B.[25]

Budiansky makes the usual assumption of an axisymmetric buckling for the uniform pressure on a shallow portion of a clamped spherical shell. He notes the lack of agreement among existing theories and attributes this, at least in part, to the waviness of shell distortions, which tend to increase with decreasing shell thickness.

His approach is to begin with the three equilibrium equations and use force-distortion relations and a stress function to simplify the equations. Further development is made through the use of a shallowness assumption and the boundary conditions. The shallowness assumption is $z = H[1-(\frac{r}{a})^2]$. This is the representation of the spherical shape by a parabolic curve.

Budiansky introduces a geometrical parameter λ and non-dimensional variables to obtain two differential equations. The manipulation of these differential equations is through the use of operators, the Hankel transformation and Fourier transforms, the inversion formula, Kelvin functions, and the boundary conditions. The two integral equations which result are solved numerically by an iterative procedure, either by regarding the pressure parameter as prescribed and monotonically increasing or by regarding the average deflection as specified. Values of p_{cr} are tabulated for ranges of λ from 3.5 to 13.

Budiansky also develops values for p_{cr} based on initial imperfections where the shape of the surface with the initial imperfection is $Z_o = H\left[1-\left(\frac{r}{a}\right)^2 - \varepsilon\, e(r)\right]$ where $e(r) = \left[1-\left(\frac{r}{a}\right)^2\right]^2$ and ε is taken as plus or minus 0.025 and 0.05. The procedure for the solution is the same as for the initially perfect shell. Values of p_{cr} are tabulated for ranges of λ from 4 to 12.

Chien, Wei-Zang[13]

Chien assumes a shell with a small curvature and constant thickness. Using equilibrium equations in spherical polar coordinates, and then making small angle approximations, he classifies the problem as to a particular type using tensor notation. Chien then obtains two nonlinear partial differential equations in two

unknowns. By assuming rotational symmetry, two differential equations are developed. These equations involve α, the slope of the meridian line in the strained state and β/θ which is the radial membrane stress.

$$\theta \frac{d^2\alpha}{d\theta^2} + \frac{d\alpha}{d\theta} - \frac{\alpha}{\theta} - \frac{R^2}{D}\alpha\beta + \frac{P^o R^3 \theta^2}{2D} = 0$$

$$\theta \frac{d^2\beta}{d\theta^2} + \frac{d\beta}{d\theta} - \frac{\beta}{\theta} + h(\alpha^2 - \theta^2) = 0$$

In these equations, P^o is the sum of the boundary forces on the upper and lower surface, the thickness is 2h, $\alpha = \frac{1}{R}\frac{dw}{d\theta} + \theta$

$\beta = \frac{1}{R^2}\frac{d\chi}{d\theta}$ and $D = \frac{2h^3}{3(1-\sigma^2)}$

Chien notes that these equations are the fundamental ones for the determination of the buckling pressure of a small segment of a spherical shell.

Neglecting two terms in these equations results in the equation developed by von Karman and Tsien:[4]

$$\theta \frac{d^2\alpha}{d\theta^2} + \frac{d\alpha}{d\theta} - \frac{\alpha}{\theta} = \frac{hR^2}{D}\theta\alpha(\alpha^2 - \theta^2) - P^o\frac{\theta^2 R^3}{2D}$$

Friedrichs, K. O.[5]

The purpose of this theory is to examine one of the assumptions made in a previous development by von Karman and Tsien.[4] The assumption being that the displacement is vertical, that is it is parallel to the axis of symmetry.

By linearizing the problem, Friedrichs finds the influence of the vertical deflection assumption is so strong as to double the buckling load. The von Karman-Tsien assumption alters the order of magnitude of the minimum buckling load with respect to the shell thickness.

Friedrichs purposes a somewhat different procedure for obtaining the buckling load. He uses a boundary layer action which has the advantage of buckling no longer being restricted to only a segment of the shell. A rotationally symmetric deflection is still assumed. Friedrichs does not obtain final results, however, and notes that the correct asymptotic situation for buckled shells is still unknown.

In discussing the minimum and intermediate buckling loads, he notes that von Karman and Tsien found stable states of equilibrium different from zero when the pressure was above a certain minimum value and below the theoretical buckling pressure. Friedrichs questions why the shell should leave the stable unbuckled state and jump to a state with higher potential energy and remain there.

Gjelsvik A. and S. R. Bodner[33]

Gjelsvek and Bodner develop an energy expression for both symmetrical and nonsymmetrical snap buckling of uniformly loaded clamped spherical caps. The difference in the two cases is

the inclusion of more terms in the strain and curvature change relations of the non-symmetrical situation making the membrane and bending strain energy expressions more complicated.

The means of obtaining a solution is identical for each case. The total energy expression is obtained in terms of an assumed deflection function and the resulting expression minimized to yield the upper buckling load and the equal-energy load which corresponds to the lower buckling load. The upper buckling pressure is:

$$p = \frac{2E}{(R/t)^2}\left[\frac{7}{1350} + \frac{7}{57\lambda} + \left(\frac{\lambda}{10} - \frac{1}{\lambda}\right)\left(\frac{66}{225} - \frac{14}{57\lambda^2}\right)^{1/2}\right]$$

and the equal energy pressure is $p = \frac{2E}{(R/t)^2}\left[\frac{77}{1350} + \frac{7}{57\lambda}\right]$.

They also find a minimum value for which buckling can occur of $\lambda^2 \leq 10$. In these expressions $\lambda = \beta^2 \frac{R}{t}$, p is the buckling pressure, E is the modulus of elasticity, R is the radius of curvature, t is the thickness and β is half the opening angle. The development implies a restriction of a shallow shell. It is noted that the upper buckling load increases with the geometric parameter indicating an unbounded pressure value.

The final equations for the nonsymmetric situation are not included although it is noted the development is similar.

Grigolyuk, E. I.[29]

From the equations of Marguerre on equilibrium of shallow shells and through a change of variables, polar coordinates,

boundary conditions, power series, and Bubnov's method, Grigolyuk arrives at two nonlinear equations. He assumes

$w = (\rho^2-1)^2 (w_0 + w_1 \rho^4 \cos n\theta)$ for the deflection function. In this expression $\rho = r/b$ where r is the radius of the base of the piece middle surface and b is the radius of the parallel circle. The two equations are: $p^* = K_1 W_0 + K_2 W_0^2 + K_3 W_0^3 + K_4 W_0 W_1^2 + K_5 W_1^2$

and $0 = W_1 (L_1 + L_2 W_1^2 + L_3 W_0 + L_4 W_0^2)$

In these equations $W_0 = \frac{w_0}{H}$, $W_1 = \frac{w_1}{H}$, $p^* = p\frac{b^4}{EhH^3}$ where w is the middle surface deflection, h is the thickness, H is the rise above the base plane, $H = \frac{R}{2}\alpha_0^2$, and p is the pressure.

Homewood, R. H., Brine, A. C., and Johnson, A. E. Jr.[27]

This publication concerns the results of experimental work on spherical caps. Eight spun shells of hot rolled steel were tested. The shells were thickest at the center and thinnest at the edge. Thickness variations were determined by ultrasonic means. Two types of shells were used with the two radii being 40 inches and 78 inches. The ratio of radius to thickness varied from 160 to 1250. A shell was considered shallow if the height to base radius ratio was less than 1/8. However, the authors note that there were no important differences in buckling characteristics or results which could be attributed to "non shallow" shells.

An oil pressure was applied to the convex surface of the shell with pressures measured with Bourdon-tube pressure gages or electronic pressure transducers. Buckling occurred abruptly and the buckles remained for most shells after removal of the pressure. Tests on shells returning to the original position caused buckling to reoccur at the same location and at approximately the same pressure.

For small values of the geometric parameter, the authors note the deformation mode is a single half-wave across the shell with a maximum deflection at the center. As the value of this parameter increases slightly, the maximum deflection shifts to both sides of the center with a slightly reduced center deflection. The center deflection is reduced considerably in the intermediate range of the geometric parameter to the point where the deformation mode is essentially two half-waves across the shell. For the larger values of the parameter, the deformation mode changes to three half-waves across the shell.

They suggest an asymmetrical buckle pattern is possibly more critical than the symmetrical one. This may account in part for the unconservative theoretical results since all the theories are based on symmetrical buckling. The authors used high speed motion pictures to show that although the final buckled shape may be symmetric, the intermediate stages of buckling are antisymmetric.

In another development,[33] where tests were carried out at the same laboratory, the authors discuss the relative merits of plastic as a model material. They point out that the advantages are a low modulus of elasticity and an excellent thickness tolerance in thin sheets for cellulose nitrate and polyvinyl chloride. The disadvantages mentioned are those of creep and sensitivity to temperature and humidity changes.

They indicate an uncorrected value of about 400,000 psi for the modulus of elasticity. However, there was a large scatter which they could not attribute solely to temperature effects. Poisson's ratio was found to be 0.35. To account for the effect of creep, they used a six minute waiting period between application of the load and taking of strain data.

The authors used 3/16 inch thick sheets of methyl methnaylate, Plexiglas II-UVA. The shell had a radius of 40 inches and the section had a radius of 16.1 inches. The shells were formed to a spherical shape from a flat sheet of plastic by the vacuum snapback method. A considerable thickness variation was noted with the shells thickest at the edge and thinnest at the center.

von Karman, Theodore and Tsien, Hsue-Shen[4]

The authors note, even at this early data, a discrepancy between prediction of the theory and experimental evidence.

They mention a linear theory for a complete spherical shell based on the work of Love which is

$$\sigma_{cr} = \frac{Et/R}{\sqrt{3(1-\nu^2)}} = .606\frac{Et}{R} \quad \text{for } \nu = 0.3$$

They believe there is an essential difference between the physical process of the buckling of a flat plate and a curved shell which is not embraced by previous theory.

Consider the load deflection curve for a spherical cap under external pressure, as shown in Figure 30. The cap starts in position 1 and assumes position 3 through the action of pressure. The strain energy is zero in either position but cannot be zero for an intermediate position. Neglecting bending stiffness, the load deflection curve is as pictured in Figure 31, or with the edges clamped it has the lower shape. An anti-symmetrical deformation or initial irregularities may alter the shape of the curve.

In the test of shells, it is likely the point B is observed experimentally while it is point A which the theory predicts. This explains some of the discrepancy. Thus great care must be taken in the experimental work to accurately determine point A.

To develop a theory, the authors make the following assumptions:

1. The solid angle of the segment is small.
2. The deflection is rotationally symmetric.
3. The deflection of any element of the shell is parallel to the axis of rotational symmetry.

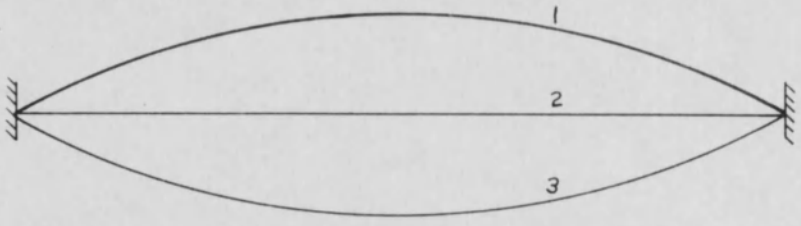

FIGURE 30

Spherical Cap

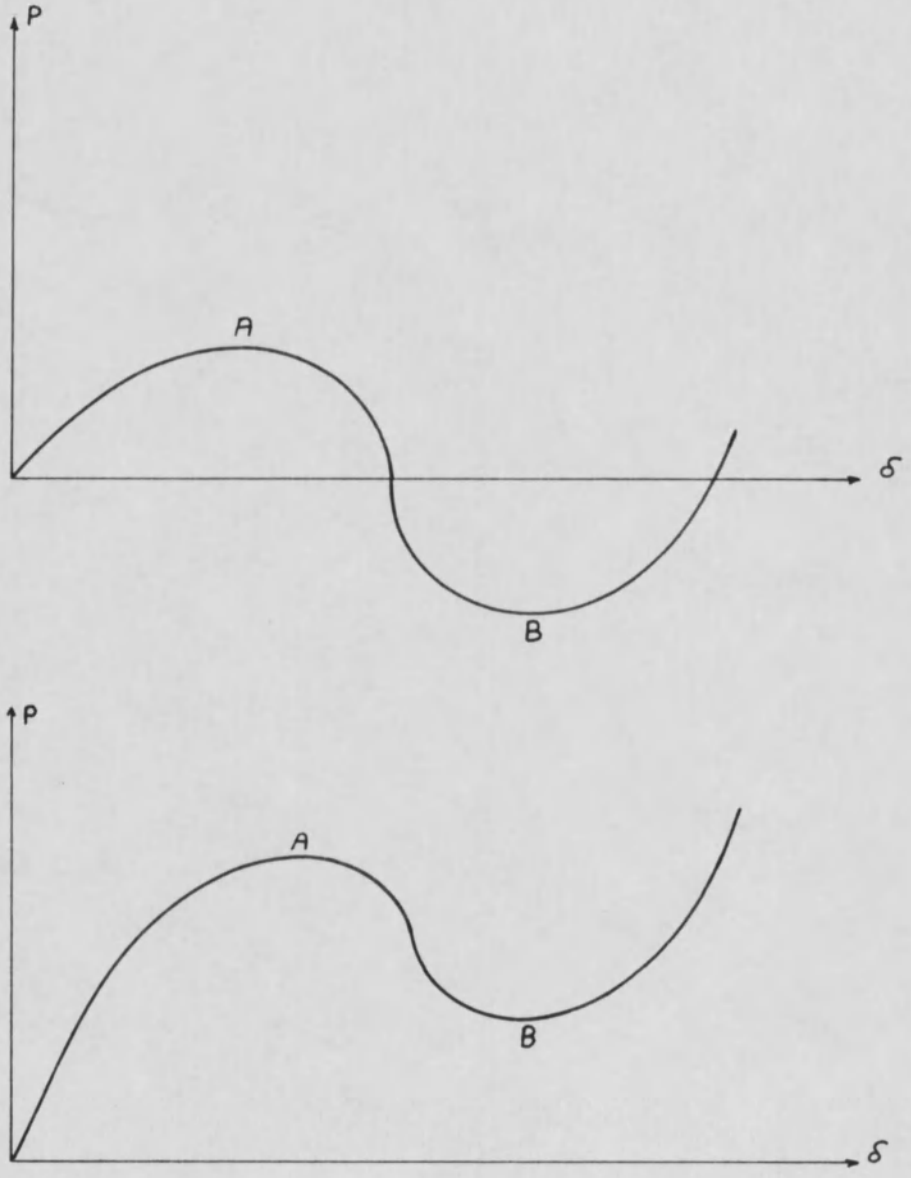

FIGURE 31

Load-Deflection Curves

4. Poisson's ratio can be neglected.

They develop a relationship for the total energy of the system and then minimize this to obtain an equilibrium position. Using boundary conditions and a shallow shell assumption yields a non-linear second order differential equation. The load deflection curve is calculated using the Rayleigh-Ritz method after assuming a deflection function satisfying the boundary conditions. The equation is $\frac{\sigma}{E} = \frac{4}{5}\left(\frac{\delta}{R} - \frac{3\delta^2}{R^2\beta^2} + \frac{16\delta^3}{7R^3\beta^3}\right) + \frac{8t^2\delta}{3R^3\beta^4}$. In this expression, σ is the uniform compressive stress produced by p ($\sigma = p\frac{R}{t}$), R is the radius of curvature, δ is the center deflection, t is the thickness, and β is half the angle of the shell.

This expression is minimized by differentiating it with respect to β^2 . The value of β^2 making $\frac{\sigma}{E}$ a minimum is then substituted back into the expression yielding:

$$\frac{\sigma}{E}\Big|_{\substack{R \\ \overline{t} \\ MIN}} = \frac{4}{5}\frac{\delta}{t}\,\frac{1+\frac{3}{280}\left(\frac{\delta}{t}\right)^2}{1+\frac{24}{35}\left(\frac{\delta}{t}\right)^2}$$

This gives an envelope curve whose maximum is $\sigma = .4908\frac{Et}{R}$ which is the smallest value, for any peak, through which the load passes, for the shell to collapse. The minimum value of the load keeping the shell in a deflected shape is $\sigma = .2377\frac{Et}{R}$.

When the energy expression is modified to include the strain produced by uniform compression prior to buckling, von Karman and Tsien find the upper value as $\sigma = 1.4606\frac{Et}{R}$ while the lower one is $\sigma = .18258\frac{Et}{R}$. For the lower stress $\beta = 3.8218\left(\frac{t}{R}\right)^{\frac{1}{2}}$

The authors emphasize that the upper buckling load can be approached experimentally only if extreme precaution is taken both in the manufacture of the specimen and in the testing. With the imperfections and tolerances in engineering practice, they claim the buckling load will invariably be very near the lower buckling load. They also note that it is the lower buckling value which is specified for design. This is because of their hypothesis that the shell jumps to the lower buckling value without reaching the classic buckling load.

Klein, Bertram[21,22]

Klein uses different parameters in an attempt to reduce the scatter shown by previous theories and experiments. In the past, plots of K versus R/t have been used. In this, K is the variable coefficient in the equation $\sigma = K E_r \frac{t}{R}$. E_r is the reduced modulus of elasticity, $\sigma_{cr} = \rho_{cr} \frac{R}{2t}$ is the initial collapse stress, R is the radius of curvature, h is the rise of the shell above the base plane, and t is the thickness. Note that for a perfect shell, K = 0.606.

Klein suggests use of an eccentricity parameter as $e/\sqrt{Rt}$ where e is the average maximum initial departure from the mean radius of the shell. Thus the eccentricity is a function of both thickness and curvature variations. Plotting $\frac{\sigma}{E_r}$ versus $\frac{R}{t}$ then reduces the scatter.

Murray, F. J. and Wright, Frank W.[11]

These authors discuss previous theoretical works pointing out the methods of solving the basic differential equations and the difficulties with each approach. They propose a step-by-step method of integrating the differential equations. Murray and Wright eliminate the small angle assumption, do not drop any terms, and thus claim a higher accuracy.

The normalized pressure parameter is $u = pR/2Et$, where p is the pressure, R is the radius of curvature, t is the thickness, and E is the modulus of elasticity. Numerical computations are carried out in complete detail for a clamped spherical cap with $R/t = 362.5$. Values are obtained for the upper buckling load and the minimum buckling load.

The authors discuss the von Karman-Tsien[4] energy equations and point out the nonlinear terms which were dropped cannot truly be neglected.

The upper and minimum buckling loads are explained as follows: The upper buckling load is the point when buckling occurs as the pressure increases. As the pressure is decreased and the shell jumps back to the unbuckled state, the minimum buckling load is the pressure at which the buckle disappears.

Computing machine limitations make it difficult to determine values for shells with an opening of greater than 23°.

Murray and Wright show that for the R/t ratio they used, the von Karman-Tsien minimum buckling load is about half of theirs. They also point out discrepancies between their results and those of Kaplan and Fung.[19] They do indicate good agreement with the results of Keller and Reiss[7] for the plot of critical buckling loads, P versus ρ .

The results of Murray and Wright indicate that for B above 0.10, where $B = \frac{\tan \theta}{2}$ and θ is one half of the angle opening, the critical buckling loads are independent of the angle opening.

The authors conclude that the critical buckling loads are independent of the angle opening of the shell when the angle opening is greater than the solid angle of the dimple. They also conclude that the results of the Rayleigh-Ritz solution by von Karman and Tsien does not satisfy the equations of equilibrium.

Nash, William A. and Modeer, James R.[30]

Nash and Modeer make two different approximations in order to develop a theory for the buckling of clamped shallow spherical shells uniformly loaded on the convex side. The first approximation is the neglect of the second invariant of the middle surface strains in the expression for the total potential energy. The second approximation retains only the linear terms of the second invariant in the same expression.

The procedure in their development begins with the strain displacements which are attributed to Marguerre. The transformation to polar coordinates yields the expressions for the first and second invariants. The total potential energy is formulated by adding the membrane and bending energies and the potential energy of the pressure.

This energy expression is based on the neglect of the second invariant. Applying the Euler variational equations to this expression yields two differential equations in terms of the displacements u and w, the solution of which involves Bessel functions.

The authors show that the load-deflection relations obtained by the neglect of the second invariant are in good agreement with results obtained by more established methods.

The development using the second assumption, which retains only the linear terms in the second invariant, agrees with the experimentation of Kaplan and Fung.[19]

Either of the approximations is extremely desirable because they uncouple the governing nonlinear equations, thus reducing the computing time.

Nash and Modeer point out that the same approximation has been employed by Reiss utilizing an entirely different approach to the problem of buckling of shallow spherical caps.

Reiss, Edward L.[7,8,18,20]

Reiss introduces new parameters as $\rho = c\frac{\beta^2 R}{h}$, the geometric parameter, and $Q = \frac{1}{2} C q \frac{R^2}{E h^2}$, the loading parameter. In these expressions $C = \left[\frac{3(1-\nu^2)}{2}\right]^{1/2}$, R is the radius of the shell, β the semi-included angle, h is half the thickness, and q is the uniform pressure. He relates his parameters to those used by Kaplan and Fung as $\rho = 2^{-1/2}\lambda^2$ and $Q = 4CK = \frac{12CP}{\rho^2}$.

Through the plotting of the results of Kaplan and Fung[19] with these parameters, Reiss uncovers modes of buckling. That is there is an oscillatory behavior between Q_{cr} and ρ with peaks occurring at transition points. For ρ greater than six and less than twenty, the shell deforms with a single maximum deflection point at the center. For ρ greater than twenty and less than fifty-five, the shell deforms with a local minimum deflection point at the center and a local maximum deflection point between the center and the edge. For ρ greater than fifty-five, the shell deforms with two local maximum deflection points, one at the center and the other between the center and the edge.

He notes that with these new parameters there is a greater correlation between the theoretical and experimental results of Kaplan and Fung. Reiss also notes the need of further experimental results, particularly at the transition regions and for large values of ρ.

In a theory written with Greenberg and Keller,[8] the authors take the equations used by Chien[13] and solve them through power series expansions. They make the assumption of shallow shells but note a lack of knowledge as to the effect of the assumption on the nonshallow shell. The assumptions of thin shells and rotational symmetry are used to simplify the equations.

Differential operators and boundary conditions are employed as well as new variables γ and α before the variables are expanded in a power series in Θ. Recursion formulas are developed through which a pair of simultaneous equations are solved for each γ_i and α_i for each given P and ρ. P is the loading parameter $P = P_{2Eh^2}\left(\frac{R}{h}\right)^2$ and ρ is the geometric parameter $\rho = k^{-1/2}\Lambda^2\frac{R}{h}$. In these expressions $k = \frac{2}{3}(1-\nu^2)$, h is half the shell thickness, R is the radius of the middle surface, and Λ is the semi-angle of the shell opening.

A digital computer technique is developed in order to generate a solution. Since an iterative procedure is used for each value of ρ by increasing P, in effect an "experimental" test is performed. For $\rho = 11.312$, which would be in the middle of the first buckling mode, the radial deflection peaked at the center and fell off at the edge. For $\rho = 23.5$, the deformations are similar to the first mode for low loads. However, at higher loads the maximum deflection is located somewhere between the center and

the edge. With $\rho = 32$, the action is similar to $\rho = 23.5$. At $\rho = 52.2$, another transition is observed.

The authors compare a plot of P versus reduced center deflection for their results with the work of Kaplan and Fung for various values of the geometric parameter. They note only a fair agreement for low values, but a better agreement at higher values. They attribute the difficulty at low values to the increased importance of initial imperfections in shallow shells and also the difficulty in measuring the radius properly in shallow shells. They still indicate the presence of transition points. The lack of theoretical and experimental agreement is explained as being due to the situation where a small error in experimental determination of the geometric parameter leads to a large error in P_{cr}. They note that in some cases the numerical results predict greater P_{cr} than the experiments while in other cases the opposite is true.

In a publication written with Keller,[7] the authors consider the pressure deflection curve for a shallow spherical cap as shown in Figure 32. They point out that for $P_L < P < P_U$, there exists three possible equilibrium states for each pressure, but only one state outside the range for each pressure. The various branches are explained as follows: OU-unbuckled, LN-buckled, UL-unstable. P_l and P_u are then the lower and upper buckling loads.

They point out previously used methods of solving the

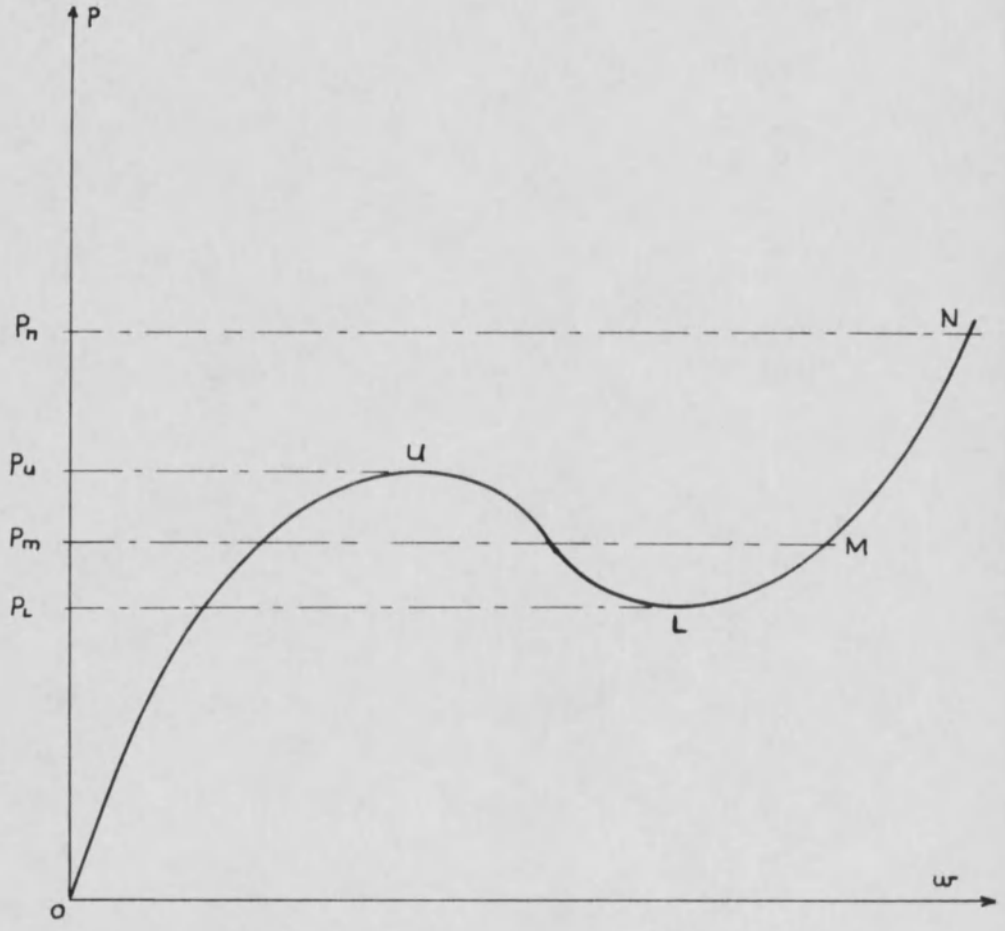

FIGURE 32

Pressure-Deflection Curve

buckling problem of a clamped spherical cap by using perturbation methods, power series, and linerizations. Keller and Reiss propose solving by iterations of a finite difference approximation of the boundary value problem.

The assumptions of a thin shallow shell as well as small strains and finite but small deflections are made. The differential equations are formulated as well as the difference equations.

Results indicate that ϱ_o , the value which separates caps that can buckle from those that cannot, must lie between six and eight. They determine P_l and P_u for values of the geometric parameter up to twenty. The intermediate buckling load P_m is determined from the point of intersection of the curves of potential energy versus P for the buckled and unbuckled states.

In a different publication concerning the modes of deformation,[20] Reiss points out that in modes I and III, the curvatures at the center are positive, while for mode II, the curvature is negative at the center. Thus there must exist values of the geometric parameter for which the curvature vanishes.

As to the situation of symmetric or nonsymmetric buckling, Reiss points out that the results of Kaplan and Fung were nearly all symmetric which they attributed to large initial symmetric irregularities. In the experimental work of Kloppel and Jungbluth on non-shallow shells, the buckles formed at the boundary. This they

attributed to initial stress and thickness variations which were large near the boundary.

In another theory,[18] Reiss's approach is to linearize the original nonlinear problem. He develops two linearized problems; the first called the linear eigenvalue problem is obtained by assuming the stress is constant and that the total vertical force at a particular point is equal to the vertical force produced along the edge by the external pressure. This yields $P_{cr} = \frac{\omega_0^2}{\varrho}$ where $\varrho = \kappa^{-1/2} \lambda^2 \frac{R}{h}$ and $\omega^2 = P/\varrho$.

Problem B, the linear elasticity problem for the bending of a shallow spherical cap, determines the transitional values of ϱ_i^* . He is able to obtain expressions for P_{cr} for various ranges of the geometrical parameter.

Reiss notes agreement with previous work except for the transitional values being higher than previously observed. He attributes the discrepancy to the failure to achieve a truly clamped edge in experimentation and the assumption of a shallow shell. He then suggests empirical formulas which modify the original expressions for P_{cr}.

Reissner, Eric[14-17]

Reissner does not specifically solve the buckling problem, but he has developed general equations which can be applied to

particular problems, such as the buckling of clamped spherical caps. In one development,[15] he begins with the equations of the linear theory of shallow shells, attributed to Marguerre. By manipulation, three differential equations are obtained in terms of the displacement components. Neglecting the longitudinal inertia effect and introducing a stress function, Reissner obtains two differential equations in terms of the stress function and the vertical displacement. He then analyzes the effect of the inertia terms through an order of magnitude analysis and determines the conditions under which the effect of longitudinal inertia is negligible compared to the effect of the transverse inertia.

In another theory,[16] he is concerned primarily with vibrations rather than buckling. The original equations are useful, however.

In a different publication,[17] Reissner develops equations for symmetrical bending of thin elastic shallow shells.

In an additional development,[14] Reissner obtains equations of equilibrium for shallow spherical shells as well as relationships between strain and stress resultants and strain and displacement quantities. Neglecting transverse shearing forces and introducing a stress function along with a load potential, he obtains two fourth order differential equations in terms of stress resultants and vertical displacements. He then reduces the governing differential

equations to two independent second order equations. In this paper he solves the equations for certain particular types of loading and edge conditions.

Simons, Roger M.[2]

Simons starts with the differential equations for small finite deflections of a thin shallow spherical shell of uniform thickness subjected to a uniform normal pressure which Reissner[14] developed. Using stress resultants, geometric and load parameters, boundary conditions and a change of variables, he manipulates the equations to a more favorable form. The geometric parameter is $\mu = m\sqrt{\frac{R}{h}}\alpha$, and the load parameter is $\gamma = \frac{m^6}{4}\rho\frac{R^4}{Eh^4}$. In these expressions m is $\left[12(1-\nu^2)\right]^{\frac{1}{4}}$, R is the base radius, h is the thickness, α is half the opening angle, and ρ is the uniform normal pressure. Simons uses a series form for the new variables and obtains recursion formulas for the coefficients. To obtain the leading coefficients he expresses the solution in a closed form in terms of Kelvin functions assuming the loading parameter is zero. He also develops a method for making the leading coefficients successively more accurate.

Simons explains the unstable state as being that state of the smallest inward pressure for which a decrease of pressure is accompanied by an increase of center deflection. Thus there is an assumption of symmetric buckling.

Introducing W, where W = w(o)/h, the ratio of the center deflection to the thickness, and W is a function of both the load parameter and the geometric parameter, the buckling criteria becomes $\frac{dW}{d\gamma} = \infty$. The smallest γ satisfying this is the critical value. Using a power series for W and manipulation, Simons determines the instability condition as $\mu^4 \geq \frac{3C_1C_4}{C_2^2 - 3C_1C_3}$. That is, instability occurs only if the inequality is satisfied. Instability cannot occur for a flat plate nor for a shell which is too shallow. The critical value of γ_{cr} is:

$$\gamma_{cr} = \frac{-1}{27C_1^2C_5^2}\left\{C_2\left[(2C_2^2 - 9C_1C_3)\mu^4 - 9C_1C_4\right]\mu^2 - 2\left[(C_2^2 - 3C_1C_3)\mu^4 - 3C_1C_4\right]^{\frac{3}{2}}\right\}$$

In these expressions $C_1 = 2(4-\mu)$; $C_2 = -3(13-3\nu)$; $C_3 = 9(5-\nu)$; $C_4 = 2304(1-\nu)$; $C_5 = 576(1-\nu)$

He notes the classical buckling pressure for a complete sphere is $-\mu^4$.

In comparing his results with those of Kaplan and Fung,[19] he notes a lack of agreement which he attributes to his assumption of γ and μ both being small. Therefore, his results are valid only for small values of these parameters.

Thurston, G. A.[31]

Thurston explains the disagreement with previous results as being caused by the fact that the solution for the nonlinear problem must be formulated as a sequence of linear problems. This

makes it difficult to distinguish between instability in the sequence of numerical calculations and points of instability of the differential equations which correspond to the classical buckling theory.

He begins with the equations of Reissner[14] and introduces parameters and new variables. The geometric parameter is $\mu^2 = \frac{m^2 a \alpha^2}{h} = 2m^2 \frac{H}{h}$ and the load parameter is $\gamma = \frac{m^6 a^4 \alpha^4}{4Eh^4} p$. In these expressions a is the radius, α is half the opening angle, h is the thickness, H is the rise above the base plane, and p is the pressure.

The equations are solved by assuming an approximate solution and then solving for the corrections. By this procedure, the nonlinear terms can be neglected since they are small as compared to the linear ones. A repeated application through a computer program leads to the solution.

Both the upper and lower buckling load curves are obtained. He notes the upper one agrees with Budiansky[25] and Weinitschke[9] while the lower one agrees with Keller and Reiss.[7] The experiments of Kaplan and Fung[19] lie between the two curves.

Tsien, Hsue-Shen[6,12]

Due to objections raised in a publication by Friedrichs,[5] Tsien[6] revises an earlier theory of von Karman and Tsien.[4]

Starting with the energy expression for the difference

between the sum of the additional strain energies of extension and bending and the virtual work of the external pressure, assuming a radial displacement function and minimizing the energy function, Tsien obtains a minimum value of the buckling stress when the amplitude of the buckle is small.

He notes the volume change due to an incompressible fluid pressure in a closed chamber is $\frac{v}{(1-\nu)t} = \frac{\sigma R}{Et} + \frac{\lambda t/R}{6(1-\nu)} \zeta \xi$. In this expression v is the volume change per unit area of shell surface, λ is the ratio of the area of a hemisphere with radius R to the area of a spherical segment; $\lambda = \frac{1}{1-\cos\theta}$, $\zeta = \theta^2 \frac{R}{t}$ and $\xi = \frac{fR}{t}$ when the radial displacement is defined as $\frac{w}{R} = f\left[1-\left(\frac{\alpha}{\beta}\right)^2\right]^2$ or f is the ratio of the maximum radial displacement at the center of the buckle to the radius of the shell.

Using the condition that the unbuckled and buckled equilibrium states have the same strain energy and the same volume change, Tsien obtains a curve of initial buckling stress and final buckling stress versus $\frac{R}{\lambda t}$. This curve shows the failing stress parameter $\sigma_i^* \frac{R}{Et}$ actually decreases with increasing values of R/t if λ remains constant.

He notes results of tests at California Institute of Technology, using water pressure on a clamped spherical cap where $\theta = 17°45'$ show agreement with his curves.

If a shell segment is loaded by fluid pressure when the fluid

is drawn from a large reservoir with a free surface, the small change of volume during buckling will not appreciably alter the fluid level in the reservoir. This hypothesis of Tsien leads to a different buckling stress parameter which is constant;

$$\sigma_3^* \frac{R}{Et} = \frac{\sqrt{5(1-\nu^2)}}{3}$$

In another theory,[12] Tsien presents an explanation of the strain energy versus deflection curve, Figure 33. Through this study a lower buckling load is observed. If a typical curve is considered, branches OC and AD correspond to stable equilibrium configurations and branch BC corresponds to an unstable configuration. Point B is seen to be a transition point from stable to unstable equilibrium.

Tsien states that previous work indicated that the load corresponding to point A was the lower buckling load. The energy represented by the vertical distance from A to the curve BC is the minimum external excitation required to cause buckling at point A. However, if the external excitation is large, buckling can occur at B' and the minimum external excitation required is the vertical distance from B' to B. This amount of energy is absorbed by the structure during buckling. Therefore, the lower buckling load is the load corresponding to point B'.

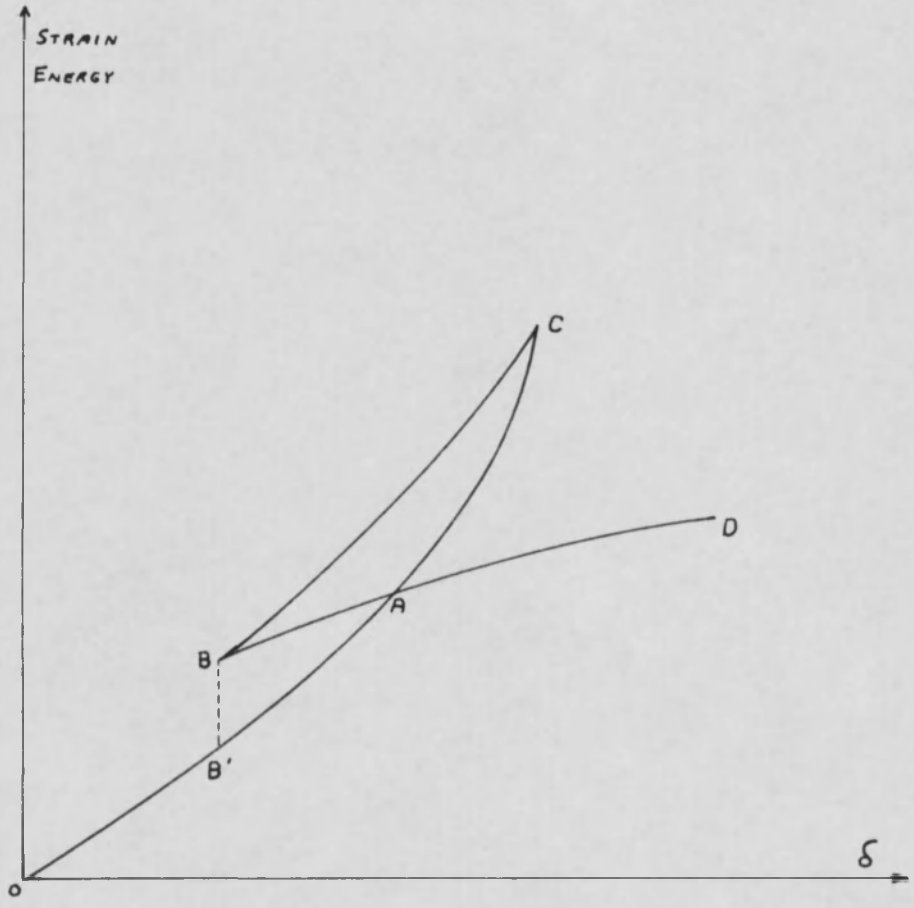

FIGURE 33

Strain Energy versus Deflection Coordinate

von Willich, Gideon P. R.[24]

von Willich makes assumptions regarding material properties that are of the usual type: homogeneous, isotropic and linearly elastic with the same modulus of elasticity in tension as in compression. The shell is assumed to have a constant thickness and this thickness is small. Further, he assumes that the deflections are symmetric about the axis and that the shell is shallow. In addition, the Euler-Bernoulli hypothesis is adopted, that is, normals to the middle surface before deformation remain normal after deformation and are inextensional.

Based upon these limitations, von Willich derives the energy equations for bending of the middle surface, extension of the middle surface and the potential energy of the applied pressure. He then assumes a deflected shape with the energy expression containing unknown parameters. An application of the principle of minimum potential energy yields these parameters.

Throughout the development, von Willich uses the parabolic equation $z = \frac{1}{2a}(r_o^2 - r^2)$ to define the surface of the shell.

von Willich determines critical values only for small values of the geometric parameter.

Weinitschke, Hubertus[9,10,23]

Weinitschke lists the following simplifying assumptions:

a. Euler-Bernoulli hypothesis

b. Deformations are rotationally symmetric

c. Tangential displacements of the middle surface are small compared with normal displacements

d. The radius of curvature is large compared to the shell length making the shells shallow

e. Uniform normal pressure is the only load

f. The thickness is uniform

Weinitschke uses the equations developed by Reissner[14] with dimensionless variables. The geometric parameter is $\mu^2 = 2m^2 \frac{H}{h} = \frac{m^2 a \alpha^2}{h}$, and the load parameter is $\gamma = \frac{m^6 a^4 \alpha^4}{4 E h^4} p$. In these expressions, a is the radius of curvature, α is the semiangle opening, h is the thickness, H is the rise of the shell from the base plane, $m^2 = [12(1-\nu^2)]^{\frac{1}{2}}$, and p is the uniform normal pressure. He also uses a parameter p where $p = p/q = \frac{\gamma}{\mu^4}$. Q is the buckling load of a complete spherical shell under uniform pressure given by the linear theory.

Introducing W where $W(\gamma) = \frac{w(0)}{h}$, the normal deflection at the apex divided by the thickness, the buckling criteria is $\frac{d\gamma}{dW} = 0$ and γ_c is a relative maximum of the function $\gamma(W)$.

He discusses the solution of the problem through use of power series with an iteration procedure applicable to a digital computer.

Weinitschke indicates agreement between his work and all previous theoretical results for low values of the geometric parameter. He notes a lack of agreement with experimental results and indicates the irregularities in shape and thickness account for the discrepancy. He is not able to account for these irregularities always producing lower buckling loads, however. He mentions the possibility of an instability associated with nonsymmetrical buckling or a wrinkling.

A previous development[23] notes the purpose being to apply the power series method used by Simons[2] for shallow shells. This paper uses a much smaller range of the geometric parameter.

In another previous publication,[10] Weinitschke comments on the discussion of apparent scattering in test data for the critical load. He notes that Klein[21] attributes the scatter to initial specimen irregularities and Reiss[20] interprets the scatter on the basis of sudden changes of the shape of the normal deflection of the shell. That is that there is an oscillation of P_{cr}, the dimensionless buckling load, with peaks at the transition values. Weinitschke presents results which support Klein.

Budiansky and Weinitschke[26] have written a publication which shows their stability curves to be in agreement despite the differences in their independent theories. A lack of agreement with the experimental results of Kaplan and Fung[19] is mentioned. They

indicate the need for a theoretical analysis assuming unsymmetrical buckling and unsymmetrical imperfections.

APPENDIX B

This section includes the test of an axial specimen with longitudinal and lateral strain gages in order to determine the modulus of elasticity and Poisson's ratio for the material.

AXIAL TEST DATA

Gage - A7
Gage Factor - 1.99
Transverse Sensitivity - -0.01

Width - 0.976 in.
Thickness - 0.031 in.
Area - 0.03065 in.^{2}

LOAD pounds	STRESS psi	GAGE READINGS longitudinal x 10^{-6}	GAGE READINGS lateral x 10^{-6}	STRAINS longitudinal x 10^{-6}	STRAINS lateral x 10^{-6}
50	163	12-1722	10-767	0	0
60	196	1841	761	119	-6
70	228	1956	756	234	-11
80	261	14- 72	751	350	-16
90	294	192	745	470	-22
100	326	311	739	589	-28
80	261	72	750	352	-17
70	228	12-1956	757	234	-10
60	196	1840	761	118	-6
50	163	1724	766	2	-1
60	196	1840	761	118	-6
80	261	14- 76	752	354	-12

LOAD pounds	STRESS psi	GAGE READINGS longitudinal x 10^{-6}	GAGE READINGS lateral x 10^{-6}	STRAINS longitudinal x 10^{-6}	STRAINS lateral x 10^{-6}
100	326	316	739	594	-28
120	457	879	713	1157	-54
140	522	1265	gage failed	1543	
176	specimen failed				

A linear relationship exists between load and strain up to about 90 pounds of load.

Modulus of elasticity $E = \frac{294-196}{(470-119) \times 10^{-6}} = 2.79 \times 10^5$ psi

Poisson's ratio $= \frac{-(-22-0)}{470} = 0.47$

APPENDIX C

This section contains the results of tests run on the vacuum former to develop the best forming technique. The various techniques are discussed in Chapter Three. The following data sheets consist of the thickness and radius of curvature measurements at each of the grid points as well as the values of standard deviation of thickness and radius of curvature. Actually the radius of curvature measurements are gage readings of the outer surface of the shell which can be converted to the radius of curvature of the middle surface of the shell by the formula $R = g/2 + \frac{1}{8g} - t/2$, where R is the radius of curvature of the middle surface, g is the gage reading and t is the thickness of the shell at that point. Variable settings are included on each data sheet.

FORMING TECHNIQUE DATA SHEET

TEST: 1

PER CENT ON: 75%

VACUUM TIME: Abt 3 Sec

SET TIME: Abt 10 Sec

MATERIAL SHEET: 1

CYCLE TIME: 100 Sec

DISTANCE OF FORM FROM PLATFORM: 6.3 in

OTHER COMMENTS: Holes in plate too small. Plexiglass plate unsatisfactory. Shell reheated and reformed adjusting frame height. Wood 3/4" below chamber.

Average Thickness: .025 in
Average Curvature: .035 in
Thickness Standard Deviation: .0025 in
Curvature Standard Deviation: .0025 in

POINT	THICKNESS in x 10^{-3}	CURVATURE in x 10^{-3}
1	27	24
2	25	36
3	28	36
4	28	33
5	28	35
6	28	36
7	29	36
8	26	36
9	26	37
10	25	35
11	23	37
12	25	36
13	26	35
14	26	36
15	26	35
16	25	35
17	25	35
18	24	37
19	20	35
20	19	32
21	16	35
22	24	35
23	24	35
24	27	36
25	20	35

FORMING TECHNIQUE DATA SHEET

TEST: 2

CYCLE TIME: 100 Sec

PER CENT ON: 75%

DISTANCE OF FORM FROM PLATFORM: 6 in

VACUUM TIME: Abt 3 Sec

OTHER COMMENTS: Material not hot enough.

SET TIME: Abt 10 Sec

MATERIAL SHEET: 1

Average Thickness: .022 in.
Average Curvature: .035 in.
Thickness Standard Deviation: .0042 in.
Curvature Standard Deviation: .0018 in.

POINT	THICKNESS in x 10^{-3}	CURVATURE in x 10^{-3}
1	27	27
2	27	37
3	28	37
4	28	36
5	28	35
6	28	36
7	27	35
8	26	36
9	27	35
10	22	36
11	21	36
12	23	35
13	23	34
14	22	35
15	22	35
16	21	34
17	21	34
18	19	36
19	17	35
20	18	34
21	17	35
22	17	35
23	17	34
24	17	35
25	17	35

FORMING TECHNIQUE DATA SHEET

TEST: 3

CYCLE TIME: 80 Sec

PER CENT ON: 75%

DISTANCE OF FORM FROM PLATFORM: 6 in

VACUUM TIME: Abt 3 Sec

OTHER COMMENTS: Plastic too hot.

SET TIME: Abt 10 Sec

MATERIAL SHEET: 1

Average Thickness: .021 in
Average Curvature: .034 in
Thickness Standard Deviation: .0059 in
Curvature Standard Deviation: .0026 in

POINT	THICKNESS in x 10^{-3}	CURVATURE in x 10^{-3}
1	29	27
2	29	38
3	26	35
4	26	35
5	27	36
6	26	37
7	28	36
8	28	36
9	29	35
10	23	37
11	22	36
12	23	35
13	21	34
14	18	33
15	19	33
16	24	35
17	25	36
18	14	34
19	17	34
20	12	31
21	11	30
22	14	31
23	15	31
24	15	37
25	13	31

FORMING TECHNIQUE DATA SHEET

TEST: 4

CYCLE TIME: 40 Sec

PER CENT ON: 50%

DISTANCE OF FORM FROM PLATFORM: 6 in

VACUUM TIME: Abt 5 Sec

OTHER COMMENTS: Not hot enough.

SET TIME: Abt 15 Sec

MATERIAL SHEET: 1

Average Thickness: .024 in
Average Curvature: .035 in
Thickness Standard Deviation: .0041 in
Curvature Standard Deviation: .0018 in

POINT	THICKNESS in x 10^{-3}	CURVATURE in x 10^{-3}
1	30	27
2	28	35
3	29	36
4	29	35
5	29	35
6	29	35
7	29	36
8	29	36
9	28	36
10	24	34
11	23	35
12	24	34
13	24	35
14	24	35
15	23	35
16	22	34
17	22	35
18	18	35
19	19	35
20	20	35
21	20	35
22	19	34
23	20	37
24	19	34
25	19	36

FORMING TECHNIQUE DATA SHEET

TEST: 5

CYCLE TIME: 120 Sec

PER CENT ON: 50%

DISTANCE OF FORM FROM PLATFORM: 6 in

VACUUM TIME: Abt 5 Sec

OTHER COMMENTS: Too hot, holes on edge.

SET TIME: Abt 15 Sec

MATERIAL SHEET: 1

Average Thickness: .024 in
Average Curvature: .035 in
Thickness Standard Deviation: .0043 in
Curvature Standard Deviation: .0018 in

POINT	THICKNESS in x 10^{-3}	CURVATURE in x 10^{-3}
1	30	28
2	29	36
3	29	36
4	29	36
5	29	36
6	28	36
7	28	35
8	30	35
9	29	35
10	24	35
11	23	34
12	22	34
13	22	34
14	22	36
15	24	36
16	25	36
17	25	37
18	20	35
19	20	34
20	19	35
21	18	36
22	18	36
23	19	36
24	18	38
25	18	36

FORMING TECHNIQUE DATA SHEET

TEST: 6

CYCLE TIME: 60 Sec

PER CENT ON: 50%

DISTANCE OF FORM FROM PLATFORM: 6 in

VACUUM TIME: Abt 5 Sec

OTHER COMMENTS: Not a sharp edge.

SET TIME: Abt 15 Sec

MATERIAL SHEET: 1

Average Thickness: .023 in
Average Curvature: .035 in
Thickness Standard Deviation: .0043 in
Curvature Standard Deviation: .0020 in

POINT	THICKNESS in x 10^{-3}	CURVATURE in x 10^{-3}
1	29	27
2	28	35
3	28	36
4	28	37
5	28	38
6	28	37
7	27	37
8	29	36
9	27	36
10	23	36
11	22	35
12	21	34
13	22	35
14	22	36
15	23	35
16	24	36
17	23	34
18	18	38
19	18	35
20	18	36
21	18	35
22	18	34
23	17	35
24	17	35
25	18	35

FORMING TECHNIQUE DATA SHEET

TEST: 7

CYCLE TIME: 30 Sec

PER CENT ON: 85%

DISTANCE OF FORM FROM PLATFORM: 6 in

VACUUM TIME: Abt 5 Sec

OTHER COMMENTS: Not a sharp edge.

SET TIME: Abt 15 Sec

MATERIAL SHEET: 1

Average Thickness: .023 in
Average Curvature: .035 in
Thickness Standard Deviation: .0043 in
Curvature Standard Deviation: .0018 in

POINT	THICKNESS in x 10^{-3}	CURVATURE in x 10^{-3}
1	29	28
2	28	36
3	28	36
4	28	36
5	28	36
6	27	36
7	27	37
8	27	37
9	28	37
10	23	35
11	24	35
12	24	36
13	23	34
14	22	35
15	21	34
16	21	34
17	22	34
18	18	35
19	18	35
20	18	35
21	17	36
22	17	36
23	17	34
24	18	33
25	18	36

FORMING TECHNIQUE DATA SHEET

TEST: 8

CYCLE TIME: 80 Sec

PER CENT ON: 50%

DISTANCE OF FORM FROM PLATFORM: 6 in

VACUUM TIME: Abt 5 Sec

OTHER COMMENTS: Too hot, holes on edge.

SET TIME: Abt 15 Sec

MATERIAL SHEET: 1

Average Thickness: .023 in
Average Curvature: .035 in
Thickness Standard Deviation: .0047 in
Curvature Standard Deviation: .0019 in

POINT	THICKNESS	CURVATURE
1	29	27
2	29	36
3	29	37
4	28	35
5	29	36
6	30	37
7	29	36
8	28	37
9	29	37
10	24	36
11	23	36
12	23	34
13	24	34
14	23	35
15	23	35
16	22	34
17	23	35
18	18	36
19	17	35
20	18	35
21	19	35
22	17	35
23	17	35
24	17	34
25	18	37

FORMING TECHNIQUE DATA SHEET

TEST: 9

CYCLE TIME: 30 Sec

PER CENT ON: 35%

DISTANCE OF FORM FROM PLATFORM: 6 in

VACUUM TIME: Abt 5 Sec

OTHER COMMENTS: Edges not sharp.

SET TIME: Abt 15 Sec

MATERIAL SHEET: 1

Average Thickness: .025 in
Average Curvature: .035 in
Thickness Standard Deviation: .0039 in
Curvature Standard Deviation: .0019 in

POINT	THICKNESS in x 10^{-3}	CURVATURE in x 10^{-3}
1	31	27
2	30	35
3	30	35
4	29	36
5	30	36
6	29	35
7	29	36
8	29	35
9	29	36
10	24	35
11	25	36
12	24	35
13	24	35
14	24	35
15	24	34
16	24	34
17	24	35
18	20	38
19	20	36
20	20	37
21	20	37
22	21	35
23	20	34
24	20	35
25	21	35

FORMING TECHNIQUE DATA SHEET

TEST: 10

CYCLE TIME:

PER CENT ON:

DISTANCE OF FORM FROM PLATFORM:

VACUUM TIME:

OTHER COMMENTS: Unformed flat disk.

SET TIME:

MATERIAL SHEET: 2

Average Thickness: .0314 in
Average Curvature:
Thickness Standard Deviation: .0005 in
Curvature Standard Deviation:

POINT	THICKNESS in x 10^{-3}	CURVATURE in x 10^{-3}
1	32	Not Measured
2	32	"
3	32	"
4	31	"
5	31	"
6	31	"
7	31	"
8	32	"
9	32	"
10	32	"
11	32	"
12	31	"
13	31	"
14	31	"
15	32	"
16	32	"
17	31	"
18	31	"
19	32	"
20	31	"
21	31	"
22	31	"
23	31	"
24	31	"
25	31	"

FORMING TECHNIQUE DATA SHEET

TEST: 11

CYCLE TIME: 30 Sec

PER CENT ON: 40%

DISTANCE OF FORM FROM PLATFORM: 6 in

VACUUM TIME: Abt 5 Sec

OTHER COMMENTS: Rim added, plaster added to top, not enough vacuum.

SET TIME: Abt 10 Sec

MATERIAL SHEET: 2

Average Thickness: .025 in
Average Curvature: .033 in
Thickness Standard Deviation: .0045 in
Curvature Standard Deviation: .0032 in

POINT	THICKNESS in x 10^{-3}	CURVATURE in x 10^{-3}
1	31	33
2	29	26
3	31	30
4	29	32
5	26	33
6	28	28
7	29	26
8	29	31
9	29	27
10	24	36
11	24	34
12	23	35
13	23	34
14	25	35
15	25	36
16	26	36
17	25	35
18	19	36
19	20	34
20	19	36
21	18	34
22	18	36
23	19	34
24	18	34
25	18	35

FORMING TECHNIQUE DATA SHEET

TEST: 12

CYCLE TIME: 30 Sec

PER CENT ON: 30%

DISTANCE OF FORM FROM PLATFORM: 6 in

VACUUM TIME: Abt 5 Sec

OTHER COMMENTS: Holes in plate made larger, edge did not hold.

SET TIME: Abt 10 Sec

MATERIAL SHEET: 2

Average Thickness: .023 in
Average Curvature:
Thickness Standard Deviation: .0040 in
Curvature Standard Deviation:

POINT	THICKNESS in x 10^{-3}	CURVATURE
1	30	Not Measured
2	28	"
3	26	"
4	27	"
5	28	"
6	28	"
7	27	"
8	27	"
9	27	"
10	24	"
11	24	"
12	23	"
13	25	"
14	22	"
15	23	"
16	24	"
17	25	"
18	17	"
19	19	"
20	19	"
21	18	"
22	18	"
23	19	"
24	18	"
25	18	"

FORMING TECHNIQUE DATA SHEET

TEST: 13

CYCLE TIME: 80 Sec

PER CENT ON: 50%

DISTANCE OF FORM FROM PLATFORM: 5.75 in

VACUUM TIME: Abt 5 Sec

OTHER COMMENTS: This was reheated and developed a hole in the edge.

SET TIME: Abt 10 Sec

MATERIAL SHEET: 2

Average Thickness: .024 in
Average Curvature: .033 in
Thickness Standard Deviation: .0035 in
Curvature Standard Deviation: .0026 in

POINT	THICKNESS in x 10^{-3}	CURVATURE in x 10^{-3}
1	27	32
2	28	30
3	29	32
4	28	30
5	29	30
6	28	30
7	28	30
8	28	29
9	29	29
10	24	35
11	26	37
12	23	35
13	23	34
14	23	34
15	24	34
16	25	35
17	24	35
18	20	36
19	20	36
20	19	36
21	20	35
22	20	34
23	20	35
24	20	36
25	20	36

FORMING TECHNIQUE DATA SHEET

TEST: 14

CYCLE TIME: 40 Sec

PER CENT ON: 40%

DISTANCE OF FORM FROM PLATFORM: 6.25 in

VACUUM TIME: Abt 5 Sec

OTHER COMMENTS: Vacuum applied quickly. Still not a sharp edge.

SET TIME: Abt 10 Sec

MATERIAL SHEET: 2

Average Thickness: .023 in
Average Curvature: .032 in
Thickness Standard Deviation: .0042 in
Curvature Standard Deviation: .0028 in

POINT	THICKNESS in x 10^{-3}	CURVATURE in x 10^{-3}
1	29	32
2	27	27
3	27	26
4	26	29
5	26	28
6	28	28
7	28	29
8	28	30
9	28	31
10	23	34
11	24	34
12	24	34
13	24	34
14	24	34
15	23	34
16	23	33
17	22	33
18	18	35
19	17	34
20	17	34
21	17	34
22	16	36
23	17	35
24	18	34
25	18	34

FORMING TECHNIQUE DATA SHEET

TEST: 15

CYCLE TIME: 40 Sec

PER CENT ON: 40%

DISTANCE OF FORM FROM PLATFORM: 6.3 in

VACUUM TIME: Abt 5 Sec

OTHER COMMENTS: Hump at top sanded, not a sharp edge.

SET TIME: Abt 10 Sec

MATERIAL SHEET: 2

Average Thickness: .023 in
Average Curvature: .033 in
Thickness Standard Deviation: .0048 in
Curvature Standard Deviation: .0032 in

POINT	THICKNESS in x 10^{-3}	CURVATURE in x 10^{-3}
1	29	34
2	29	35
3	28	35
4	29	28
5	28	25
6	28	24
7	28	27
8	29	35
9	28	35
10	22	34
11	24	35
12	24	34
13	24	35
14	24	35
15	23	35
16	24	34
17	23	33
18	18	34
19	17	33
20	17	34
21	17	33
22	17	34
23	16	35
24	17	35
25	17	34

FORMING TECHNIQUE DATA SHEET

TEST: 16

PER CENT ON: 40%

VACUUM TIME: Abt 5 Sec

SET TIME: Abt 10 Sec

MATERIAL SHEET: 2

CYCLE TIME: 80 Sec

DISTANCE OF FORM FROM PLATFORM: 5.32 in

OTHER COMMENTS: Silicone helped a little in release; it was reheated since first forming was not a sharp edge.

Average Thickness: .025 in
Average Curvature: .033 in
Thickness Standard Deviation: .0028 in
Curvature Standard Deviation: .0030 in

POINT	THICKNESS in x 10^{-3}	CURVATURE in x 10^{-3}
1	28	32
2	28	33
3	28	26
4	27	26
5	28	26
6	29	33
7	29	35
8	29	36
9	29	35
10	25	34
11	26	34
12	26	35
13	26	35
14	24	35
15	24	34
16	24	33
17	24	34
18	22	34
19	22	33
20	22	35
21	22	34
22	21	36
23	22	36
24	22	36
25	22	35

FORMING TECHNIQUE DATA SHEET

TEST: 17-25

CYCLE TIME: Reheated 240 Sec

PER CENT ON: 30%

DISTANCE OF FORM FROM PLATFORM: 6.25

VACUUM TIME: 5 Sec

OTHER COMMENTS: Still not a sharp edge.

SET TIME: Abt 15 Sec

MATERIAL SHEET: 2

Average Thickness: .026 in
Average Curvature: .034 in
Thickness Standard Deviation: .0043 in
Curvature Standard Deviation: .0016 in

POINT	THICKNESS in x 10^{-3}	CURVATURE in x 10^{-3}
1	32	27
2	30	34
3	31	34
4	30	33
5	30	35
6	30	35
7	30	35
8	30	35
9	30	35
10	25	33
11	26	34
12	28	35
13	26	34
14	26	33
15	25	34
16	24	34
17	25	34
18	21	34
19	19	33
20	19	33
21	21	33
22	20	34
23	20	33
24	20	34
25	21	34

FORMING TECHNIQUE DATA SHEET

TEST: 26-28

CYCLE TIME: 60 Sec

PER CENT ON: 60%

DISTANCE OF FORM FROM PLATFORM: 5.6 in

VACUUM TIME: Abt 5 Sec

SET TIME: Abt 10 Sec

OTHER COMMENTS: Reheated, changing amount of heat on and plate height. Holes developed on edge.

MATERIAL SHEET: 2

Average Thickness: .027 in
Average Curvature: .035 in
Thickness Standard Deviation: .0027 in
Curvature Standard Deviation: .0014 in

POINT	THICKNESS in x 10^{-3}	CURVATURE in x 10^{-3}
1	30	32
2	29	36
3	30	37
4	30	37
5	30	37
6	29	37
7	30	35
8	30	36
9	29	35
10	25	35
11	24	34
12	22	34
13	24	34
14	26	34
15	25	36
16	25	35
17	25	36
18		
19		
20		
21		
22		
23		
24		
25		

FORMING TECHNIQUE DATA SHEET

TEST: 29

CYCLE TIME: 40 Sec

PER CENT ON: 60%

DISTANCE OF FORM FROM PLATFORM: 5.6 in

VACUUM TIME: Abt 5 Sec

OTHER COMMENTS: Hole on edge but forming complete.

SET TIME: Abt 10 Sec

MATERIAL SHEET: 2

Average Thickness: .026 in
Average Curvature: .035 in
Thickness Standard Deviation: .0042 in
Curvature Standard Deviation: .0008 in

POINT	THICKNESS in x 10^{-3}	CURVATURE in x 10^{-3}
1	30	33
2	30	35
3	29	36
4	30	36
5	30	36
6	30	36
7	30	35
8	31	35
9	30	35
10	25	34
11	24	35
12	23	35
13	24	34
14	26	34
15	25	34
16	26	35
17	26	34
18	21	36
19	21	35
20	19	36
21	20	35
22	20	35
23	21	35
24	20	34
25	20	34

FORMING TECHNIQUE DATA SHEET

TEST: 30-31

CYCLE TIME: 60 Sec

PER CENT ON: 60%

DISTANCE OF FORM FROM PLATFORM: 5.8 in

VACUUM TIME: Abt 5 Sec

SET TIME: Abt 10 Sec

OTHER COMMENTS: Frame moved on #30 so reheated. Edge holes caused incomplete forming.

MATERIAL SHEET: 2

Average Thickness: .027 in
Average Curvature: .035 in
Thickness Standard Deviation: .0030 in
Curvature Standard Deviation: .0009 in

POINT	THICKNESS in x 10^{-3}	CURVATURE in x 10^{-3}
1	30	35
2	29	36
3	30	37
4	30	36
5	29	36
6	30	37
7	28	36
8	29	36
9	29	35
10	24	35
11	23	35
12	23	35
13	24	34
14	24	35
15	23	35
16	24	34
17	23	35
18		
19		
20		
21		
22		
23		
24		
25		

FORMING TECHNIQUE DATA SHEET

TEST: 32-33

CYCLE TIME: 60 Sec

PER CENT ON: 50%

DISTANCE OF FORM FROM PLATFORM: 6 in

VACUUM TIME: Abt 5 Sec

OTHER COMMENTS: #32 re-heated with plate raised. Holes on edge of #33 caused incomplete forming.

SET TIME: Abt 10 Sec

MATERIAL SHEET: 2

Average Thickness: .027 in
Average Curvature: .035 in
Thickness Standard Deviation: .0027 in
Curvature Standard Deviation: .0013 in

POINT	THICKNESS in x 10^{-3}	CURVATURE in x 10^{-3}
1	30	33
2	29	36
3	29	36
4	29	36
5	29	36
6	30	35
7	29	38
8	28	37
9	29	37
10	24	35
11	25	34
12	25	34
13	24	36
14	23	35
15	24	35
16	23	36
17	23	34
18		
19		
20		
21		
22		
23		
24		
25		

FORMING TECHNIQUE DATA SHEET

TEST: 34

CYCLE TIME: 40 Sec

PER CENT ON: 50%

DISTANCE OF FORM FROM PLATFORM: 6 in

VACUUM TIME: Abt 5 Sec

OTHER COMMENTS: #16 reheated, holes in edge.

SET TIME: Abt 10 Sec

MATERIAL SHEET: 2

Average Thickness: .024 in
Average Curvature: .036 in
Thickness Standard Deviation: .0031 in
Curvature Standard Deviation: .0015 in

POINT	THICKNESS in x 10^{-3}	CURVATURE in x 10^{-3}
1	28	32
2	27	36
3	28	36
4	29	36
5	29	36
6	28	36
7	28	37
8	29	37
9	28	37
10	23	34
11	23	35
12	24	35
13	24	35
14	24	34
15	23	34
16	23	34
17	23	34
18	21	36
19	21	37
20	21	37
21	21	36
22	20	34
23	21	38
24	22	36
25	22	37

FORMING TECHNIQUE DATA SHEET

TEST: 35

CYCLE TIME: 50 Sec

PER CENT ON: 50%

DISTANCE OF FORM FROM PLATFORM: 6.25 in

VACUUM TIME: Abt 5 Sec

OTHER COMMENTS: #15 reheated.

SET TIME: Abt 10 Sec

MATERIAL SHEET: 2

Average Thickness: .024 in
Average Curvature: .035 in
Thickness Standard Deviation: .0043 in
Curvature Standard Deviation: .0009 in

POINT	THICKNESS in x 10^{-3}	CURVATURE in x 10^{-3}
1	29	35
2	28	37
3	28	35
4	28	36
5	27	35
6	28	35
7	28	36
8	28	37
9	28	37
10	21	36
11	25	36
12	24	35
13	24	35
14	24	36
15	23	35
16	23	35
17	22	35
18	20	34
19	19	35
20	18	35
21	18	35
22	18	35
23	19	35
24	19	36
25	18	34

FORMING TECHNIQUE DATA SHEET

TEST: 36

CYCLE TIME: 50 Sec

PER CENT ON: 50%

DISTANCE OF FORM FROM PLATFORM: 6 in

VACUUM TIME: 5 Sec after plastic drapes

OTHER COMMENTS: #14 re-heated, hump sanded slightly. Forming looked good until hole formed causing a rounding at edge.

SET TIME: Abt 10 Sec

MATERIAL SHEET: 2

Average Thickness: .026 in
Average Curvature: .034 in
Thickness Standard Deviation: .0025 in
Curvature Standard Deviation: .0021 in

POINT	THICKNESS in x 10^{-3}	CURVATURE in x 10^{-3}
1	26	27
2	28	35
3	28	34
4	28	33
5	28	34
6	28	36
7	28	36
8	28	37
9	28	36
10	23	33
11	24	34
12	24	35
13	24	35
14	23	35
15	22	34
16	22	34
17	22	34
18		
19		
20		
21		
22		
23		
24		
25		

FORMING TECHNIQUE DATA SHEET

TEST: 37

CYCLE TIME: 50 Sec

PER CENT ON: 50%

DISTANCE OF FORM FROM PLATFORM: 6 in

VACUUM TIME: 10 Sec - As frame comes down

OTHER COMMENTS: #11 re-formed. It was tight before hole formed.

SET TIME: Abt 10 Sec

MATERIAL SHEET: 2

Average Thickness: .025 in
Average Curvature: .035 in
Thickness Standard Deviation: .0041 in
Curvature Standard Deviation: .0011 in

POINT	THICKNESS in x 10^{-3}	CURVATURE in x 10^{-3}
1	30	33
2	30	36
3	30	37
4	30	37
5	30	36
6	30	35
7	30	35
8	31	37
9	30	36
10	24	34
11	25	35
12	24	35
13	24	34
14	25	35
15	26	36
16	24	35
17	24	34
18	21	36
19	21	37
20	21	36
21	19	35
22	20	36
23	21	35
24	20	35
25	20	36

FORMING TECHNIQUE DATA SHEET

TEST: 38

CYCLE TIME: 50 Sec

PER CENT ON: 40%

DISTANCE OF FORM FROM PLATFORM: 5.33 in

VACUUM TIME: 5 Sec - After shell drapes

OTHER COMMENTS: #9 re-heated, hump sanded slightly. Hole in edge again.

SET TIME: Abt 10 Sec

MATERIAL SHEET: 1

Average Thickness: .026 in
Average Curvature: .035 in
Thickness Standard Deviation: .0027 in
Curvature Standard Deviation: .0014 in

POINT	THICKNESS in x 10^{-3}	CURVATURE in x 10^{-3}
1	28	30
2	29	35
3	28	36
4	29	36
5	29	36
6	29	36
7	29	36
8	29	35
9	30	35
10	24	35
11	24	35
12	23	35
13	23	34
14	24	36
15	24	36
16	23	35
17	25	35
18		
19		
20		
21		
22		
23		
24		
25		

FORMING TECHNIQUE DATA SHEET

TEST: 39

CYCLE TIME: 50 Sec

PER CENT ON: 40%

DISTANCE OF FORM FROM PLATFORM: 5.33 in

VACUUM TIME: Abt 10 Sec - As frame comes down

OTHER COMMENTS: #7 re-heated. Looked close until edge hole developed.

SET TIME: Abt 10 Sec

MATERIAL SHEET: 1

Average Thickness: .024 in
Average Curvature: .034 in
Thickness Standard Deviation: .0032 in
Curvature Standard Deviation: .0018 in

POINT	THICKNESS in x 10^{-3}	CURVATURE in x 10^{-3}
1	27	28
2	29	35
3	28	34
4	28	35
5	28	36
6	28	36
7	28	35
8	27	36
9	28	35
10	24	34
11	25	35
12	25	35
13	24	35
14	23	33
15	23	32
16	22	32
17	23	33
18	21	33
19	20	35
20	21	35
21	20	36
22	20	35
23	20	36
24	20	34
25	21	35

FORMING TECHNIQUE DATA SHEET

TEST: 40

CYCLE TIME: 50 Sec

PER CENT ON: 40%

DISTANCE OF FORM FROM PLATFORM: 5.33 in

VACUUM TIME: 1 Sec as frame comes down

OTHER COMMENTS: #6 re-heated, hump sanded again.

SET TIME: Abt 10 Sec

MATERIAL SHEET: 1

Average Thickness: .024 in
Average Curvature: .035 in
Thickness Standard Deviation: .0031 in
Curvature Standard Deviation: .0015 in

POINT	THICKNESS in x 10^{-3}	CURVATURE in x 10^{-3}
1	25	29
2	27	34
3	28	36
4	27	37
5	28	35
6	28	35
7	26	35
8	28	34
9	26	33
10	26	35
11	25	34
12	25	34
13	25	34
14	25	33
15	26	35
16	26	35
17	26	35
18	20	35
19	20	35
20	20	36
21	20	35
22	20	36
23	20	35
24	20	34
25	20	34

FORMING TECHNIQUE DATA SHEET

TEST: 41

CYCLE TIME: 50 Sec

PER CENT ON: 50%

DISTANCE OF FORM FROM PLATFORM: 6 in

VACUUM TIME: 1 Sec after it drapes

OTHER COMMENTS: #4 re-heated. Hole in edge.

SET TIME: 10 Sec

MATERIAL SHEET: 1

Average Thickness: .027 in
Average Curvature: .035 in
Thickness Standard Deviation: .0019 in
Curvature Standard Deviation: .0008 in

POINT	THICKNESS in x 10^{-3}	CURVATURE in x 10^{-3}
1	29	37
2	29	36
3	29	35
4	28	34
5	27	35
6	29	34
7	28	35
8	29	35
9	29	34
10	25	35
11	24	34
12	25	34
13	25	35
14	26	35
15	26	35
16	25	36
17	24	35
18	19	
19	20	
20	20	
21	20	
22	19	
23	19	
24	19	
25	19	

FORMING TECHNIQUE DATA SHEET

TEST: 42

CYCLE TIME: 60 Sec

PER CENT ON: 35%

DISTANCE OF FORM FROM PLATFORM: 5.33 in

VACUUM TIME: 2 Sec as frame comes down

OTHER COMMENTS: Reheated

SET TIME: Abt 15 Sec

MATERIAL SHEET: 3

Average Thickness: .028 in
Average Curvature: .035 in
Thickness Standard Deviation: .0031 in
Curvature Standard Deviation: .0016 in

POINT	THICKNESS in x 10^{-3}	CURVATURE in x 10^{-3}
1	32	29
2	31	36
3	32	36
4	32	35
5	33	36
6	31	35
7	32	36
8	32	36
9	33	36
10	27	34
11	28	35
12	28	35
13	29	35
14	29	35
15	29	35
16	28	34
17	27	33
18	25	36
19	24	38
20	25	35
21	24	33
22	25	35
23	25	35
24	25	37
25	25	35

FORMING TECHNIQUE DATA SHEET

TEST: 43-44

CYCLE TIME: 60 Sec

PER CENT ON: 50%

DISTANCE OF FORM FROM PLATFORM: 5.33 in

VACUUM TIME: 5 Sec as frame comes down

OTHER COMMENTS: Reheated

SET TIME: Abt 15 Sec

MATERIAL SHEET: 3

Average Thickness: .027 in
Average Curvature: .035 in
Thickness Standard Deviation: .0032 in
Curvature Standard Deviation: .0013 in

POINT	THICKNESS in x 10^{-3}	CURVATURE in x 10^{-3}
1	30	32
2	31	36
3	31	36
4	31	36
5	32	36
6	31	36
7	31	36
8	30	36
9	31	36
10	26	33
11	26	33
12	26	34
13	25	33
14	27	34
15	26	33
16	26	34
17	26	34
18	23	36
19	22	34
20	23	35
21	23	35
22	25	37
23	24	36
24	23	35
25	25	36

FORMING TECHNIQUE DATA SHEET

TEST: 45

CYCLE TIME: 50 Sec

PER CENT ON: 35%

DISTANCE OF FORM FROM PLATFORM: 5.33 in

VACUUM TIME: 5 Sec as frame comes down

OTHER COMMENTS: Loss of air due to improper adjustment.

SET TIME: Abt 15 Sec

MATERIAL SHEET: 3

Average Thickness: .026 in
Average Curvature: .034 in
Thickness Standard Deviation: .0036 in
Curvature Standard Deviation: .0019 in

POINT	THICKNESS in x 10^{-3}	CURVATURE in x 10^{-3}
1	29	27
2	30	36
3	31	36
4	31	36
5	30	35
6	30	34
7	30	34
8	32	35
9	30	35
10	25	33
11	24	32
12	26	32
13	26	33
14	27	34
15	26	34
16	26	34
17	25	33
18	21	35
19	21	36
20	21	35
21	22	36
22	24	34
23	23	33
24	22	35
25	22	35

APPENDIX D

This section contains the results of the buckling tests for each of the shell types. The description of the testing is in Chapter Three. This section includes the buckling pressure and volume change for each shell tested.

BUCKLING TEST DATA SHEET

Shape: I Sheet: 5 Rise: 3.51 in.

Shell Number	Buckling Pressure p in psi	Radius of Curvature R in inches	Thickness t in in.	Vol. Change V in in.^{3}
1	5.1	3.60	.023	-
2	5.0	3.41	.023	-
3	4.0	3.50	.022	-
4	5.0	3.41	.024	-
5	3.6	3.70	.023	-
6	4.8	3.70	.023	-
7	4.3	3.60	.024	-
8	3.9	3.60	.021	2.5
9	3.7	3.60	.020	1.4
10	-	-	-	-
11	-	-	-	-

BUCKLING TEST DATA SHEET

Shape: I Sheet: 6 Rise: 3.51 in.

Shell Number	Buckling Pressure p in psi	Radius of Curvature R in inches	Thickness t in in.	Vol. Change V in $in.^3$
1	4.4	3.41	.025	-
2	5.3	3.50	.024	2.8
3	4.7	3.50	.025	2.8
4	5.3	3.50	.024	4.4
5	5.0	3.50	.024	-
6	5.2	3.50	.025	3.8
7	5.1	3.70	.024	3.3
8	5.1	3.50	.026	-
9	4.5	3.50	.025	-
10	5.5	3.70	.025	-
11	-	-	-	-

BUCKLING TEST DATA SHEET

Shape: I Sheet: 7 Rise: 3.51 in.

Shell Number	Buckling Pressure p in psi	Radius of Curvature R in inches	Thickness t in in.	Vol. Change V in $in.^3$
1	6.1	3.41	.025	2.0
2	6.2	3.41	.024	2.1
3	6.4	3.50	.025	2.4
4	5.9	3.50	.024	1.7
5	5.3	3.50	.024	2.6
6	6.6	3.50	.026	3.6
7	3.9	3.50	.025	-
8	6.0	3.50	.026	4.2
9	5.9	3.50	.024	-
10	3.9	3.41	.025	3.0
11	4.8	3.50	.026	-

BUCKLING TEST DATA SHEET

Shape: I Sheet: 8 Rise: 3.51 in.

Shell Number	Buckling Pressure p in psi	Radius of Curvature R in inches	Thickness t in in.	Vol. Change V in $in.^3$
1	6.4	3.50	.024	2.1
2	6.0	3.50	.025	2.0
3	6.4	3.50	.026	2.1
4	5.7	3.41	.025	-
5	4.5	3.41	.024	1.6
6	6.0	3.50	.025	2.3
7	6.3	3.50	.025	2.0
8	5.2	3.50	.023	3.9
9	6.2	3.41	.026	-
10	5.7	3.41	.025	3.1
11	6.4	3.50	.025	4.8

BUCKLING TEST DATA SHEET

Shape: I Sheet: 9 Rise: 3.51 in.

Shell Number	Buckling Pressure p in psi	Radius of Curvature R in inches	Thickness t in in.	Vol. Change V in in.^{3}
1	Leak	-	-	-
2	4.7	3.60	.021	-
3	2.7	3.60	.021	1.9
4	3.8	3.60	.021	-
5	3.2	3.60	.021	2.3
6	3.4	3.41	.021	2.7
7	3.8	3.60	.021	-
8	3.8	3.60	.021	-
9	3.01	3.41	.020	1.4
10	3.4	3.50	.021	-
11	4.3	3.41	.022	1.8

BUCKLING TEST DATA SHEET

Shape: II Sheet: 10 Rise: 2.65 in.

Shell Number	Buckling Pressure p in psi	Radius of Curvature R in inches	Thickness t in in.	Vol. Change V in $in.^3$
1	Leak	-	-	-
2	3.4	3.96	.023	-
3	4.1	3.97	.024	-
4	4.5	3.60	.024	-
5	3.6	3.96	.023	-
6	4.1	3.60	.024	2.6
7	4.7	3.97	.024	-
8	4.0	3.96	.023	3.9
9	3.8	3.60	.024	3.5
10	4.2	3.60	.023	4.9
11	4.0	3.60	.024	-

BUCKLING TEST DATA SHEET

Shape: II Sheet: 11 Rise: 2.65 in.

Shell Number	Buckling Pressure p in psi	Radius of Curvature R in inches	Thickness t in in.	Vol. Change V in $in.^3$
1	4.7	3.97	.026	-
2	4.8	3.97	.025	-
3	5.6	3.60	.025	5.7
4	5.3	3.60	.025	5.2
5	5.4	3.60	.025	3.5
6	4.4	3.60	.025	4.2
7	5.0	3.97	.026	4.3
8	4.8	3.60	.026	3.9
9	5.3	3.97	.026	5.6
10	5.1	3.60	.025	5.8
11	5.0	3.97	.025	-

BUCKLING TEST DATA SHEET

Shape: II Sheet: 12 Rise: 2.65 in.

Shell Number	Buckling Pressure p in psi	Radius of Curvature R in inches	Thickness t in in.	Vol. Change V in $in.^3$
1	4.3	3.97	.026	5.6
2	4.9	3.97	.026	4.8
3	5.4	3.60	.026	-
4	5.5	3.60	.025	-
5	4.6	3.60	.025	3.1
6	4.4	3.97	.025	3.1
7	4.5	3.60	.025	3.8
8	4.8	3.97	.026	3.6
9	5.1	3.60	.026	4.2
10	5.1	3.97	.026	-
11	Leak	-	-	-

BUCKLING TEST DATA SHEET

Shape: III Sheet: 13 Rise: 2.12 in.

Shell Number	Buckling Pressure p in psi	Radius of Curvature R in inches	Thickness t in in.	Vol. Change V in $in.^3$
1	4.6	4.34	.028	3.1
2	4.5	4.34	.028	3.6
3	4.2	4.34	.027	3.5
4	4.1	4.20	.027	4.1
5	4.7	4.34	.028	4.6
6	4.6	4.34	.029	4.0
7	4.2	4.34	.027	4.0
8	4.4	4.20	.028	4.5
9	4.9	4.20	.028	5.5
10	4.8	4.34	.028	4.8
11	5.1	4.34	.027	4.6

BUCKLING TEST DATA SHEET

Shape: III Sheet: 14 Rise: 2.12 in.

Shell Number	Buckling Pressure p in psi	Radius of Curvature R in inches	Thickness t in in.	Vol. Change V in $in.^3$
1	4.5	4.34	.028	-
2	4.5	4.34	.028	-
3	4.9	4.20	.029	3.6
4	5.4	4.34	.029	3.6
5	4.3	4.20	.028	3.7
6	5.4	4.20	.029	4.6
7	4.9	4.20	.028	3.6
8	4.5	4.20	.027	3.9
9	4.7	4.20	.028	-
10	4.9	3.94	.029	3.9
11	5.0	3.94	.029	3.8

BUCKLING TEST DATA SHEET

Shape: III Sheet: 15 Rise: 2.12 in.

Shell Number	Buckling Pressure p in psi	Radius of Curvature R in inches	Thickness t in in.	Vol. Change V in in.^{3}
1	4.4	3.94	.027	4.2
2	4.9	4.20	.027	4.1
3	4.3	4.34	.028	4.3
4	4.9	4.20	.028	4.2
5	4.9	4.20	.027	-
6	4.9	4.20	.029	-
7	4.6	4.34	.028	-
8	4.3	3.94	.028	4.4
9	4.5	3.82	.027	4.6
10	4.9	3.94	.027	3.4
11	4.3	4.34	.028	3.6

BUCKLING TEST DATA SHEET

Shape: IV Sheet: 16 Rise: 1.53 in.

Shell Number	Buckling Pressure p in psi	Radius of Curvature R in inches	Thickness t in in.	Vol. Change V in in.^{3}
1	3.3	5.46	.032	3.2
2	Leak	-	-	-
3	3.4	5.46	.032	3.9
4	3.4	5.24	.033	3.3
5	3.2	5.46	.031	3.0
6	3.4	5.46	.032	2.8
7	Leak	-	-	-
8	Leak	-	-	-
9	3.6	5.24	.031	-
10	3.1	5.46	.030	3.6
11	3.4	5.46	.031	3.7

BUCKLING TEST DATA SHEET

Shape: IV Sheet: 17 Rise: 1.55 in.

Shell Number	Buckling Pressure p in psi	Radius of Curvature R in inches	Thickness t in in.	Vol. Change V in $in.^3$
1	Leak	-	-	-
2	3.3	5.24	.032	4.5
3	3.3	5.24	.031	-
4	3.1	5.46	.032	-
5	3.3	5.24	.030	3.8
6	3.2	5.24	.030	-
7	3.1	5.24	.030	-
8	3.3	5.24	.030	2.2
9	3.3	5.24	.031	2.2
10	3.2	5.24	.030	-
11	3.3	5.46	.030	3.7

BUCKLING TEST DATA SHEET

Shape: IV Sheet: 18 Rise: 1.53 in.

Shell Number	Buckling Pressure p in psi	Radius of Curvature R in inches	Thickness t in in.	Vol. Change V in in.^{3}
1	3.5	5.24	.031	2.4
2	3.2	5.24	.031	2.2
3	3.6	5.24	.032	2.4
4	3.6	5.24	.031	-
5	3.5	5.46	.031	2.1
6	3.2	5.46	.031	2.1
7	3.2	5.24	.031	-
8	3.3	5.24	.031	2.0
9	3.4	5.46	.031	2.0
10	3.0	5.46	.031	3.8
11	2.8	5.24	.030	3.5

BUCKLING TEST DATA SHEET

Shape: V Sheet: 19 Rise: 0.96 in.

Shell Number	Buckling Pressure p in psi	Radius of Curvature R in inches	Thickness t in in.	Vol. Change V in in.^{3}
1	1.1	9.64	.031	1.2
2	1.1	9.64	.031	.9
3	1.0	9.64	.030	-
4	1.1	9.64	.031	1.1
5	1.0	9.64	.030	1.1
6	1.0	9.64	.030	.9
7	1.0	9.64	.032	1.0
8	1.1	9.64	.031	1.8
9	1.1	9.64	.030	-
10	1.0	9.64	.031	-
11	1.0	9.64	.033	-

BUCKLING TEST DATA SHEET

Shape: V Sheet: 20 Rise: 0.96 in.

Shell Number	Buckling Pressure p in psi	Radius of Curvature R in inches	Thickness t in in.	Vol. Change V in in.^{3}
1	1.1	9.64	.031	.9
2	1.1	9.64	.031	1.2
3	1.1	9.64	.031	.9
4	1.2	9.64	.032	1.0
5	1.1	9.64	.030	1.0
6	1.1	9.64	.032	1.0
7	1.2	9.64	.032	1.4
8	1.1	9.64	.030	-
9	1.1	9.64	.033	-
10	1.1	9.64	.031	1.0
11	1.1	9.64	.032	.9

BUCKLING TEST DATA SHEET

Shape: V Sheet: 21 Rise: 0.96 in.

Shell Number	Buckling Pressure p in psi	Radius of Curvature R in inches	Thickness t in in.	Vol. Change V in $in.^3$
1	1.0	9.64	.033	1.7
2	1.1	9.64	.033	.9
3	1.1	9.64	.033	.9
4	1.1	9.64	.033	.9
5	1.1	9.64	.032	1.0
6	1.2	9.64	.032	.9
7	1.1	9.64	.032	-
8	1.1	9.64	.032	.9
9	1.1	9.64	.032	1.2
10	1.1	9.64	.032	.9
11	Leak	-	-	-

APPENDIX E

This section contains the results of the pressure-volume readings. The data sheets indicate the mercury level in the manometer for a corresponding water level in the water chamber for shells where these quantities were recorded. The mercury level is related to pressure and the water level is related to volume change. The curves show the pressure-volume relation for each shape.

PRESSURE-VOLUME DATA SHEET

Shell Number 5-5

WATER LEVEL in inches	MERCURY LEVEL in inches
.5	0
2.0	.7
3.0	1.3
4.0	1.7
5.0	2.3
6.0	2.8
8.0	3.5
8.3	3.5

PRESSURE-VOLUME DATA SHEET

Shell Number 5-6

WATER LEVEL in inches	MERCURY LEVEL in inches
.4	.1
1.0	.3
2.0	.7
3.0	1.2
4.0	1.6
5.0	2.0
6.0	2.4
7.0	2.7
8.0	2.9
9.0	3.5
10.0	4.0
11.0	4.5
12.0	4.7
12.5	4.7

PRESSURE-VOLUME DATA SHEET

Shell Number 6-6

WATER LEVEL in inches	MERCURY LEVEL in inches
0	.2
1.0	1.2
2.0	2.3
3.0	3.3
4.0	4.5
4.9	5.2

Shell Number 6-7

WATER LEVEL in inches	MERCURY LEVEL in inches
0	.1
1.0	1.5
2.0	2.5
3.0	3.6
4.0	4.9
4.2	5.1

PRESSURE-VOLUME DATA SHEET

Shell Number 10-10

WATER LEVEL in inches	MERCURY LEVEL in inches
0	.4
1.0	1.7
2.0	2.6
3.0	2.8
4.0	3.3
5.0	3.6
6.0	4.0
6.3	4.1

Shell Number 10-11

WATER LEVEL in inches	MERCURY LEVEL in inches
.8	.1
1.0	.6
2.0	1.4
3.0	2.1
4.0	2.5
5.0	3.7
5.4	3.9

PRESSURE-VOLUME DATA SHEET

Shell Number 11-10

WATER LEVEL in inches	MERCURY LEVEL in inches
0	.4
1.0	1.0
2.0	1.6
3.0	2.3
4.0	3.0
5.0	3.6
6.0	4.3
7.0	4.9
7.4	5.1

Shell Number 11-11

WATER LEVEL in inches	MERCURY LEVEL in inches
0	.4
1.0	.9
2.0	1.4
3.0	1.9
4.0	2.4
5.0	3.0
6.0	3.6
7.0	4.1
8.0	4.7
8.7	5.0

PRESSURE-VOLUME DATA SHEET

Shell Number 12-10

WATER LEVEL in inches	MERCURY LEVEL in inches
0	.2
1.0	.6
2.0	1.1
3.0	1.6
4.0	2.1
5.0	2.6
6.0	3.1
7.0	3.7
8.0	4.3
9.0	4.9
9.6	5.1

Shell Number 13-9

WATER LEVEL in inches	MERCURY LEVEL in inches
0	.3
1.0	1.1
2.0	1.9
3.0	2.7
4.0	3.5
7.0	4.9

PRESSURE-VOLUME DATA SHEET

Shell Number 14-9

WATER LEVEL in inches	MERCURY LEVEL in inches
.1	.1
1.0	.7
2.0	1.5
3.0	2.2
4.0	3.0
5.0	3.7
6.7	4.6

Shell Number 15-9

WATER LEVEL in inches	MERCURY LEVEL in inches
0	.2
1.0	1.1
2.0	1.9
3.0	2.7
4.0	3.4
5.0	4.0
5.9	4.4

PRESSURE-VOLUME DATA SHEET

Shell Number 16-10

WATER LEVEL in inches	MERCURY LEVEL in inches
0	.2
1.0	1.2
2.0	1.9
3.0	2.6
4.0	2.9
4.6	3.0

Shell Number 16-11

WATER LEVEL in inches	MERCURY LEVEL in inches
0	.4
1.0	1.4
2.0	2.3
3.0	3.0
4.0	3.3
4.7	3.3

PRESSURE-VOLUME DATA SHEET

Shell Number 17-10

WATER LEVEL in inches	MERCURY LEVEL in inches
.3	.1
1.0	1.0
2.0	2.0
3.0	2.8
3.8	3.1

Shell Number 17-11

WATER LEVEL in inches	MERCURY LEVEL in inches
0	.4
1.0	1.3
2.0	2.0
3.0	2.7
4.0	3.2
4.7	3.2

PRESSURE-VOLUME DATA SHEET

Shell Number 18-10

WATER LEVEL in inches	MERCURY LEVEL in inches
0	.4
1.0	1.0
2.0	1.6
3.0	2.2
4.0	2.7
4.8	2.9

Shell Number 18-11

WATER LEVEL in inches	MERCURY LEVEL in inches
0	.3
1.0	1.0
2.0	1.6
3.0	2.1
4.0	2.5
4.4	2.6

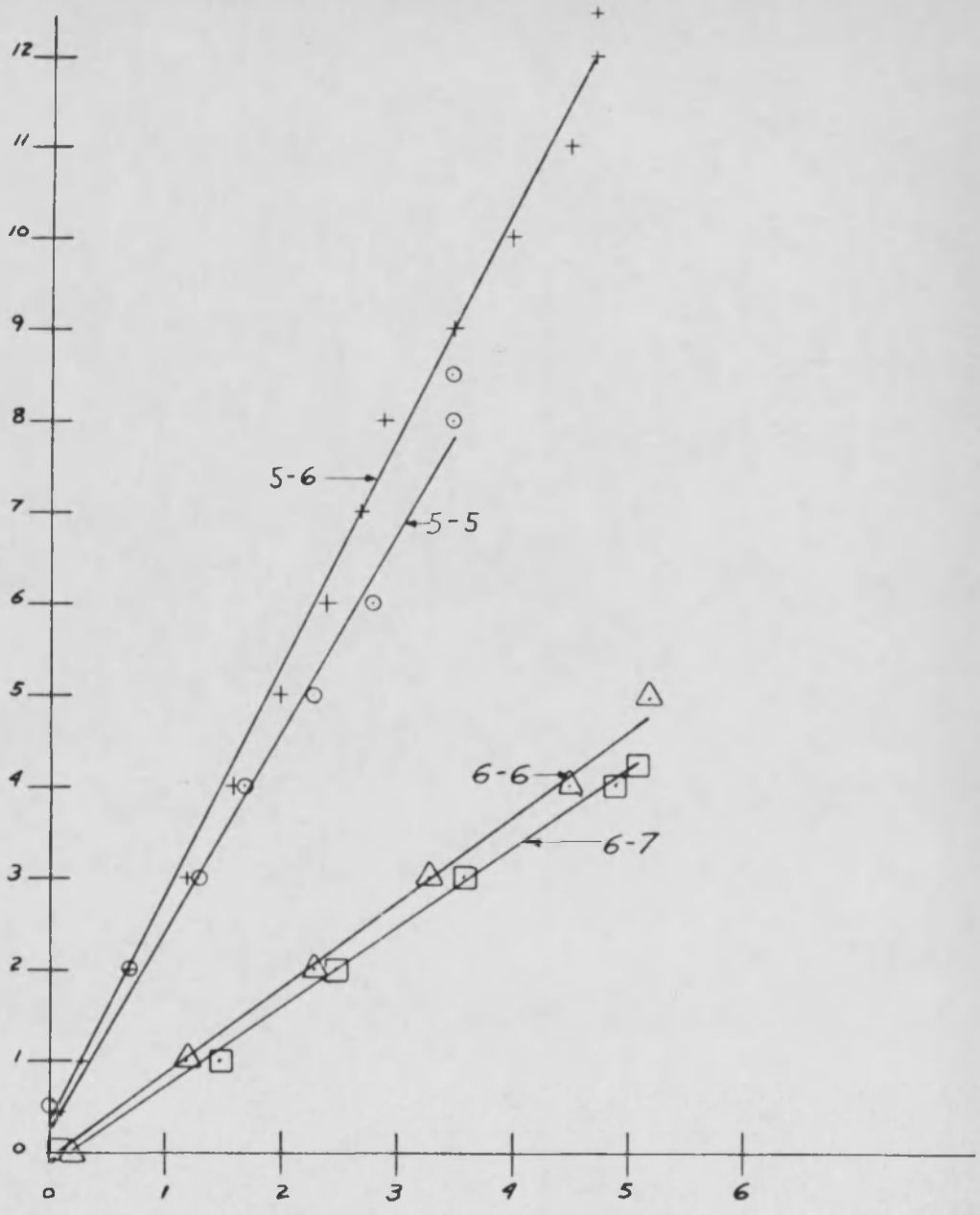

FIGURE 34

Pressure-Volume Curves for Shape I

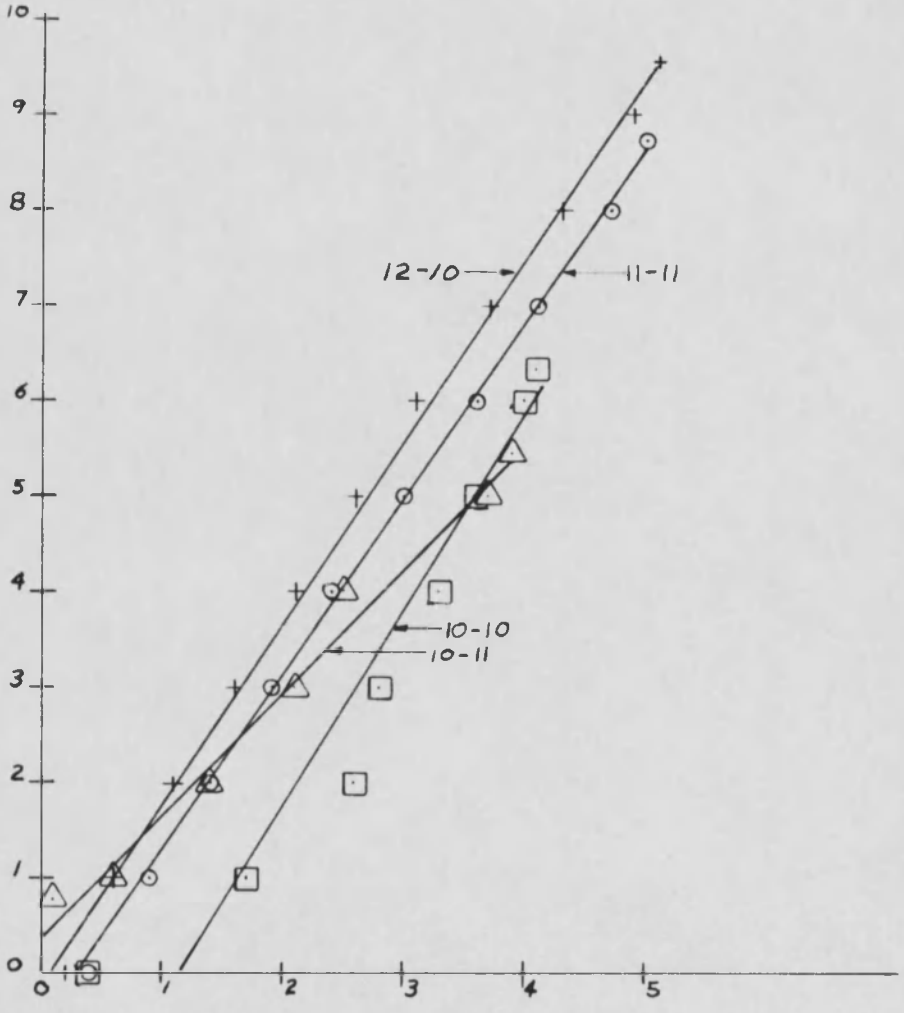

FIGURE 35

Pressure-Volume Curves for Shape II

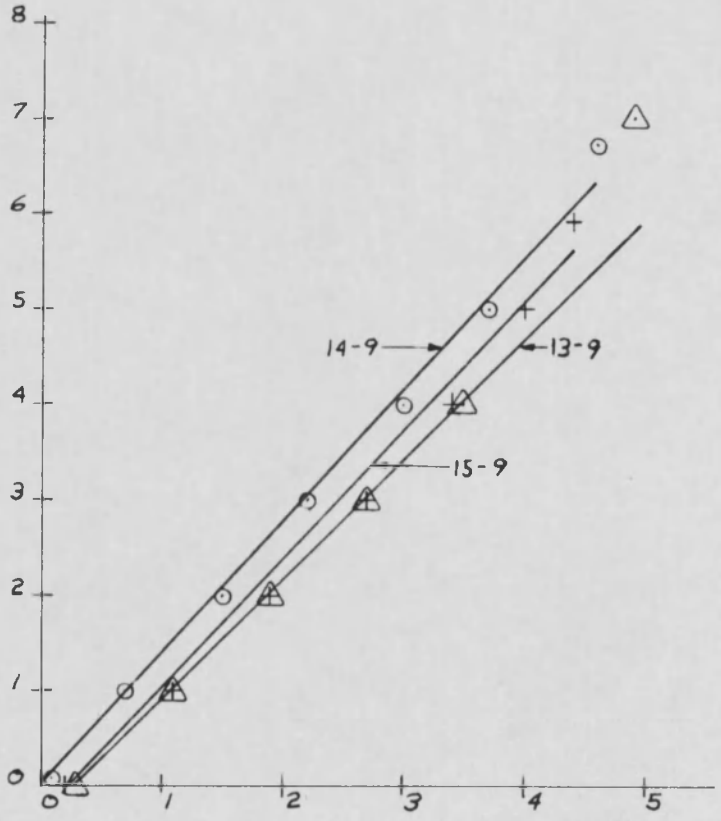

FIGURE 36

Pressure-Volume Curves for Shape III

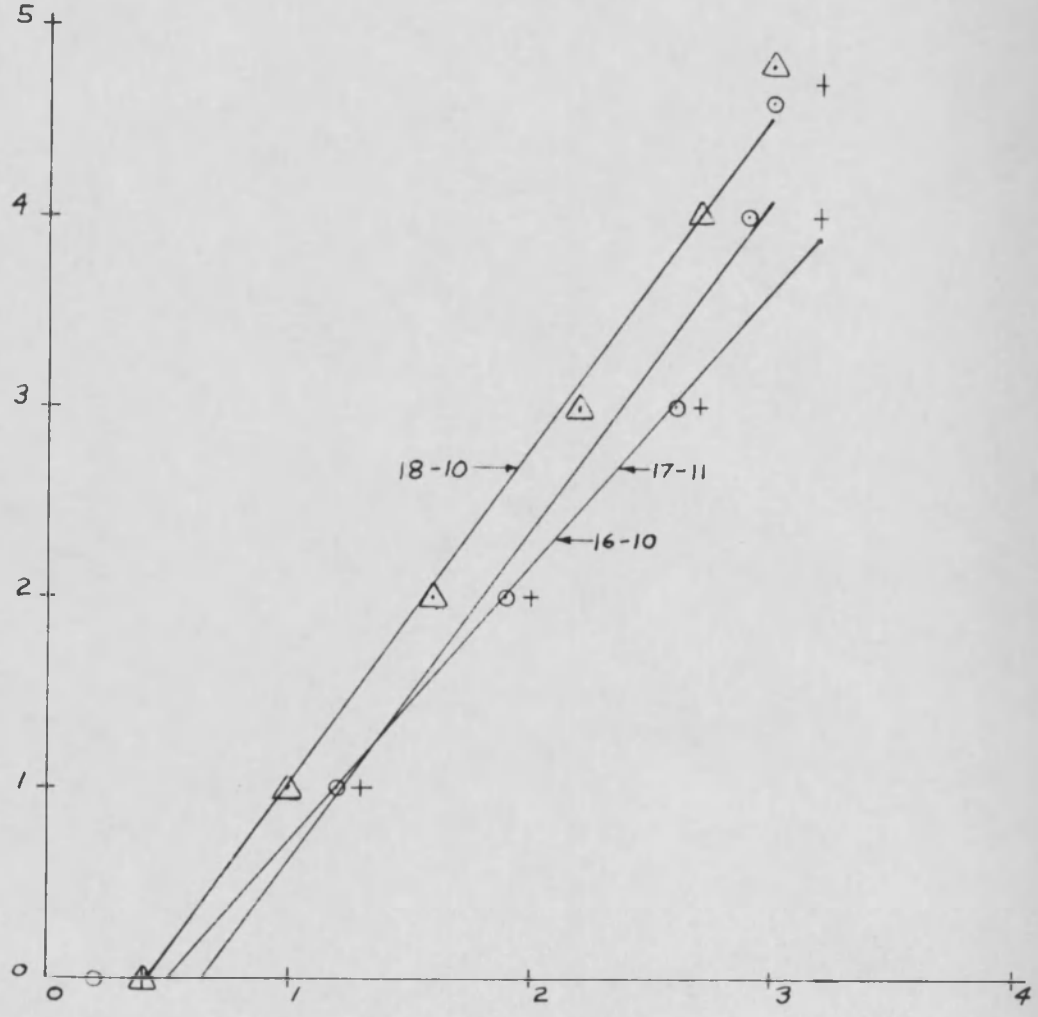

FIGURE 37

Pressure-Volume Curves for Shape IV

LIST OF REFERENCES

1. ARCHER, Robert R. "Stability Limits for a Clamped Spherical Shell Segment Under Uniform Pressure," Quarterly of Applied Mathematics, Vol. 15, January 1958.

2. SIMONS, Roger M. "A Power Series Solution of the Non-Linear Equations for Axi-Symmetrical Bending of Shallow Spherical Shells," Journal of Mathematics and Physics, Vol. 35, July 1956.

3. KARMAN, Th. von, DUNN, Louis G., and TSIEN, Hsue-Shen. "The Influence of Curvature on the Buckling Characteristics of Structures," Journal of the Aeronautical Sciences, Vol. 7, May 1940.

4. KARMAN, Th. von, and TSIEN, Hsue-Shen. "The Buckling of Spherical Shells by External Pressure," Journal of the Aeronautical Sciences, Vol. 7, December 1939.

5. FRIEDRICHS, K. O. "On the Minimum Buckling Load for Spherical Shells," Theodore von Karman Anniversary Volume, 1941.

6. TSIEN, Hsue-Shen. "A Theory for the Buckling of Thin Shells," Journal of the Aeronautical Sciences, Vol. 9, August 1942.

7. KELLER, Herbert B., and REISS, Edward L. "Spherical Cap Snapping," Journal of the Aeronautical Sciences, Vol. 26, October 1959.

8. REISS, Edward L., GREENBERG, Herbert J., and KELLER, Herbert B. "Nonlinear Deflections of Shallow Spherical Shells," Journal of the Aeronautical Sciences, Vol. 24, July 1957.

9. WEINITSCHKE, Hubertus. "On the Nonlinear Theory of Shallow Spherical Shells," Journal of the Society for Industrial and Applied Mathematics, Vol. 6, September 1958.

10. WEINITSCHKE, Hubertus. "On the Stability Problem for Shallow Spherical Shells," Journal of Mathematics and Physics, Vol. 38, January 1960.

11. MURRAY, F. J., and WRIGHT, Frank W. "The Buckling of Thin Spherical Shells," Journal of the Aerospace Sciences, Vol. 28, March 1961.

12. TSIEN, Hsue-Shen. "Lower Buckling Load in the Non-Linear Buckling Theory for Thin Shells," Quarterly of Applied Mathematics, Vol. 5, July 1947.

13. CHIEN, Wei-Zang. "The Intrinsic Theory of Thin Shells and Plates, Part III-Application to Thin Shells," Quarterly of Applied Mathematics, Vol. 2, April 1944.

14. REISSNER, Eric. "Stresses and Small Displacements of Shallow Spherical Shells, I and II," Journal of Mathematics and Physics, Vol. 25, January 1946.

15. REISSNER, Eric. "On Transverse Vibrations of Thin Shallow Elastic Shells," Quarterly of Applied Mathematics, Vol. 13, July 1955.

16. REISSNER, Eric. "On Axi-Symmetrical Vibrations of Shallow Spherical Shells," Quarterly of Applied Mathematics, Vol. 13, October 1955.

17. REISSNER, Eric. "Symmetric Bending of Shallow Shells of Revolution," Journal of Mathematics and Mechanics, Vol. 7, March 1958.

18. REISS, Edward L. "Axially Symmetric Buckling of Shallow Spherical Shells under External Pressure," Journal of Applied Mechanics, Vol. 25, December 1958.

19. KAPLAN, A., and FUNG, Y. C. "A Nonlinear Theory of Bending and Buckling of Thin Elastic Shallow Spherical Shells," NACA Technical Note 3212, August 1954.

20. REISS, Edward L. "On the Non-Linear Buckling of Shallow Spherical Domes," Journal of the Aeronautical Sciences, Vol. 23, October 1956.

21. KLEIN, Bertram. "Parameters Predicting the Internal and Final Collapse Pressures of Uniformly Loaded Spherical Shells," Journal of the Aeronautical Sciences, Vol. 22, January 1955.

22. KLEIN, Bertram. "Further Remarks on the Collapse Pressures of Uniformly Loaded Spherical Shells," Journal of the Aeronautical Sciences, Vol. 24, April 1957.

23. WEINITSCHKE, Hubertus. "On the Buckling Problem of Shallow Spherical Shells under External Pressure," Journal of the Aeronautical Sciences, Vol. 25, February 1958.

24. WILLICH, Gideon P. R. von. "The Elastic Stability of Thin Spherical Shells," Journal of the Engineering Mechanics Division, Proceedings of the American Society of Civil Engineers, Vol. 85, No. EM 1, January 1959.

25. BUDIANSKY, B. "Buckling of Clamped Spherical Shells," Proceedings of the Symposium on The Theory of Thin Elastic Shells, Delft, August 1959.

26. BUDIANSKY, Bernard, and WEINITSCHKE, Hubertus. "On Axisymmetrical Buckling of Clamped Shallow Spherical Shells," Journal of the Aerospace Sciences, Vol. 27, July 1960.

27. HOMEWOOD, R. H., BRINE, A. C., and JOHNSON JR., A. E. Buckling Instability of Monocoque Shells, Research and Advanced Development Division, Avco Corporation, Technical Report RAD-TR-9-59-20, August 1959.

28. JOHNSON, A. E., and HOMEWOOD, R. H. "Stress and Deformation Analysis from Reduced Scale Plastic Model Testing," Experimental Mechanics, September 1961.

29. GUGOLYUK, E. I. "On the Unsymmetrical Snapping of Shells of Revolution," Proceedings on the Symposium on the Theory of Thin Elastic Shells, Delft, August 1959.

30. NASH, William A., and MODEER, James R. Certain Approximate Analyses of the Nonlinear Behavior of Plates and

Shallow Shells. Florida Engineering and Industrial Experiment Station, Technical Paper 193, Vol. 14, No. 10, October 1960.

31. THURSTON, G. A. "A Numerical Solution of the Nonlinear Equations for Axisymmetric Bending of Shallow Spherical Shells," Journal of Applied Mechanics, Vol. 28, December 1961.

32. PAHL, Peter Jan, and SOOSAAR, Keto. Structural Models for Architectural and Engineering Education. Cambridge 39, Massachusetts: School of Engineering, Massachusetts Institute of Technology, 1964.

33. GJELSVIK, A., and BODNER, S. R. "Nonsymmetrical Snap Buckling of Spherical Caps," Journal of the Engineering Mechanics Division, Proceedings of the American Society of Civil Engineers, Vol. 88, No. EM 5, October 1962.